High-efficiency water splitting by optimizing piezo photocatalytic synergy in $Bi_{0.5}Na_{0.5}TiO_3$ optimized with $RGO-Co_3O_4$

By

Farah Mumtaz

(Registration No: 00000328039)

Department of Materials Engineering

School of Chemical and Materials Engineering

National University of Sciences & Technology (NUST)

Islamabad, Pakistan

(2024)

High-efficiency water splitting by optimizing piezo photocatalytic synergy in $Bi_{0.5}Na_{0.5}TiO_3$ optimized with RGO-Co_3O_4

By

Farah Mumtaz

(Registration No: 00000328039)

A thesis submitted to the National University of Sciences and Technology, Islamabad,

in partial fulfillment of the requirements for the degree of

Master of Science in
Nanoscience and Engineering

Supervisor: Dr. Mohsin Saleem

School of Chemical and Materials Engineering

National University of Sciences & Technology (NUST)

Islamabad, Pakistan

(2024)

THESIS ACCEPTANCE CERTIFICATE

THESIS ACCEPTANCE CERTIFICATE

Certified that final copy of MS thesis written by Ms **Farah Mumtaz** (Regn No 00000328039), of School of Chemical & Materials Engineering (SCME) has been vetted by undersigned, found complete in all respects as per NUST Statues/Regulations, is free of plagiarism, errors, and mistakes and is accepted as partial fulfillment for award of MS degree. It is further certified that necessary amendments as pointed out by GEC members of the scholar have also been incorporated in the said thesis.

Signature: _____

Name of Supervisor: **Dr Mohsin Saleem**

Date: ___11/03/2024___

Signature (HOD): _____

Date: ___20/5/24___

Signature (Dean/Principal): _____

Date: ___20. 5. 2024___

TH - 1

National University of Sciences & Technology (NUST)

MASTER'S THESIS WORK

Formulation of Guidance and Examination Committee (GEC)

Name: **Farah Mumtaz**   NUST Reg No: **00000328039**

Department: **Department of Materials Engineering**   Specialization: **Master of Science in Nanoscience & Engineering**

Credit Hour Completed: **24.0**   CGPA: **3.75**

Course Work Completed

S/No:	Code:	Title:	Core/Elective:	CH:	Grade:
1.	MSE-854	Characterization Of Materials	Compulsory	3.0	A
2.	RM-898	Research Methodology	Additional	2.0	Q
3.	NSE-813	Essentials of Nanoscience and Engineering	Compulsory	3.0	A
4.	CHE-815	Nano Catalysis	Compulsory	3.0	B
5.	MSE-856	Nano Material and Processing	Compulsory	3.0	A
6.	MSE-872	Composite Materials	Elective	3.0	A
7.	NSE-961	Surface Coatings and Thin Films	Elective	3.0	B+
8.	NSE-842	Nano Materials For Energy Applications	Elective	3.0	A
9.	ESE-829	Functional Nanomaterials for Renewable Energy	Elective	3.0	B+

Date **09 - Dec - 2022**   Student's Signature

Thesis Committee

1. Name: **Mohsin Saleem (Supervisor)**   Signature
   Department: **Department of Materials Engineering**

2. Name: **Tayyaba Noor (Cosupervisor)**   Signature
   Department: **Department of Chemical Engineering**

3. Name: **Sofia Javed (Internal)**   Signature
   Department: **Department of Materials Engineering**

4. Name: **Zeeshan Ali (Internal)**   Signature
   Department: **Department of Materials Engineering**

Date: **09 - Dec - 2022**   Signature of Head of Department:

APPROVAL

Date: **09 - Dec - 2022**   Signature of Dean/Principal:

School of Chemical & Materials Engineering (SCME) (SCME) H-12 Campus,

TH – 4

National University of Sciences &Technology (NUST)

MASTER'S THESIS WORK

We hereby recommend that the dissertation prepared under our supervision by Regn No & Name: <u>00000328039 Farah Mumtaz</u>

Title: <u>High Efficiency Water Splitting by Optimizing Piezo-Photo Catalytic Synergy in Bi$_{0.5}$Na$_{0.5}$TiO$_3$ Optimized with RGO-Co$_3$O$_4$.</u>

Presented on: <u>22 Feb 2024</u>   at: <u>1400 hrs in SCME (Seminar Hall)</u>

Be accepted in partial fulfillment of the requirements for the award of Masters of Science degree in **Nanoscience & Engineering**.

Guidance & Examination Committee Members

Name: <u>Dr Zeeshan Ali</u>   Signature:_____

Name: <u>Dr Sofia Javed</u>   Signature:_____

Name: <u>Dr Tayyaba Noor</u> Co-Supervisor)   Signature:_____

Supervisor's Name: <u>Dr Mohsin Saleem</u>   Signature:_____

Dated: <u>22—02-2024</u>

Head of Department

Date <u>26/3/24</u>

Dean/Principal

Date <u>26-3-2024</u>

School of Chemical &Materials Engineering (SCME)

AUTHOR'S DECLARATION

I Farah Mumtaz hereby state that my MS thesis titled "High-efficiency water splitting by optimizing piezo photocatalytic synergy in $Bi_{0.5}Na_{0.5}TiO_3$ optimized with $RGO-Co_3O_4$" is my own work and has not been submitted previously by me for taking any degree from National University of Sciences and Technology, Islamabad or anywhere else in the country/ world.

At any time if my statement is found to be incorrect even after I graduate, the university has the right to withdraw my MS degree.

Name of Student: Farah Mumtaz

Date: 22 May 2024

PLAGIARISM UNDERTAKING

I solemnly declare that research work presented in the thesis titled "High-efficiency water splitting by optimizing piezo photocatalytic synergy in $Bi_{0.5}Na_{0.5}TiO_3$ optimized with $RGO\text{-}Co_3O_4$" is solely my research work with no significant contribution from any other person. Small contribution/ help wherever taken has been duly acknowledged and that complete thesis has been written by me.

I understand the zero-tolerance policy of the HEC and National University of Sciences and Technology (NUST), Islamabad towards plagiarism. Therefore, I as an author of the above titled thesis declare that no portion of my thesis has been plagiarized and any material used as reference is properly referred/cited.

I undertake that if I am found guilty of any formal plagiarism in the above titled thesis even after award of MS degree, the University reserves the rights to withdraw/revoke my MS degree and that HEC and NUST, Islamabad has the right to publish my name on the HEC/University website on which names of students are placed who submitted plagiarized thesis.

Student Signature: _____

Name: Farah Mumtaz

DEDICATION

"I dedicate this thesis to my beloved parents, sister, husband, and kids."

ACKNOWLEDGEMENTS

TABLE OF CONTENTS

REFERENCES 78

LIST OF TABLES

LIST OF FIGURES

LIST OF SYMBOLS, ABBREVIATIONS AND ACRONYMS

EDX   Energy Dispersive X-Ray

SEM   Scanning Electron Microscope

XRD   X-ray Powder Diffraction

FTIR   Fourier-Transform Infrared Spectroscopy

nm   Nanometers

CV   Cyclic Voltammetry

GCD   Galvanostatic Charge Discharge

EIS   Electrochemical Impedance Spectroscopy

ABSTRACT

Utilizing strain-induced polarization to amplify the performance of photo-catalytic water-splitting systems has garnered significant attention. However, achieving efficient charge separation, high underwater suspension efficiency, and sustained cyclic stability remains a persistent challenge. In this study, we employed a classic low temperature ball milling technique to synthesize rhombohedral phase $B_{0.5}Na_{0.5}TiO_3$ as matrix material for our composite catalyst. One-step superimposed reduced graphene oxide with cobalt oxide loading RGO-Co_3O_4 is used as reinforcement. We report a 14.79% increase in H_2 evolution with the addition of reinforcement and optimal H_2 evolution was achieved with 5% RGO-Co_3O_4 517 µmol/g-h. After the introduction of simultaneous photo and piezoelectric potential by using ultrasonicator H_2 evolution is much enhanced 109 µmol/g-h surpassing individual piezo catalysis 66 µmol/g-h and photo catalysis 64 µmol/g-h. Herein, we explore the utilization of alternative wastewater using manure and seawater as a replacement for distilled water revealing improved H_2 evolution that is 1.8% and 50.4% respectively that is more than distilled water along with other useful biogases. Additionally, the catalyst demonstrates remarkable performance without a sacrificial agent further highlighting its exceptional potential. Moreover, we also uncover the role of Co_3O_4 as a co-catalyst and RGO as a promoter for water splitting. This work provides insight into harnessing and designing ingenuous composites for efficient and stable piezo photo catalysts for efficient and stable water-splitting systems.

Keywords: Water Splitting, Electrochemical Properties, Hydrogen Evolution.

CHAPTER 1: INTRODUCTION

1.1   Introduction

The evolution of fuel from firewood to modern renewable fuels is a testimony of human creativity and ambition. It underpins ethical, environmental, and geopolitical challenges for humanity as their quest for fuel is coined with their survival. In today's world waste water and energy shortages have posed serious challenges for scientific researchers in their pursuits of a cleaner environment. [3, 4]

Environmental contamination has overall disrupted the natural ecosystem which affects the safety of life on Earth. A recent surge in energy demands with excessive use of fossil fuels, and their high environmental foot print have posed a serious obstacle to a green environment. [5]
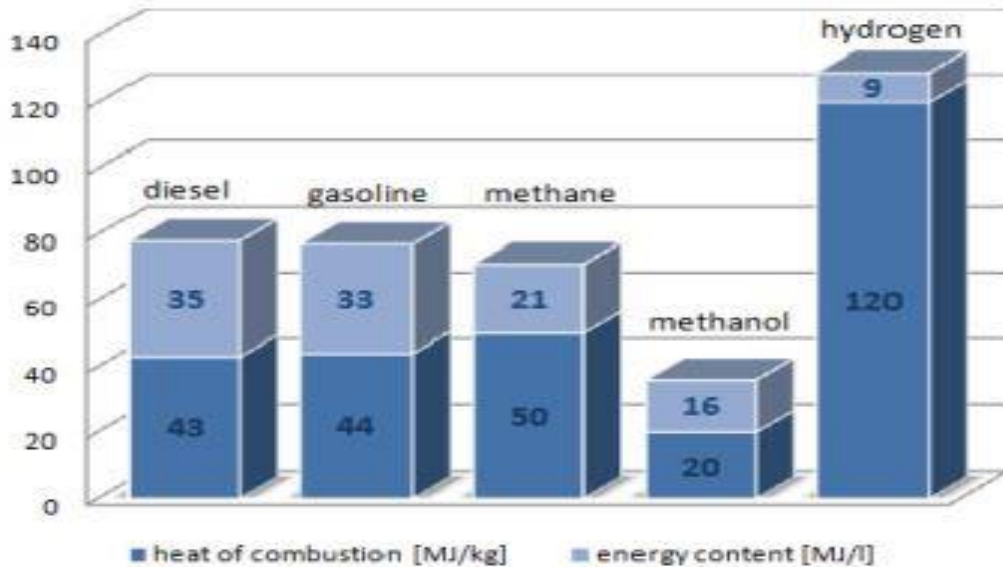
Figure 1.1: Shows a comparison between the energy density of hydrogen versus other fossil fuels[6]

In the past few decades, catalysis emerged as an encouraging approach towards clean water, soil, and green fuels, which includes photo catalysis, piezo catalysis, piezo-photo catalysis, and pyro-electric catalysis. New and sophisticated catalysts are used to

harness abundant and natural primary energy sources like solar e.g. photons, mechanical e.g. piezo and triboelectric, and thermal e.g. pyro electrics. Photo catalysis is the most common and widely investigated whereas piezo and pyro-electric catalysis is more recent approaches.[7, 8]

Although a variety of renewable alternatives are available the key challenge remains to efficiently convert either this renewable energy directly into electricity or in the production of fuel with desired energy density as offered by existing fuel setup. Furthermore, energy density considerations outnumber other renewable contenders in the energy arena where its energy density is three times more than that of gasoline.[6]

1.2   Water Splitting

Water splitting technology plays a crucial role in the development of green fuels particularly in hydrogen production which is believed to be a clean and sustainable energy source. Photocatalysis is the most widely used process where electronic transitions from valance to conduction band take place in photoactive materials.

In the streak of photocatalysts specifically for water splitting reactions semiconductors as oxides, sulfides, and selenides have been tried and tested over years for wastewater dye degradation and hydrogen production. [9-11] However, their optimization in terms of band gaps, suitable energy positions for desired reactions, low charge recombination, high photo and water stability, low toxicity, and cost remains a challenge. [12]

High band gaps of common semiconductors limit their direct use as they make the catalyst more UV active and reduce its overall solar energy utilization. Extensive structural and band gap engineering is required to generate hydrogen under direct light irradiation. [13]

Electron hole pairs generated through photo excitations trigger desired reactions. However, a high band gap and charge recombination hampers the performance of a photocatalyst. It demands to devise new and more efficient mechanisms for water splitting reactions to increase yield.[14, 15]

At the same time, mechanical energy is another abundant form of green energy available in nature as wind, tide, vibration, sonication, and atmospheric pressure. Certain materials can harness this energy into electrical energy and are termed piezo materials. Charge separation in piezo materials takes place by mechanical stress triggering water-splitting reactions. [8]
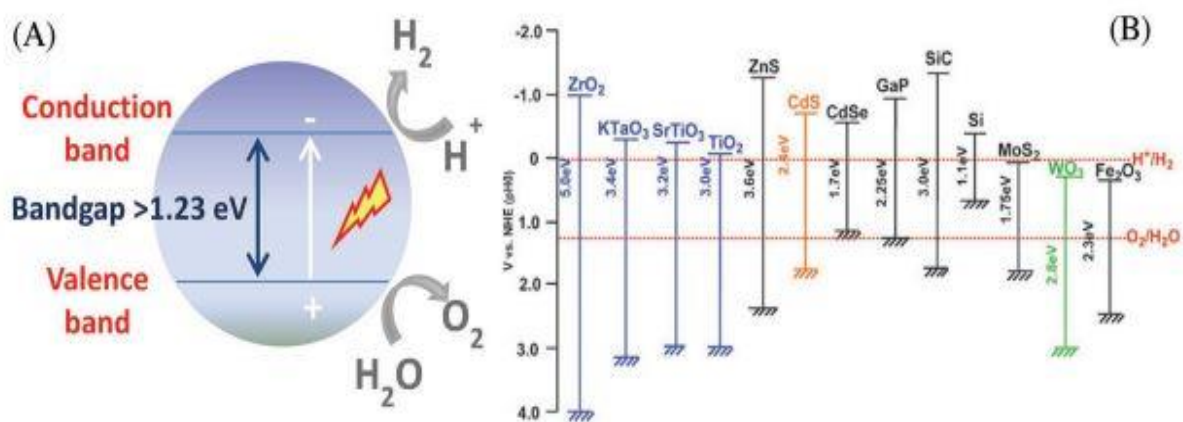
Figure 1.2: Schematics (A) water splitting over photoactive material and (B) band structures of semiconductor materials vs redox potential for water splitting [16]
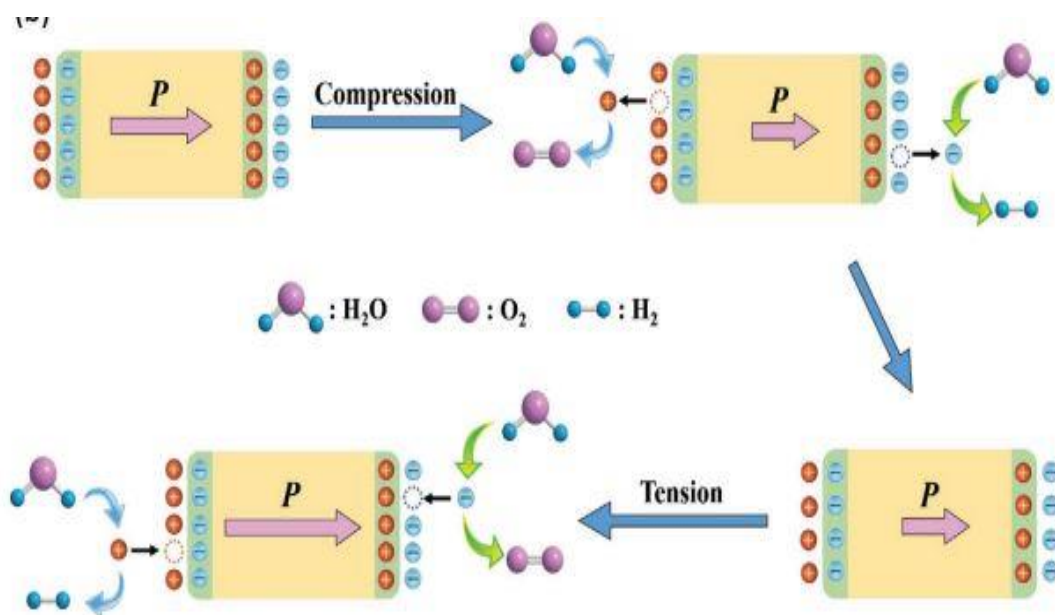
Figure 1.3: Schematics of piezo catalysis for water splitting [17]

Piezo-photo catalysis is an innovative concept that combines two fundamental concepts piezo-electricity and photo-catalysis. piezo active materials generate electrical charges when subjected to mechanical stress, whereas photo-catalysts utilize light energy to create electron-hole pairs that drive chemical reactions leading to water splitting.[18-20]

Internal polarization caused by mechanical stress induces strain in the photocatalyst thus altering its electronic configuration and facilitating charge carriers separation. This strain-induced effect not only enhances charge separation but also its mobility. Convergences of these two concepts have synergistic effects that can improve the efficiency and yield of water-splitting reactions. [21]Although certain materials perform well as either piezo or photocatalysts however same material provides better H_2 yield due to the synergic effect of piezo-photo catalysis. [22, 23]

In recent years, perovskite materials have garnered substantial attention in the field of photovoltaics due to their photo electronic properties including high light absorption and charge mobility. The same properties made them a suitable candidate for photocatalysis. [24, 25]Researchers have been working to enhance their light absorption in the visible region and devising new strategies to improve their stability in aqueous mediums. [26]
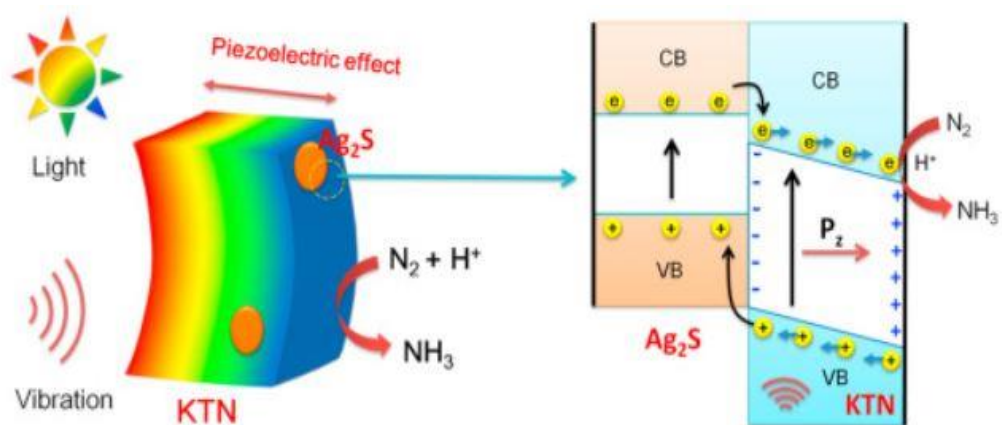
Figure 1.4: Schematics of piezo-photo catalysis for water splitting over KTN and AG$_2$S nanoparticles [27]

Perovskite being both photo and piezo-active are excellent candidate for piezo-photo catalysis and a variety of materials like titanates, niobates, and ferrates have been investigated with or without the use of metal loading. A few of the commonly investigated perovskite materials in their hybrids and composites are $Bi_{0.5} Na_{0.5} TiO_3$, $BaTiO_3$, $CaTiO_3$-$Bi_2Ti_2O_7$, $NaNbO_3$, Bi_2O_6, $BiVO_4$, $AgNbO_3$, $SrBaNb_2O_7$, and $BiFeO_3$, etc. [28-31]

Research also suggests photo-active materials in their 2D nano configuration also depict piezo nature and are excellent contenders for piezo-photo catalysis like RGO, carbon nitride cadmium sulfide, etc. These layered 2D piezo-photo materials provide an alternative material range for water-splitting reactions. Carbon nitride seems to be the most potent one although the high cost of material and slow reaction kinetics needs to be optimized. [29, 32]

However performance of piezo-photo catalysis depends upon a variety of parameters including curie temperature, piezoelectric coefficient, conductivity, band gaps, and band alignment to the redox potential of reactions. [33] Reaction kinetics is directly proportional to material conductivity, whereas a stronger piezoelectric coefficient tends to have poor conductivity. It makes material selection and design quite a strategic balance of the two. [34]

1.3   Metal-Organic Frameworks

Metal-organic frameworks MOFs are a more recent material in piezo-photo catalysis where longer polymeric chains of MOFs give more stability to metals from underwater oxidation and enhance the longevity of metal nanoparticles that are embedded in their polymeric structure. [35] Recently perovskite halides have been reinforced with non-metal as co-catalysts however very little established literature is available in domains of co-catalysts and promoters for piezo-phto catalysis. [36]

Moreover, not only hybrid materials are a new stride, but certain hybrid techniques pose new fads in the water splitting arena such as combining tribo/piezoelectric nano-generator TENG/PENG and photovoltaic prior photoelectrochemical cell. [37, 38] They eliminate the inherent limitation of external bais required for photoelectrochemical cells.

Integration of such different techniques offers room for coherence with other similar techniques like photoelectrochemical cells, photocatalysis, piezo catalysis, and piezo-photo catalysis. [39]

In this paper we have designed a hybrid composite with classic perovskite matrix using bismuth sodium titanate BNT and superimposed Co_3O_4 functionalized RGO as reinforcement. Where the RGO part of our reinforcement not only acts as an alternative to conventional metal loading for facilitating HER reaction but also improves the charge mobility inside piezo natured matrix. On the other hand, Co_3O_4 speeds up classically slow OER reaction indirectly facilitating hydrogen production. Optical properties of RGO also lower the band gap of our material and make it more visible light active to optimize full spectrum absorption. Moreover, research findings confirm the role of Co_3O_4 as a

Co-catalyst however RGO appears to be a promoter that not only improves conductivity but also improves material light absorption properties.

CHAPTER 2:   LITERATURE REVIEW

2.1   Fuel history

Fuels and human history go hand in hand in shaping societies and economies over centuries. From firewood to the rise of fossil fuel and the consistent quest for sustainable alternatives history of fuel is no less than an evolutionary journey filled with technical innovations, resource exploitation, environmental changes, and one of the most controversial reasons backing wars and affecting international alliances. [40]

2.2   Firewood

One of the most crucial milestones in human evolution was the discovery of firewood and it laid a solid foundation to inhabit new geographical regions and develop complex societies. Firewood as an early fuel till the 18th century served as society's lifeline as it not only provided warmth but also was a sole source of cooking food and provide protection from predators. [41] Growing societies and their ever-increasing need for fuel increase the scope of biomass from firewood to crop residues and animal dung. However, this reliance has its limitations and creates environmental and pollution issues in the form of deforestation and some types of air and soil pollution. [6, 42]

2.3   Coal

A seismic shift in fuel history emerged between the 18th to 19th centuries with the discovery of coal. The advent of the Industrial Revolution and the rise of coal as a new energy source not only transformed the existing industries and transportation but also laid the foundation of urban lifestyle. However, coal-led industries resulted in unprecedented economic growth and for the first time in history, fuel got coined with national security. [43] The Industrial Revolution paid huge environmental costs in the form of excessive air pollution leading to widespread respiratory problems and mining accidents that plagued communities settled around coal mines and factories.[44] Even today, coal abundance or availability of other energy-density fuels is considered necessary for the swift expansion and sustenance of industrialized nations. However, no one can deny the high carbon

footprint of coal-powered industries and its impact even goes beyond borders. Recent research advancements in coal power plants have shown to replace entire plant facilities with biomass technology to utilize existing installed capacity in the best of industrial and environmental use. [45]

2.4   Fossil fuel

In many applications, fossil oils are considered to have displaced coal and ever since are considered to dominate the transport industry. The late 19th century escorted a new candidate into the fuel world. [46]Fossil fuel with higher energy density as compared to coal and its refining into various products like kerosene, gasoline, diesel, and heavy-density oils not only makes it more efficient but also more versatile when it comes to its utility. Crude oil at its core led to the widespread adoption of automobiles, reshaping conventional transportation and instigating urban planning.[47]

The 20th century marked another pivotal shift in fuel history and revolutionized transportation by making airplanes, automobiles, trains, and ships an integral part of modern urban life.   Furthermore, it also played a crucial role in developing more technically advanced industries like a petrochemical industry that stems the foundation for plastics, new synthetic materials and fabrics, and countless consumer products.[48]

The geographical positioning of oil reserves and its global thirst led to several geopolitical conflicts over a century. The two world wars of the early 20th century brought fuel to the limelight in global geopolitics and have profoundly affected and shaped international relations over decades till date. [49, 50]Crude oil to its core is critical to military logistics and has been a driving force for innovation and development in oil extraction and redefining techniques.

These wars and conflicts catalyzed the development of technologies like jet engines and missiles that have changed the dynamics of aviation and warfare. However, OPEC (the organization of petroleum exporting countries) in the oil market emerged as a powerful player with significant influence over oil prices and its supply worldwide.[51]

2.5   Electricity

Concurrently, the late 19th and early 20th century also marked the rapid electrification of societies. The advent of electricity added a new dimension to the fuel arena and also started the foundation of modern electric green technologies. The thriving petrochemical industry backed by fossil oil mainly dominates transportation and military dynamics.[52] However advances in electrical engineering, power generation, and transmission brought light, heating, and machinery to homes and industry. On the whole, electricity emerged as a more flexible and efficient energy source that led to transformation in daily life and industrial processes.[53]

2.6   Nuclear energy

The 20th century was marked by the advent of a variety of fuel alternatives leading to numerous new technologies that revolutionized society in general. Crude oil and electricity feet can be back traced to the early 20th century however; nuclear energy came into light by the mid-twenties. [54] Initially, nuclear power plants were built to generate electricity by harnessing the massive power of nuclear reactions for softer domestic and industrial use. Later on, seemingly early promising, cleaner, and abundant energy sources emerged to be one the most challenging alternatives with complex safety concerns and immense risk of nuclear proliferation. [55] Secondly, nuclear technology with an enormous potential to be used in nuclear warfare as in WW-2 also restricts its widespread expansion thus limiting its overall potential to be used as a cleaner and safer alternative. [56]

2.6.1   Environmental concerns and renewable fuels

Early 20th century till date fossil oil remains the key contender in the energy and fuel arena however its high environmental footprint started raising red flags. The latter half of the 20th century experienced exacerbated consequences of fossil oil burning. Greenhouse gases began releasing at alarm bells rate subsequently increasing the air pollution index in urban societies. [57]Serious smog problems contributing to respiratory and air navigation problems as well as acid rains contaminating soil and causing certain health concerns are

not the only problems but it has also increased overall global warming that results in natural environmental catastrophes. [58, 59]

Growing awareness concerning the environment roots for a variety of environmental movements and regulations that aim at mitigating these harmful effects. Furthermore, they highlight the dire need to develop cleaner and safer energy alternatives. [60] However, this transition remains a dire challenge for governments to sustain their economies at the expense of deteriorating the environment or saving environment at the expense of the economy. [61]

In the early 21st century there is a noticeable surge and investment in renewable fuel sources. Biofuels introduced in the early 2000s as an alternative to fossil fuels were not only due to the soaring high prices but also to their low CO_x, SO_x, and NO_x emissions. They were cleaner alternatives, but irony remains the same as they still produce substantial amounts of carbon emissions. [62, 63]

Despite being expensive in comparison to its conventional rival i.e. crude oil conspicuous amount of funds are poured into developing new and more sustainable fuel alternatives. Emerging technologies like wind, solar, and hydropower are deployed to mature synergistic energy systems that are not only green but also increase energy independence. According to the Paris Agreement of 2015 investment in renewable sources and the environmental burden of oil exploration for developing countries like Kenya needs to be shared by the world being a collateral environmental hostage. [64]The world faces a monumental challenge while transitioning from economical fossil fuels to expansive sustainable fuel sources. Environment being the colossal opportunity cost of using economical fuel poses a serious threat to the fate of our planet and the wellbeing of our generations to come.[65]

Climate change, resource depletion, geopolitical tensions, the growing world's fuel needs, and the viability of economies underscore the perseverance of transitioning into renewable yet sustainable fuel alternatives. The nature of the problem is more tumultuous than it seems apparently because of underpinning political and economic currents as the government supporting oil explorations and imports supports fossil oil backed economies

however at the same time, government signed environmental treaties demands significant decrease in consumption and production of fossil fuels. [12, 65]
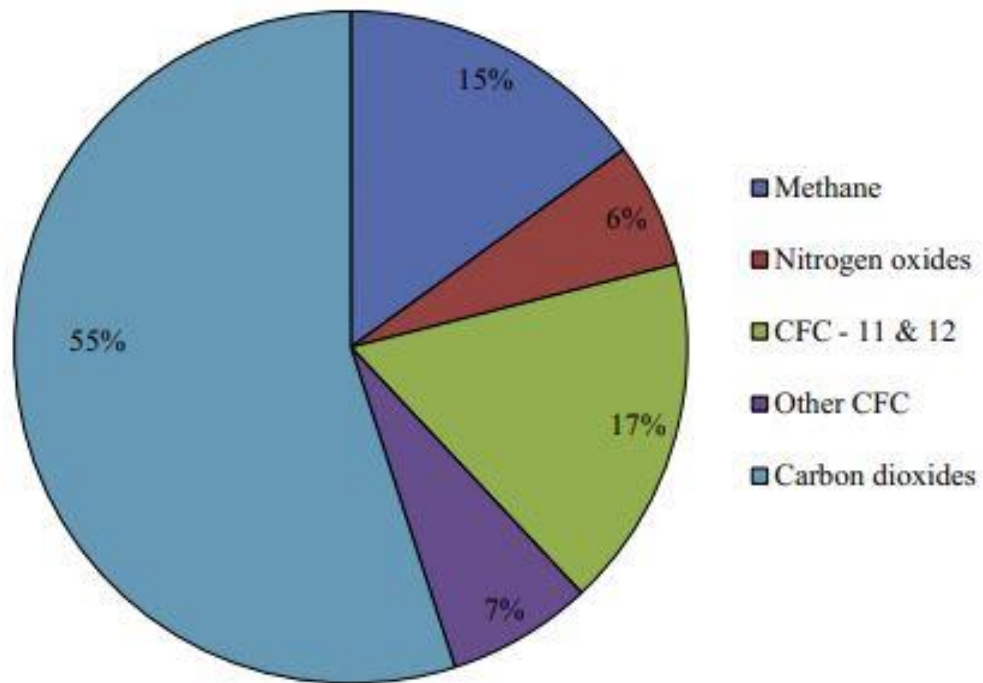
Figure 2.1: Different greenhouse gasses and their contribution to global warming[66]
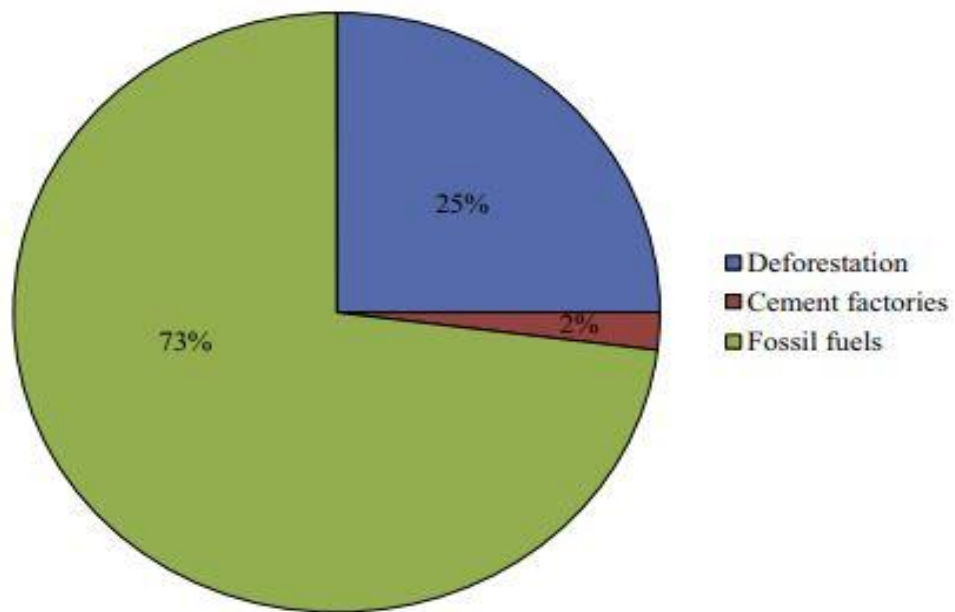
Figure 2.2: Pie chart of major CO_2 sources [66]

2.7 Renewable fuels

A diverse range of renewable fuels is available that offers a variety of sustainable energy options that interns depend upon the end application. [67] Biofuels and biogas were the earliest in the renewable forefront and can be easily used in conventional vehicles with significantly lower carbon emissions and as a natural gas alternative respectively.

Countries like Australia and Brazil have conducted numerous studies on shifting their domestic transport to biofuels. [68] Both alternatives were significantly criticized for having their carbon footprint furthermore bio bio-fuel controversy of food versus fuel limits its sustainability. [69]
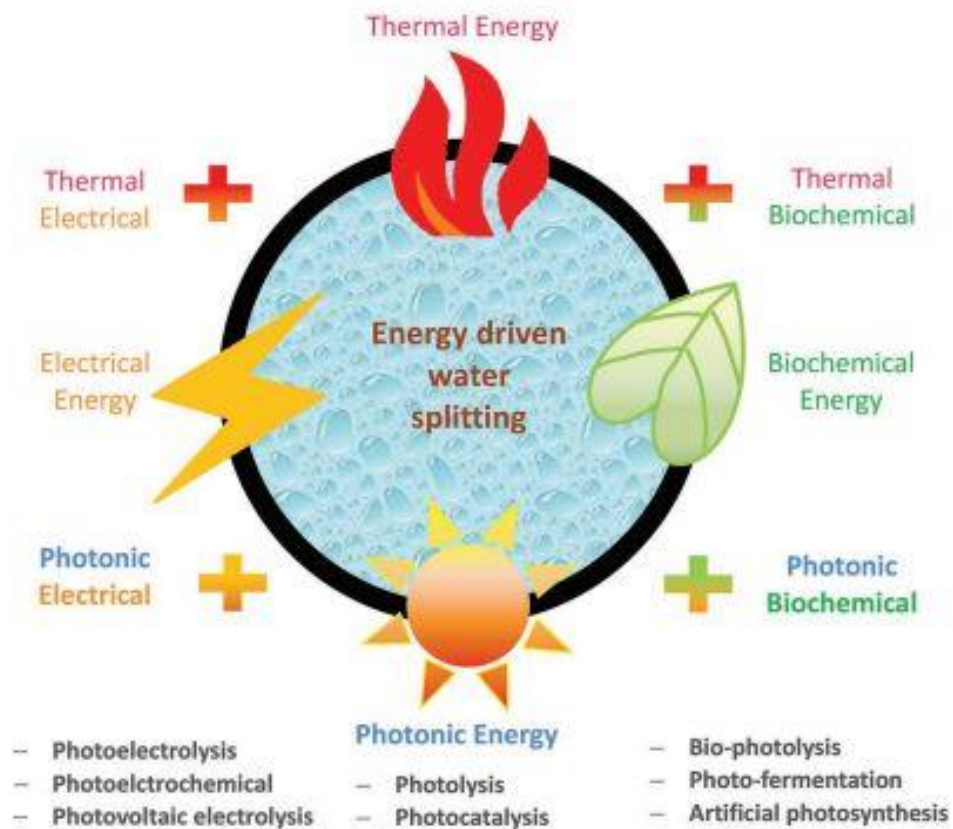
Figure 2.3: Schematics of water splitting systems with variety of energy drivers[16]

One renewable source might not have the capacity to power all fuel needs but their development and integration into existing energy systems significantly reduces fossil fuel

consumption and overall improves air quality index of metropolitan cities.[70] Geothermal energy, hydropower energy, wind energy, and solar energy emerged as sustainable contenders for renewable energy alternatives.[71, 72]

The new to this energy arena is hydrogen where hydrogen burning through fuel cells produces only one by-product which is water, and it is clean. If hydrogen is produced through some renewable source like wind or solar it has the potential to be the future green and sustainable fuel. Studies have been conducted on shifting power generation systems of different countries by fuel cells that in turn are backed by hydrogen. Future trends and studies forecast towards major energy shift and it is toward hydrogen. [73]

2.7.1   Hydrogen fuel
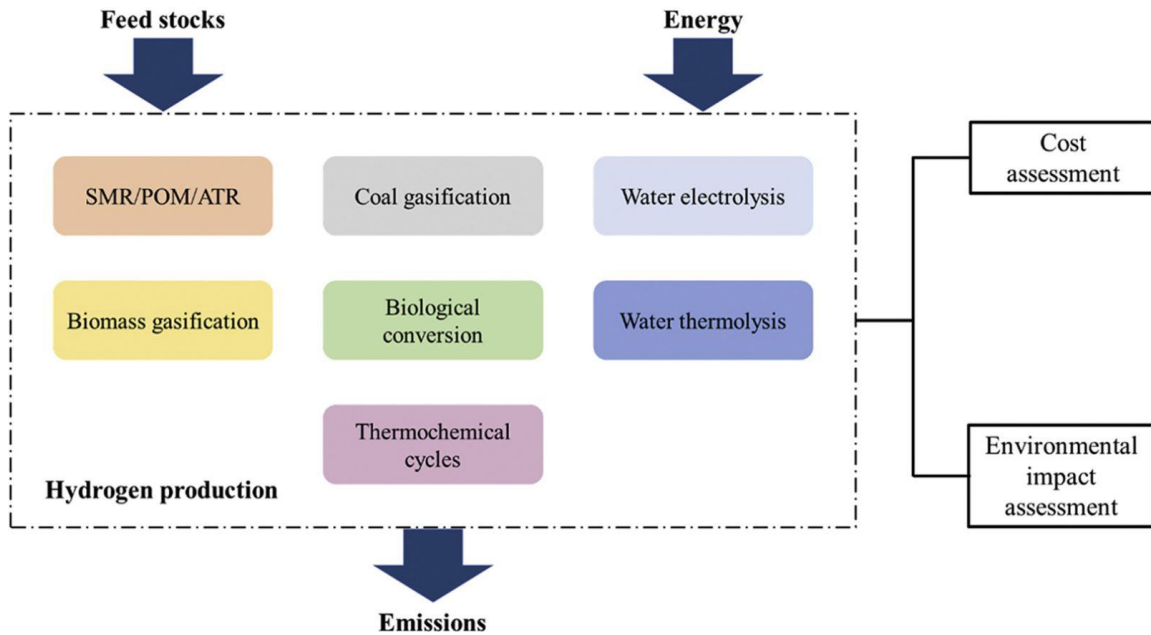
Figure 2.4: Hydrogen production methods assessment in view of cost involvement and environmental output [74]

In the global green energy landscape hydrogen status has been significantly elevated due to its small size and abundant availability. It is highly versatile energy alternative that can be incorporated into powering vehicles to generating electricity and heat. Energy storage nature of hydrogen also enables to storage of more renewable energy produced on fortunate days with high wind and sun exposure to be later used on less

fortunate days. This added versatility and green nature gives hydrogen stardom in a sustainable energy ecosystem.[75] A variety of hydrogen synthesis methods is available but a selection plays a crucial role in harnessing hydrogen for its applications like fuel cells, energy storage, and industrial processes. All the synthesis methods are assessed based on feedstock, their energy inputs, overall emissions, cost assessment, and overall environmental assessment.

2.7.2 Steam methane reforming (SMR)
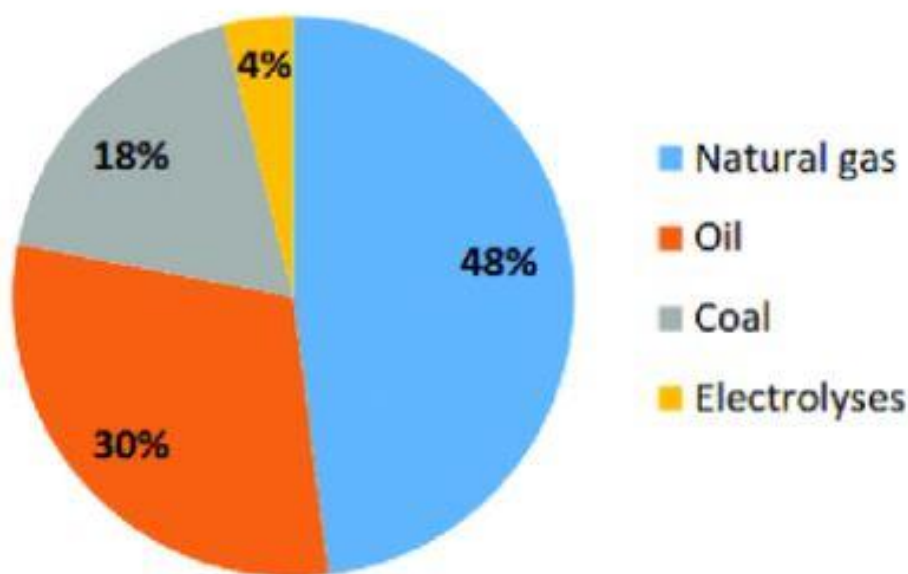
Figure 2.5: Pie chart of present H_2 production sources with maximum share of SMR fueled by natural gas[76]

Steam methane reforming (SMR) being the classical hydrogen synthesis method has been used in a variety of industries such as petrochemicals and fertilizers for over a century. It not only contributes to 98% of commercial hydrogen synthesis but also the 50% CO_2 share worldwide. The process involves reactions between methane (CH_4) and water (H_2O) producing hydrogen H_2 and carbon monoxide CO.[77] Although it is the most established and efficient hydrogen synthesis process however carbon dioxide CO_2 produced as a byproduct contributes to greenhouse gas emissions that raise serious doubts

14

about using SMR. Thus it overall makes the fuel cells powered by hydrogen from SMR a pseudo-green technology and poses a serious hurdle towards powering vehicles.[78, 79]

2.7.3   Thermochemical hydrogen production

Thermochemical hydrogen production involves high-temperature reactions using a variety of feedstocks to produce minimal greenhouse gas emissions. It requires proper reactor design depending upon the type and availability of feedstocks including water, sewerage water, biomass, industrial wastes, and fossil oils.[80] Sludge pyrolysis, biomass incineration, sulfur-iodine cycle, hybrid sulfur cycle, and partial oxidation of hydrocarbons are a few examples with potential for high production efficiency. Complex control systems, reactor designs, and expensive thermo-stable materials in addition to residual carbon emissions make it cleaner than SMR but still pose a serious challenge in the quest for green fuels.[81]

It has potential for large-scale commercial production as researchers have proposed pilot plants with two-step water splitting mechanisms. First, the temperature is increased to reduce metal oxide using concentrated sunlight to tiger water redox reaction producing hydrogen and metal oxide gain. [82]

2.7.4   Biomass gasification

Biomass gasification is similar to coal gasification technology developed in WW-2 to meet military emergency fuel needs. Basically, it converts hydrocarbons present in natural organic materials like wood, crop residues sewerage wastes, etc into a gaseous mixture containing hydrogen, carbon monoxide, carbon dioxide, and lightweight hydrocarbons.[83] The process involves heating biomass in the absence of air to produce syngas which is a mixture of CO, H_2, and other gases. However, it produces less sulfur, and ashes and releases way less carbon content in the air.[84]

This technique has its own merits and demerits as it is an overall energy-intensive process that results in a sizeable amount of energy wastage. It incorporates a variety of feedstock and results in inconsistent impurities in syngas that require an additional purification unit. On the whole, it is more of a waste disposal technique that converts

existing waste into value-added fuel rather than being a core Hydrogen source.[85] Significantly lower carbon foot print along with waste renewable nature and ease to be integration into existing waste management systems, make it a potential candidate for a cleaner secondary alternative that can be used in hybrid energy systems in the overall energy ecosystem.[86, 87]

2.7.5   Biohydrogen production

The significance of bio-hydrogen production methods can't be ignored because of their limited greenhouse emissions and low energy inputs. It employs a variety of biological reactions like aerobic and anaerobic fermentation and photo-biological reactions by exploiting a variety of microorganisms such as bacteria and algae.[88] These methods required high levels of precision and accuracy to reaction conditions as biological reactions show high specificity towards reactions. They have the added advantage to be used with existing wastewater management systems.[89] Low hydrogen yield, microbial strains, and specific nature of reaction limit its commercial potential as a major clean alternative. Although it cannot replace proper industrial hydrogen needs but can be easily integrated as a charge for fuel cells. [90]

2.7.5   Electrolysis

Before delving into hydrogen-powered fuel alternatives it is imperative to develop new technologies that are based on fundamentals of renewable energy sources like wind or solar. To make a green transition sustainable and viable, all raw materials starting from scratch should be either environmentally friendly or are existing waste materials that need some waste treatment to make them eco-friendly. On the whole water splitting technologies are developed by utilizing solar or wind power to split water into hydrogen and oxygen with essentially no carbon emissions. It overall eliminates carbon emissions that are considered a hallmark pollutant of conventional techniques.[91]

Electrolysis is the first of the green hydrogen technologies and it also underpins a core concept to develop further cleaner technologies. Water electrolysis is a sustainable

process that requires electric current to split water into its constituents i.e. hydrogen and oxygen in a specific ratio that can be used exactly in the same ratio in a fuel cells.[92]
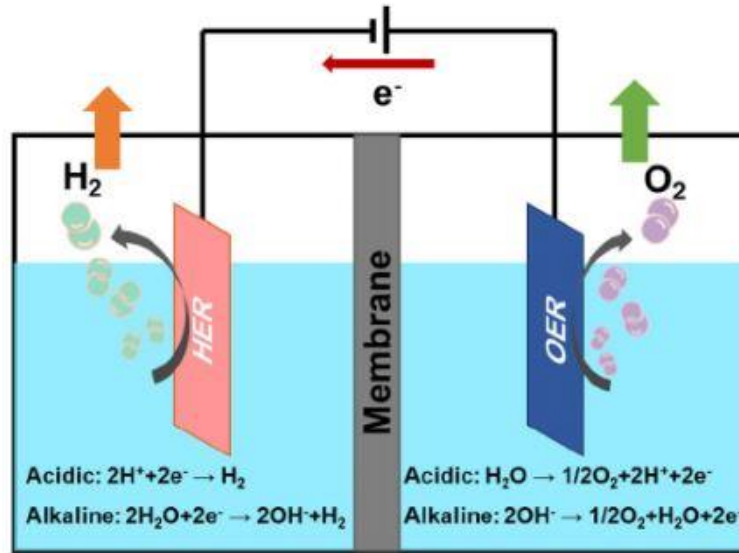
Figure 2.6: Hydrogen production methods today and years to come[93]

Broadly two different types of electrolysis are used alkaline electrolysis and proton exchange membranes (PEM). The alkaline solution is used as an electrolyte in alkaline electrolysis, and it is considered more robust but comparatively much cheaper than PEM electrolysis. On the other side, PEM electrolysis uses solid polymer as an electrolyte that results in more efficient operations and much agility towards fluctuating loads.[94, 95]

It is a more advanced technology and produces hydrogen with much higher purity but requires a renewable energy source such as wind or solar to have cleaner hydrogen in the end. It is also an essential requirement to have much pure-grade water like demineralized, deionized, or distilled water. Furthermore, high energy input and losses, use of expensive catalysts and materials especially in the case of PEM electrolysis, infrastructure for distribution and storage, and finally scaling up to meet surging global energy needs limits the widespread adoption of technology in view of its commercial potential. [96]Moreover, the role of the catalyst is the most crucial to the overall performance of water splitting reaction, it not only requires careful selection but also

17

structural and design engineering of the catalytic matrix and the catalyst itself is very crucial for optimum interfacial properties. [97]

2.8   Photo electrochemical water splitting

Solar energy is the most abundant and versatile renewable source available and the same solar energy can be used in a variety of renewable processes for the generation of hydrogen. From green heating systems to power generation or production of synthetic fuel all depends upon ingenious process design.[3]
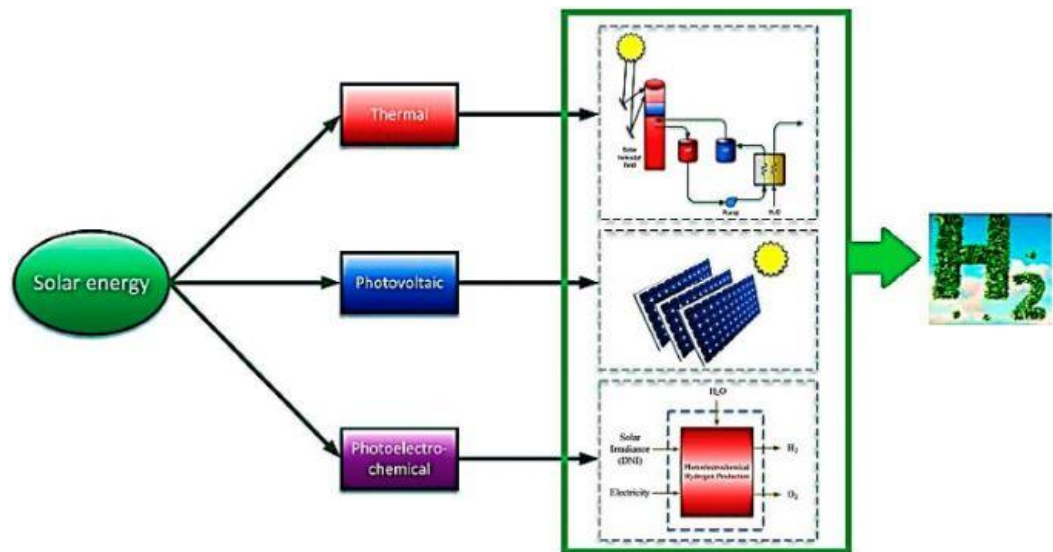
Figure 2.7: Various process powered by solar energy for hydrogen generation[3]

2.8.1   Mechanism

Photo electrochemical (PEC) water splitting is a sustainable technology to harness solar energy to produce green hydrogen. Its process is similar to electrolysis but instead of using electricity to split water, it utilizes combination of semiconductor material and solar energy. Photo irradiation of semiconductor materials generates electron-hole pairs that initiate desired water-splitting reactions.[98].

Essentially it involves photo electrodes immersed in an electrolyte solution that converts solar energy into chemical energy by splitting water into its respective derivatives i.e. hydrogen and oxygen using electron hole pairs. Early PEC cells utilize mainly titanium

18

dioxide TiO2, silicone, and zinc oxide ZnO. They offer limited efficiency as a result of poor light absorption, proper band alignments, and high charge recombination. Prompt research is required to design specialized engineering materials to spit water under sunlight while remaining environmentally friendly at the same time.[99]
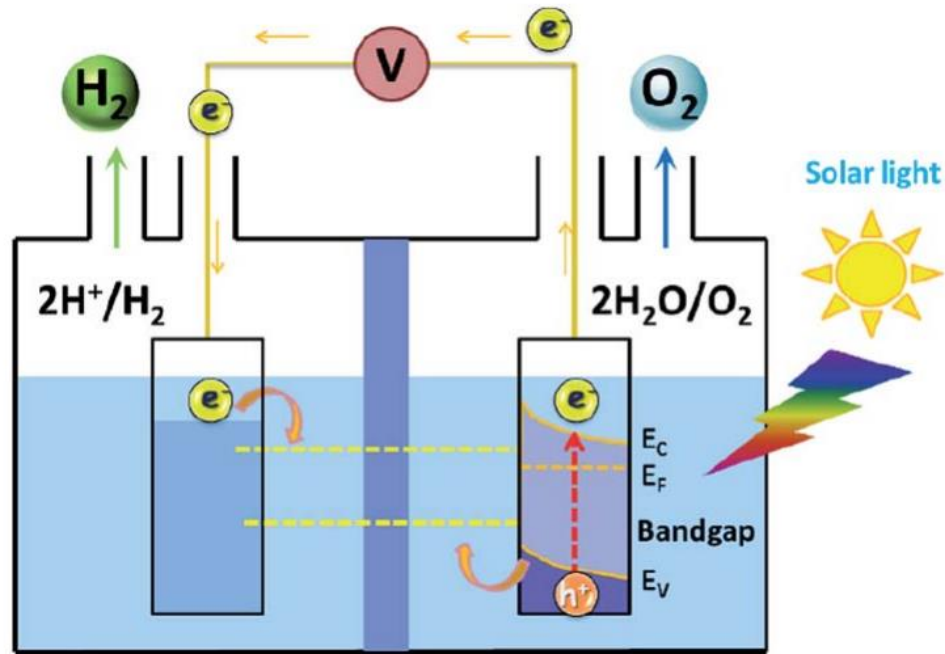
Figure 2.8: Various processes powered by solar energy for hydrogen generation[100]

2.8.2   *Materials*

The choice of photoelectrode material plays a pivotal role in the efficiency of PEC cells from the early use of simple semiconductors such as silicone to complex tandem cells today. Researchers have proposed four-step strategies to overcome silicon's inherent limitation and to harness its low band gap energy i.e. 1.1eV. Starting from surface morphology regulation to enhance light harvesting properties later followed by band engineering to reduce charge recombination issues. The addition of a protective layer reduces photo corrosion, and lastly loading photocatalyst on silicon electrode. Later researchers also followed a similar trend for other materials to enhance their photo properties. [37]

UV active semiconductors show wider band gaps with higher charge recombination rates. On the other side, visible band gap semiconductor materials show narrower band gaps with compromised quantum efficiency and poor available surface area. Metal semiconductors are broadly susceptible to photo corrosion which further limits their use.[101] Binary semiconductors like layered materials with an anisotropic nature like graphitic carbon nitride g-C_3N_4, RGO, black phosphorous, and a few chalcogenides like CdS, etc have appropriate bang gaps but their high charge recombination limits their direct application as photoelectrodes. Apart from new and more sophisticated materials more integrated and complex PEC systems are being constituted by incorporating photovoltaics PV into green hydrogen systems. [36]
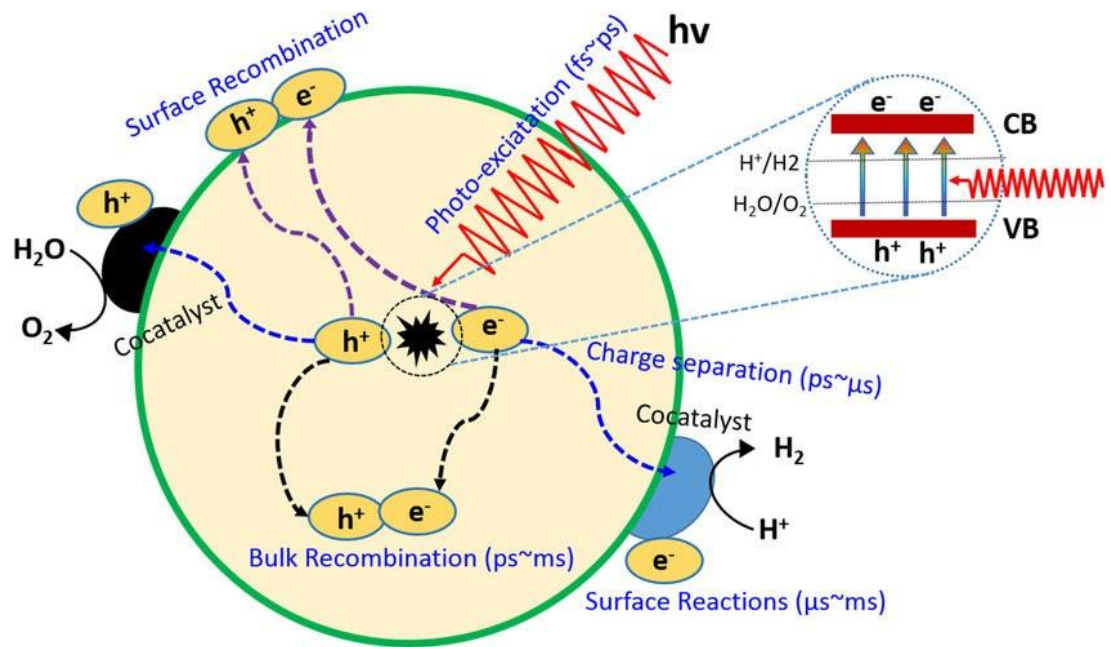
Figure 2.9: Schematics of Photo catalysis from photo excitations to charge separation and recombination followed by desired reactions[102]

Band edge and band gap of perovskite crystal structures can be engineered and custom-tailored to make them visible light active for both solar cells and PEC cells. Perovskites can be categorized based on their structure ABO_3, layered, and ABX_3 type where doping either A or B sites has a significant effect on band gaps and overall PEC cell output. A new stride in doping luminescent materials like (Ho, Er, Eu, and Nd, etc) not only narrow the band gap but also reduces the charge recombination rate.[34] Perovskite

band edges can also be managed by making their composites with binary semiconductors resulting in hetero junction systems that are capable of producing hydrogen under visible light. This area has recently gained much attention as recently researchers have been exploring more and more visible light active composites, nanostructures, and their hybrids to enhance light absorption and reduce charge recombination. On the whole, perovskite has gained a reputation as a wonder catalyst in the solar hydrogen production stage.[36]

Efficient photocatalysts are crucial for PEC water splitting systems and a variety of materials broadly in the categories of metal oxides, perovskites, organic semiconductors, and their hetero junctions have been investigated over the years. However recent studies have shown significant emphasis on perovskites especially lead-based iodides but their toxicity raises a serious objection to its application as a potent candidate for green hydrogen. Despite significant research in the field of PEC water splitting over decades it still faces several challenges that act as key milestones towards green hydrogen's future. Restricted stability of photo electrodes under tough operating conditions like corrosion and photo corrosion limits the cyclic stability of the cell and their solutions have been a core concern of recent researchers.[103]

Metals being excellent hydrogen catalysts are prone to metal oxidation under wet PEC cells whereas, n-type semiconductors are prone to photo corrosion under prolonged light irradiation. To mitigate low low-efficiency effects of photo-sensitive materials new strategies like coatings and surface passivation needs to be incorporated. Researchers have investigated a new method of metal passivation without compromising catalysis by using a triple catalytic mixture that is NiFeMo in the CNTs framework. Overall system performs well at 13.8% solar to hydrogen efficiency at 450mV over potential.[104]

2.8.3   Recent Advancements

Photo corrosion remains a compelling challenge to PEC hydrogen systems. A variety of techniques apart from just advanced engineered materials have been employed that include coating stable protective layers, surface passivation techniques, and strategically smart designed reactors that limit the contact between photo electrodes and electrolytes. Similarly, organic semiconductors and polymers such as PEC are also less

common due to their instability in water. However recent studies have investigated p-type polymers and n-type fullerene materials are passivized with Ni foils, Galn eutectic, and layered doubled hydrates as model materials. [105]

2.8.4 *Photo corrosion inhibition*

Perovskite materials being one of the key actors in the PEC stage are less prone to photo corrosion but their instability in water require certain surface treatments to mitigate their poor stability issue and improve longevity.

2.8.5 *Hybrid materials*

Nano materials like quantum dots and nanoparticles of higher order offer unique advantages in PEC schemes. Size and dimension-dependent properties make them appropriate additive materials to decorate either binary semiconductors or make unique composites with other photo-active materials. As a result, hybrid materials offer much more favorably positioned and tunable band gaps for desired applications.[36]

2.8.6 *Tandem cells*

Just like in photo voltaic concept of tandem cells can also be employed in PEC cells. Self-driven tandem cells offer solutions to eliminate external bias no matter how small the external bias is. The addition of photo voltaic PV components to the PEC system makes the overall system self-reliant.[106]

Photo electrodes made with multiple photo-sensitive materials varying in their band gaps have recently gained much attention because of their potential to improve overall cell efficiency. Depending on band gaps different materials absorb light from different regions of the overall solar spectrum and utilizing such materials increases the chances to absorb more light from different parts of the solar spectrum. [12, 107]

Tandem cells overall enhance light absorption and result in more charge generation that contributes to higher levels of hydrogen produced. The most critical parameter to evaluate PEC water splitting systems is its solar to hydrogen efficiency. Solar to hydrogen efficiency beyond 10 % is quite critical and requires careful engineering to achieve. Studies

on binary hetero-junctions report interesting findings where one junction is formed with Ti-doped hematite and the other junction is formed with Nb-doped tin oxide. Overall one junction responds to PV and the other to PEC in turn making the system self-reliant with no external bias.[36]
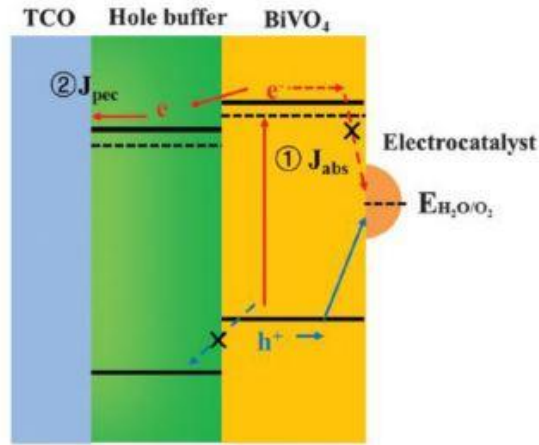
Figure 2.10: Schematics for heterojunction with $BiVO_4$ catalyst and WO_3 co-catalyst[107]

2.8.7   Integrated systems

Potential for further improvement lies solely in the integration of advanced materials and prompts engineering solutions. The single technique seems to lack in providing a solution for such an intricate technology and its commercialization is still far from happening due to the complex nature of the process, scalability, and cost effectiveness. This PV-assisted PEC technology has the potential for making self-powered smart devices on the principle of artificial photosynthesis and a variety of already tried and tested PV materials can be incorporated here as well. Researchers have explored the potential of classic GaAs as PV solar cells in double junction PV-PEC systems with InGaP as InGaP/GaAs with reported solar to hydrogen efficiency of 9%. [108] however recent advancement is a breakthrough in this field where 20.8% efficiency was reported in July 2023 and is the most efficient photoelectrochemical system reported so far. This type of PV-PEC system uses integrated halide perovskite-based tandem cell that is a smart use of cheaper catalysts for expensive green technology. [105]
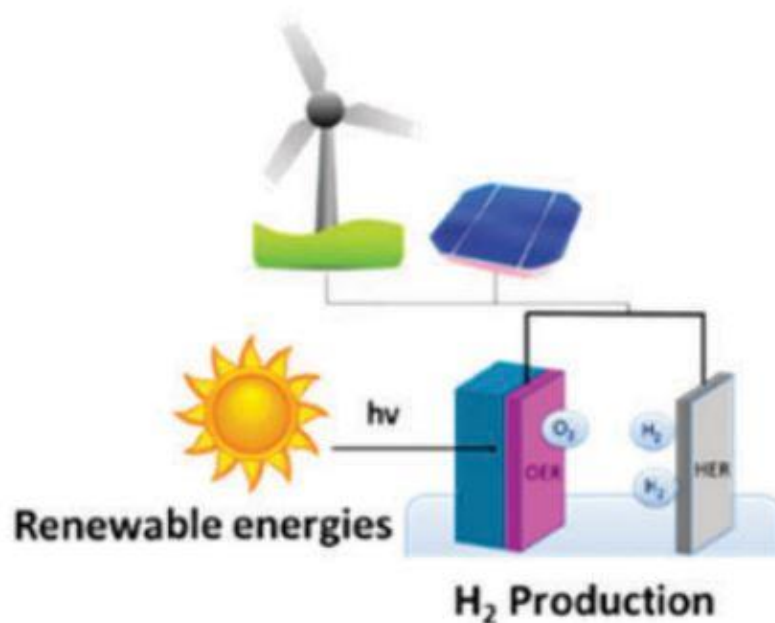
Figure 2.11: Schematics for H_2 economy unit capable to work on both internal bais (PEC system) and external bais (electrochemical system) by harnessing both solar and wind energy[109]

Sophisticated yet strategic nature of such technologies requires collaborations between academia, industry and governments to accelerate transition from lab to commercial scale. PEC has led a new stride in recent years and set the foundation of more sophisticated solar technologies in green fuel arena as artificial photosynthesis, artificial leaf, integrated solar fuel systems, photo catalysis, piezo photocatalysis, and self-powering tribo electric nano generator TENG PEC systems. The continuous dedication of researchers in PEC commercialization and the potential of its easy integration into the existing energy landscape future seem to be positive for green hydrogen.[37, 110]

2.9   Photo catalysis

2.9.1   Mechanism

Photo electro-catalytic (PECat) also called photocatalysis PC for hydrogen production is a modification of PEC production of hydrogen. Both use semiconductor materials and light irradiation to produce electron-hole pairs to carry out water-splitting

reactions. However, the mechanism, design architecture, gas synthesis, and end application of both technologies differ a lot. [111]
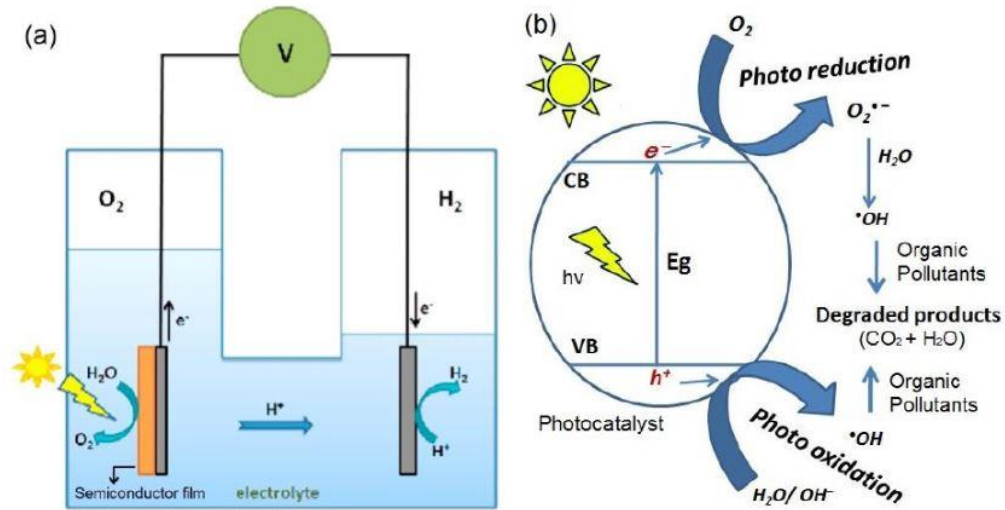
Figure 2.12: Schematics (a) Photo catalysis for water splitting and (b) photo catalysis for wastewater and organic dye degradation[112]

In PEC cell we have pair of photo electrodes generally made with some semiconducting material that are immersed in an electrolyte. Photons are absorbed by photo electrodes resulting into respective electron hole e-h+ pair that migrate to the electrode electrolyte interface. Interface becomes very important for PEC cells as reaction takes place on interface and could contribute to serious impedance issues. At the anode interface oxidation reaction takes place and oxygen is released while electrons travel through an external circuit and reach the cathode where they reduce protons to form hydrogen gas. Water oxidation results in the formation of oxygen gas, protons, and electrons where electrons travel through an external circuit while protons travel through an electrolyte and both reach the cathode where they combine to produce desired hydrogen gas. Both the gases are released at two different electrodes with high-grade purity. [101, 113]The overall reaction can be represented as

Oxidation reaction

$$H_2O + Photon \rightarrow O_2\,(g) + e^- + H^+$$

Reduction reaction

$$H^+ + e^- \rightarrow H_2 (g)$$
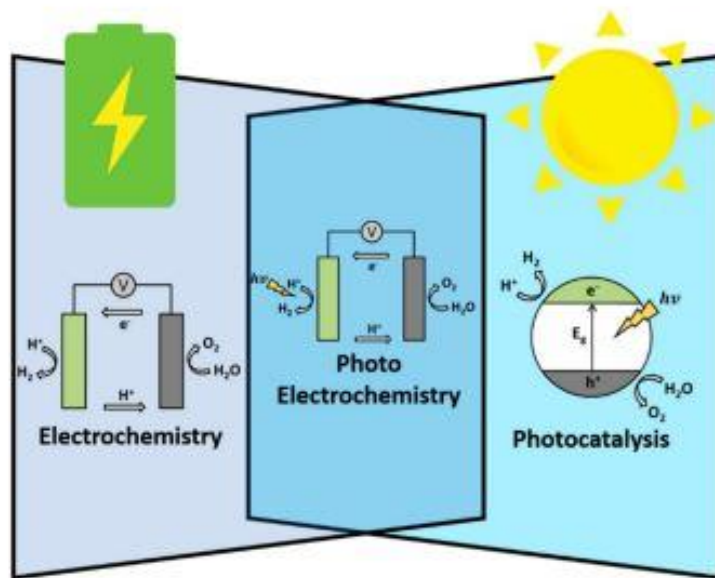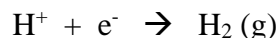
Figure 2.13: Schematics for comparison between three water splitting mechanisms Electrochemical, PEC and PECat[114]

On the other hand, photo catalysis for water, splitting uses a photo catalyst (PC) that might or might not be a semiconductor material. Traditionally photo catalysts were metal nanoparticles or p-type semiconductors of either chalcogenide or metal oxide families such as TiO2 or CdS. PC is directly added to a water reaction mixture that essentially holds few additives as sacrificial agents to facilitate a reduction reaction. [115] Similar to PEC cells when PC is exposed to light they also generate an e-h+ pair, however, e-h+ can participate in multiple redox reactions in water and other reactants present in the reaction mixture directly on the catalyst surface. It is one of the fundamental differences to the reaction mechanism as it requires no alternate pathways for e and h+ prior reduction reaction. Here catalyst surface is of great importance as it provides reaction sites for water-splitting reactions.[99]

The nature of redox reactions in PECat reaction systems is much more complex as compared to the PEC reaction scheme. A variety of reactions apart from hydrogen

evolution reaction (HER) takes place depending upon the nature and type of both catalyst and reaction mixture. Oxygen evolution reaction (OER) is not always guaranteed as other oxidation reactions might take precedence. Research has reported with perovskite halides formation of superoxide anion $O^{2\bullet-}$ different oxidation reactions result in the formation of H_2O_2 instead of O_2. [116]

Especially in the case of g-C_3N_4 embedded with some metal nanoparticles. This technique allows more complex reactions along with OER and HER especially if the reaction mixture is made from industrial wastewater or some natural organic waste. Catalysis is highly specific so the same catalyst might produce different products at different yields depending upon the nature and type of reaction mixture. [117] At the same time, instead of OER, there are high chances for hydrogen peroxide H_2O_2 to be formed and left in spent reaction mixtures with the same water samples by just changing a catalyst. Researchers have reported presence of nitrides in layered carbon sources and iodides, bromides, and chlorides in perovskites not only alter the oxidation reaction but also the overall product mixture in the end making HER more complex. [32, 118]

Band energies refer to energy levels occupied by electrons where two energy levels are of significant importance for PC materials i.e. valance band (VB) and conduction band (CB). Band gap is the difference between two levels that dictates the electrical and optical properties of PC materials and is the most crucial factor in PECat water splitting. Researchers have investigated porous $BiFeO_3$ as photoanodes for water splitting they have tried to optimize band properties through interfacial engineering [119]

Photon absorption contributing to the e^- h^+ pair takes place only when the energy of an incident photon is equal or higher than the band gap energy of PC material. Apart from just band gap structuring researchers have investigated other techniques like surface passivation and junction improvement to suppress charge recombination.

For example, $BiFeO_3$ with Ar annealing improves charge mobility and further passivation with p-type polymer polyethylenedioxytheophene PEDOT reduces its surface defects and improves p-n junction which overall suppresses charge recombination. [120]
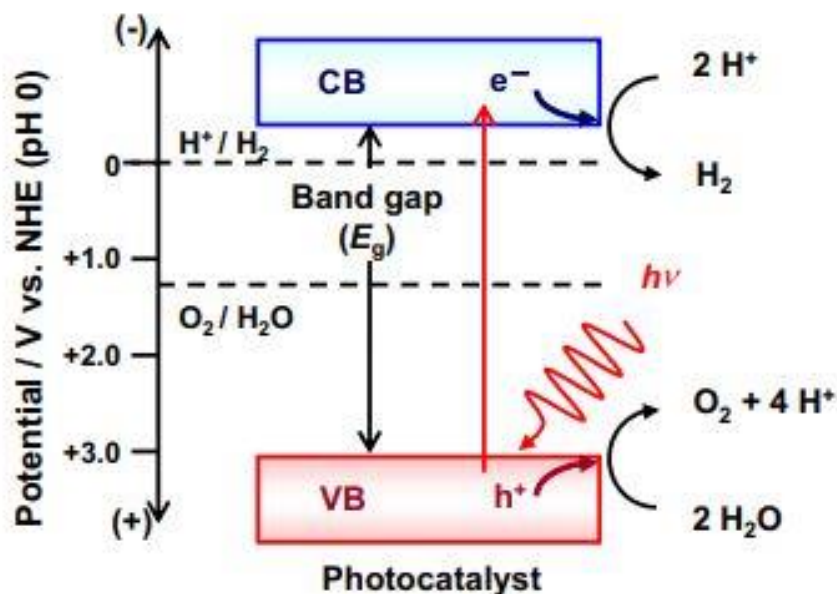
Figure 2.14: Band energy diagram for photo catalytic water splitting system[121]

The two energy levels play a crucial role in redox reactions where excited electrons present in CB participate in reduction reactions while holes left in VB can trigger oxidation reactions. Efficient PECat for water splitting requires materials with band energies that can be synchronized with the thermodynamic potential of water splitting reactions i.e. 1.23eV theoretically. Materials with band gaps higher than 1.23eV can qualify as PC materials however band gaps with CB being more negatively and VB being more positively positioned with the same band gap are preferred.[122]

Solar spectrum reaching the earth surface can be bifurcated into three main types depending upon their energy level 4 to 5% UV, 45% visible, and the remaining 49 to 50% IR. The thermodynamic potential of IR is less than 1eV and is less than the minimum potential required for water splitting and disqualifies IR active materials though they have the highest contribution to the overall solar spectrum. [14]Althoughthe thermodynamic potential of UV is between 3 to 4eV which is quite favorable and well above that of water splitting UV contribution to the overall solar spectrum is the lowest. That makes UV-active photo catalysts a poor choice for water splitting under direct sunlight exposure. Recent researchers have explored g-C_3N_4 as a potential visible light active photo catalyst through

various pretreatments, doping methods, metal depositions, surface passivation, and its composites with appropriate co-catalyst.[123]
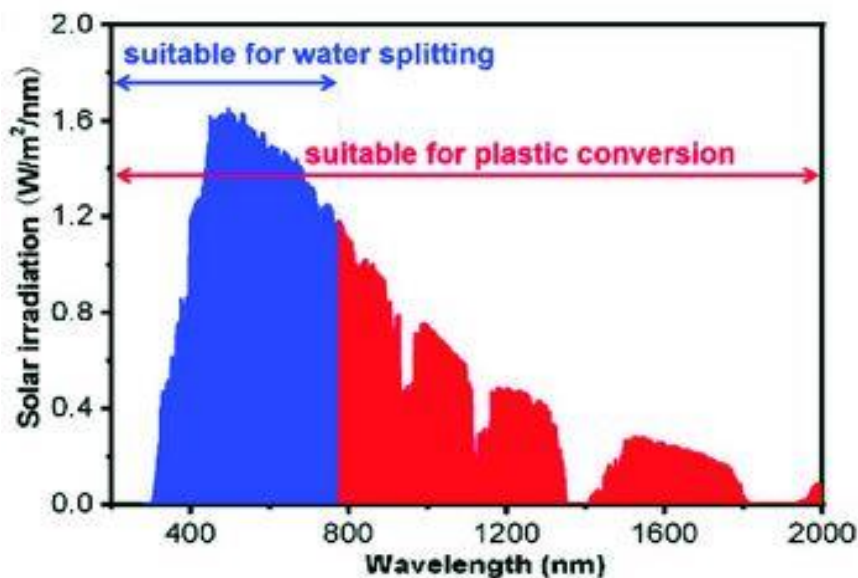
Figure 2.15: Band energy diagram for photo catalytic water splitting system [124]

However, visible light active photo catalysts hold great potential as not only their thermodynamic potential is above that of water splitting reaction but also they can make maximum use of broad range solar spectrum i.e. 45%. Furthermore, peak hours with max UV exposure on sunny days also improve efficiency by give higher yields. Generally 1.5 to 2.5eV band gap is considered to be ideal for PC materials used in sun-driven water splitting as it is in perfect alignment with visible region potential.[125] To make TiO_2 more visibly active first its composite is made with visible light active CdS then is loaded with CoO as a co-catalyst. Under visible light and 2% co-catalysts loading it results in a 7% higher yield than TiO_2 alone. [126]

2.9.2 Materials

Early researchers have extensively investigated TiO_2, ZnO, and their composite's potential as PC material however, having favorable band energy of 3.2eV that is significantly higher than the minimum requirement of 1.23eV it remained a poor choice. Although it is efficient in e^- h^+ pair generation its band energies are not properly aligned

29

with water splitting potential and results in low quantum efficiency. Researchers have investigated similar CdS with Au loading and find it much superior in water splitting in terms of hydrogen yield and quantum efficiency.[127]

Apart from water splitting TiO_2 has been proven as one of the most effective photo catalysts in wastewater dye degradation and other renewable environmental remediation processes.[128] Previous findings also suggests several methods to enhance TiO_2 performance in water splitting reactions through doping, surface modification, and band engineering to not only reduce band gap but also to improve band alignment.[129, 130]

Binary perovskites like Bismuth vanadate ($BiVO_4$) have not only been used in PEC tandem cells but also continue their stride in PECat systems due to their favorable band energies. Recent studies have shown great emphasis on speeding up slow OER reactions as they result in a steady flow of electrons for much faster HER and $BiVO_4$ proved to accelerate photocatalytic activity of water oxidation reactions. Strategies such as heterojunction formation, cocatalyst decoration on $BiVO_4$, and forming layered structures with other charge mobile materials further enhance its performance and potential in PECat systems.
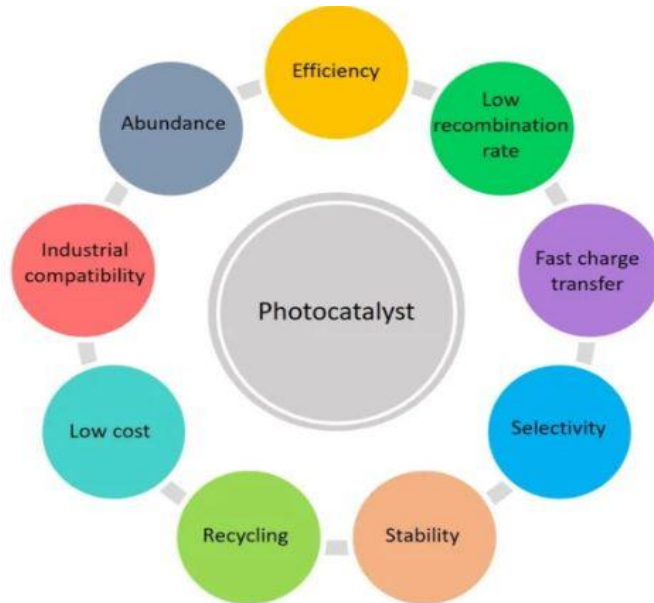
Figure 2.16: Schematics summarizes basic design requirements for high-efficiency photo catalysts [131]

Chalcogenides and metal oxides are also another category of material that offers greater potential to be used in PECat systems. Researchers have explored the potential of g-C$_3$N$_4$ as a multifunctional photo catalyst by making its composites with metal oxides like WO3 and BiVO$_4$. It makes quite a robust system that can also be deployed in PEC and PV-PEC systems.[132]

2.9.3   Tandem photocatalysis

Tandem photocatalysis is the most recent advancement in the line of PECat water splitting where the aim is to have controlled and stepwise generation of e$^-$ h$^+$ pairs while maximizing solar absorption. Different photo materials with varying band energies are combined not only to maximize utilization of the solar spectrum but also to form a heterojunction that significantly reduces charge recombination.[133]
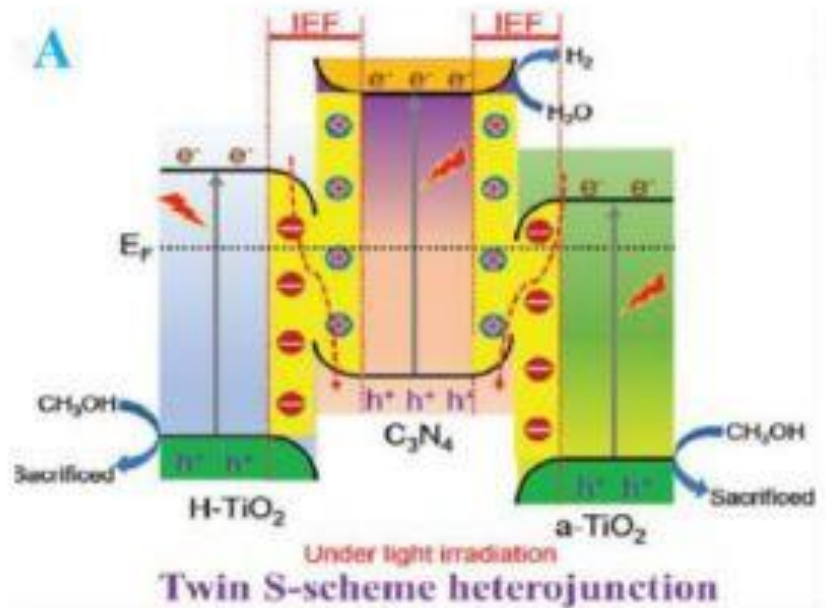
Figure 2.17: Schematics for PECat H$_2$ evolution using double s-scheme hetero junction[134]

Heterojunctions promote efficient e and h+ transfer between different materials thus they overall reduce charge recombination and improve PECat water splitting. Studies show that already tried and tested perovskite materials with appropriate bands are

combined giving entirely different yet optimized results in photo catalysis.[135] Researchers have explored a wide range of s-scheme hetero-junction photocatalysts such as TiO_2, CdS, g-C_3N_4, COF-based graphdinyne-based, ZnO, and $ZnIn_2S_4$. Their charge migration schemes in different material combinations along with their expected p-n junction are presented.[134] Metal-free 2D polymer tandems with 1.8 to 2.8eV band gaps are also the researcher's key area of interest as they offer more flexible and corrosion-resistant systems. [136]

2.9.4   MOFs

Metal organic frameworks MOFs are a more recent trend in photo materials where MOFs acts as a medium for generated e-h+ pair to flow in and out of the matrix. Researchers have investigated MnO_x as co-catalyst added in Pt based MOF matrix resulting much higher hydrogen yield and enhanced charge separation. Here Pt acts as electron site contributing HER and MnO_x as h+ carring site promoting OER.[35]

Longer polymeric chains of MOFs give more stability to metals from underwater oxidation and enhance the longevity of metal nanoparticles that are embedded in their polymeric structure. [137] Researchers have also reported conjugated polymer frameworks loaded with IrO_2 as h^+ and Palladium as- e-carrier medium for efficient water splitting. MOFs can be effectively used for loading both metal and metal oxide nanoparticles to optimize HER and OER sites. [138]
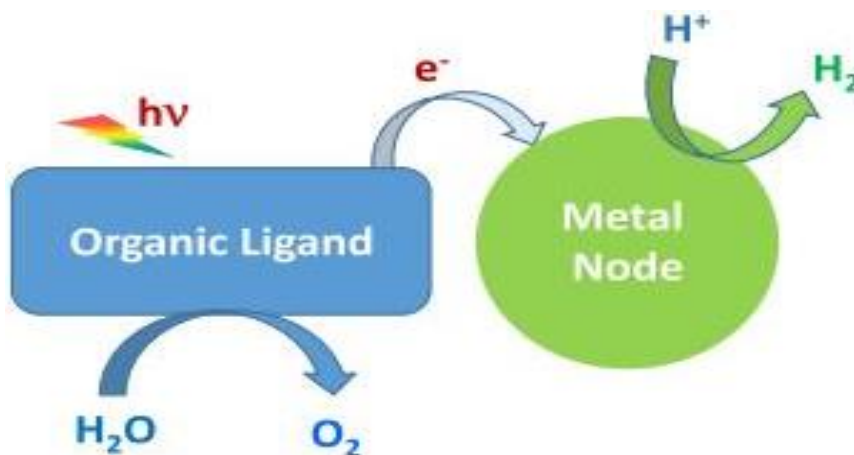
Figure 2.18: Schematics of MOF materials for photocatalytic water splitting[137]

2.10   Piezo catalysis

Piezo catalysis is a more recent development in the catalysis realm where the focus is on harnessing mechanical force or pressure to trigger chemical reactions. Mechanical energy is another abundant form of green energy available in nature as wind, tide, vibration, sonication, and atmospheric pressure. Certain materials can harness this energy into electrical energy and are termed piezo materials. [139]

2.10.1 Mechanism

This emerging branch of catalysis exploits unique properties of piezoelectric materials that generate an electric charge when subjected to mechanical stress and vice versa. Internal polarization caused by mechanical stress induces strain in the piezo catalyst thus altering its electronic configuration and facilitating charge carrier separation. [8] In piezo catalysis, piezo materials are either used as catalysts or co-catalysts to improve both the efficiency and selectivity of various chemical reactions. Strong internal current pulsations as an outcome of mechanical force induce changes in electronic structure and surface properties thereby influencing catalysis which is a completely surface-dominated phenomenon. [140, 141] Piezo current produced inside material provides altered reaction pathways that not only lowers their activation energy barrier but also improve their reaction kinetics thus ultimately leading to water electrochemical splitting. It is an innovative approach that can be fine-tuned to various renewable systems from wastewater treatment to energy storage and sustainable green fuel production. [142, 143]

Piezo catalysis can easily be incorporated into existing heterogeneous catalysis where harnessing mechanical energy yields specific chemical and electrochemical reactions. To perform water splitting reaction piezoelectric activation is required by subjecting mechanical stress to the material.

It generates electric charge at specific sites where these charges interact with water molecules adsorbed on piezo materials' surface. [144] The efficiency of piezo catalysts is crucial to the selective activation of catalytic sites on the material surface. On these sites, water molecules get physisorbed due to strong interaction between freshly produced

electric charges and water. As a result catalytic activity of adsorbed sites improves and facilitates water splitting reaction. [145] Electron-rich negative sites promote reduction reactions like dye degradation, chromium reduction, and HER while positive sites facilitate OER or other oxidation reactions like the formation of peroxides. The internal polarization as an outcome of mechanical stress generates two types of sites leading to a pair of redox reactions for water splitting. [146]

2.10.2 Materials

The most investigated piezo materials for catalysis are perovskites in the form of titanates such as lead zirconate titanate (PZT) and barium titanate $BaTiO_3$ with high piezoelectric coefficients d33. Piezoelectric coefficient is a ratio whose value indicates mechanical to electrical conversion efficiency and vice versa. The higher the d_{33} values higher the piezo effect and faster reaction kinetics will be expected. The toxic nature of PZT limits its use in environment-friendly technologies although it offers the highest d_{33} value. [147] According to established data and environmental concerns, $BaTiO_3$ offers the highest d_{33} value in lead-free piezo materials.

Researchers have reported $BaTiO_3$ with 10nm particle size under sonication alone producing 655 $\mu mol\, g^{-1}\, h^{-1}$ hydrogen. [148] Researchers have also reported organic metal-free polymeric piezo materials like polyvinylidene fluoride PVDF and PVDF-HFP as excellent materials for hydrogen production. Although the premium cost for polymeric piezo materials still opens a quest for finding efficient yet economical alternatives. [21]

To improve the efficiency of piezo catalysts classic metal catalysts are either deposited on piezo materials or embedded in their polymeric structure. Catalysts like platinum Pt, iridium Ir, and ruthenium Ru are commonly used due to their superb catalytic activity under room conditions. [8] Nanomaterials are most widely used to enhance piezo catalysis efficiency and recent research trend show the use of metal nanoparticles like Pt deposition on nano-scale piezoelectric to create highly efficient piezo catalytic systems. Researcher's most commonly used piezo material $BaTiO_3$ performance is reported to be enhanced by using Ag nanoparticles.[149] [13]

Piezo catalysis is a more advanced catalysis and offers great potential to be integrated with any other green hydrogen system such as PEC or PECat system. Such integrated systems open a way for semiconducting materials to be used in piezo catalysis.[150]

Especially in the nano range, they have an admirable ability to absorb piezo-generated charges and stimulate surface reactions crucial to water splitting. Common semiconductors used in PECat systems like ZnO, TiO_2, and WO_3 can also be used in piezo catalysis systems under nano range with or without carbon loadings.[151]

2.10.3 Integrated systems

Integration of PECat systems with piezo systems results in powerful catalysts for sustainable water-splitting systems. Perovskite oxides are versatile materials with diverse chemical compositions and tunable band gaps through doping.

Broad-range applications of these materials made them ideal choices for clean energy storage such as solar cells and supercapacitors and green fuel synthesis systems like PECat and piezo catalysis systems. [18] Materials like bismuth ferrite $BiFeO_3$, strontium titanate $SrTiO_3$, and barium titanate $BaTiO_3$ exhibit both piezoelectric and semiconducting properties that not only make them ideal choice for charge generation but also for catalyzing water splitting. [14, 15, 152]

2.10.4 2D materials

Growing research is especially inclined towards 2D materials due to their diverse and unique electrical and mechanical properties. Researchers have reported huge potential in group three Ga, In, and Se dichalcogenides and Ga holds more attention as other researchers have also explored its nitrides potential for piezo catalysis as well. [153, 154]

Commonly used 2D materials encompass transition metal dichalcogenides (TMDs) like molybdenum di sulfide MoS2 and cadmium sulfide CdS and graphene derivatives like RGO and $g-C_3N_4$. Conventional charge recombination issue is much catered by piezo-induced polarization inside material layers. [155]

2.10.5 Hybrid materials

To harness the synergistic effects of multiple materials researchers over time have developed hybrid materials. Their combinations include piezoelectric material coupled with electro catalyst, semiconductors, layered 2D sheets, dual nature materials like perovskites, and metal nanoparticles. [20]

However, along with the advantages of such systems, they can also hamper overall performance as more actors take part in reactions. Interfaces formed around a variety of materials provide alternative energy paths inside a material matrix that might reduce charge recombination but also reduce charge mobility inside material which is crucial for reaction kinetics.[22]

2.11 Piezo-photo catalysis

2.11.1 Mechanism

Piezophotocatalysis is an ingenuous technique that combines both piezo catalysis and photocatalysis in one catalytic system. Their synergic effect can produce more hydrogen by reducing charge recombination issues and enhancing charge mobility inside the catalyst due to internal polarization.

Material compromised on either side can be made efficient by the dual effect of both powerful catalytic systems.

2.11.2 Material Designed

Our piezo photocatalytic material comprises bismuth sodium titanate BNT and reduced graphene oxide RGO functionalized with cobalt oxide Co_3O_4. Investigation reveals similar but comparatively slightly superior piezo catalytic activity for water-splitting reactions.

However, under simultaneous piezo and photocatalysis hydrogen produced was significantly higher. The reaction process involved over a photocatalyst is shown in the figure below.
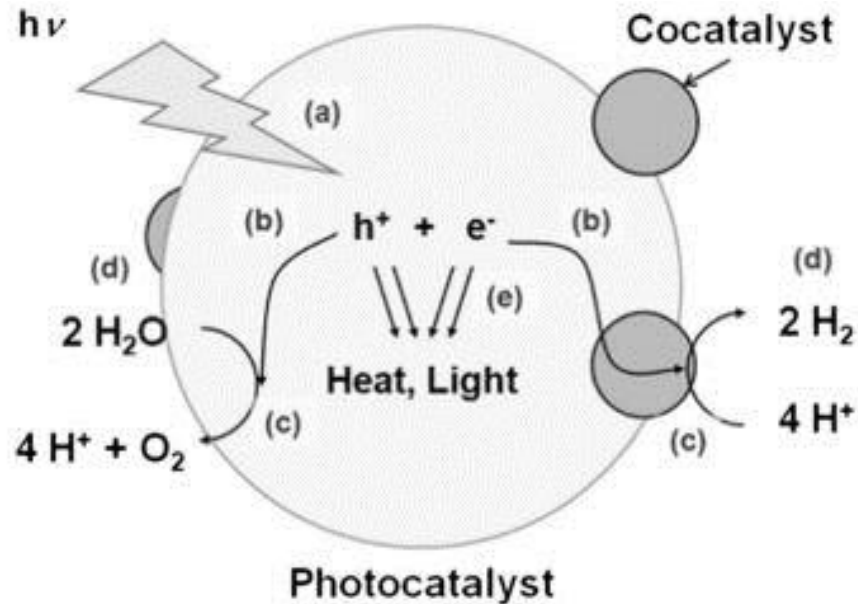
Figure 2.19: Water splitting reaction process over a catalyst. (a) light absorption, (b) charge transfer, (c)redox reactions, (d) adsorption and desorption of charged species, and (e) charge recombination[121]

The role of RGO is predominantly to improve (a) light absorption and (b) charge transfer however it can also act as a weak co-catalyst for HER. Whereas Co_3O_4 is a co-catalyst that not only provides a site for OER reaction but also provides a site for adsorption/desorption of oxidation species. In our case, large piezo matrix of BNT improves (e) charge recombination.

All parts in the reaction process must support each other to overall improve reaction kinetics. However heterogeneity of hybrid catalysts poses additional challenges due to interfaces formed and requires careful material designing to overcome barriers impeding the redox reactions [121]. The role of Co_3O_4 as co-catalyst is quite critical here as OER takes precedence and is essential for the smooth flow of negative charges to carry out desired HER.

The reaction path for water splitting can be expressed as follows.

$$BNT \leftrightharpoons BNT + h^+ + e^-$$

$$H_2O + 2h^+ \leftrightharpoons 2H^+ + 1/2O_2$$

$$2H^+ + 2e^- \leftrightharpoons H_2$$
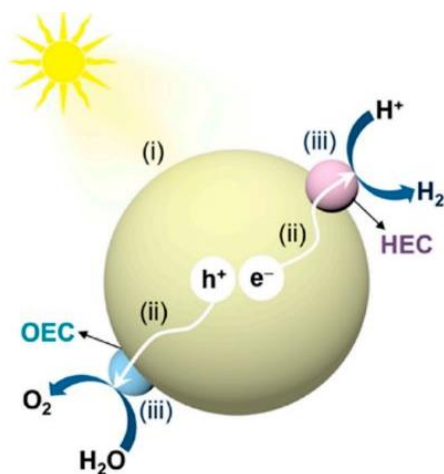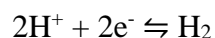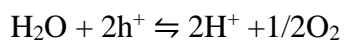
Figure 2.20: Proposed schematics for our catalyst with (i) light absorption, (ii) charge separation by heterojunction with RGO and Co_3O_4, (iii) hydrogen evolution catalyst HEC and oxygen evolution catalyst OEC active reaction sites [106]

Table 2.1: Role of Catalyst in OER

Light Absorption	Charge Separation
Adsorption and Desorption of Charged Species	Charge Transfer
Hydrogen Evolution Catalyst	Redox Reactions
Charge Recombination	Oxygen Evolution Catalyst

CHAPTER 3:   MATERIALS AND METHODS

For the synthesis of bismuth sodium titanate BNT and reduced graphene oxide decorated with cobalt oxide RGO-Co_3O_4 bottom-up approaches were used and they are discussed in detail below.

3.1   Bottom-up approach

Bottom-up approaches manufacture materials by using chemical reactions from scratch. BNT was made by bottom-up technique while graphene oxide was purchased from a vendor and reduced together with cobalt salts by one of the following

- Sol-gel [156]

- Hydrothermal/solvothermal [151]

- Co-precipitation[156]

- Micro-emulsion [157]

- Wet chemical synthesis [158]

- Chemical vapor deposition [159]

3.1.1   Sol-gel Method
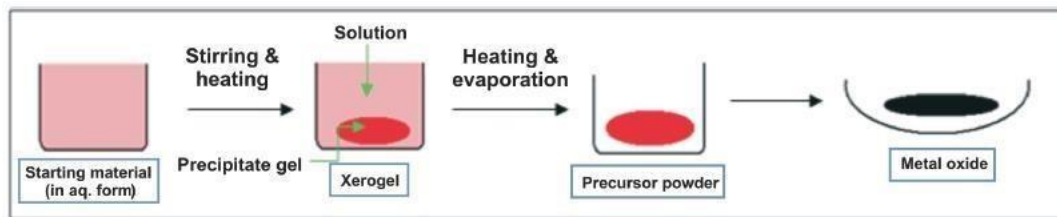
Figure 3.1: Gel schematics for metal oxide formation[156]

Hydrolysis reaction is performed by mixing reactants together that later is transformed into gel as a result of dehydration. Given thermal treatment resulted into gelation of reaction mixture.

<u>Advantages</u>

- It is an easy and affordable method

- High purity

- Good homogeneity

- Low-temperature method

<u>Drawbacks</u>

- Weak bonding

- Difficult to regulate porosity

3.1.2 *Hydrothermal/Solvo-thermal*

A hydrothermal reactor is a sealed reaction vessel heated to a temperature over its boiling point. As a result, reaction occurs under high temperature and pressure and the name hydro/solvo is given to the solvent used in the reaction. It is amongst the most common bottom-up techniques for the synthesis of small and economical nanoparticles these days. [151]

<u>Advantages</u>

- Simple method

- Changing time, temperature and concentration gives easy control over morphology

- Comparatively economical for sophisticated small 0D materials

<u>Disadvantages</u>

- Expensive autoclaves

- Safety concerns
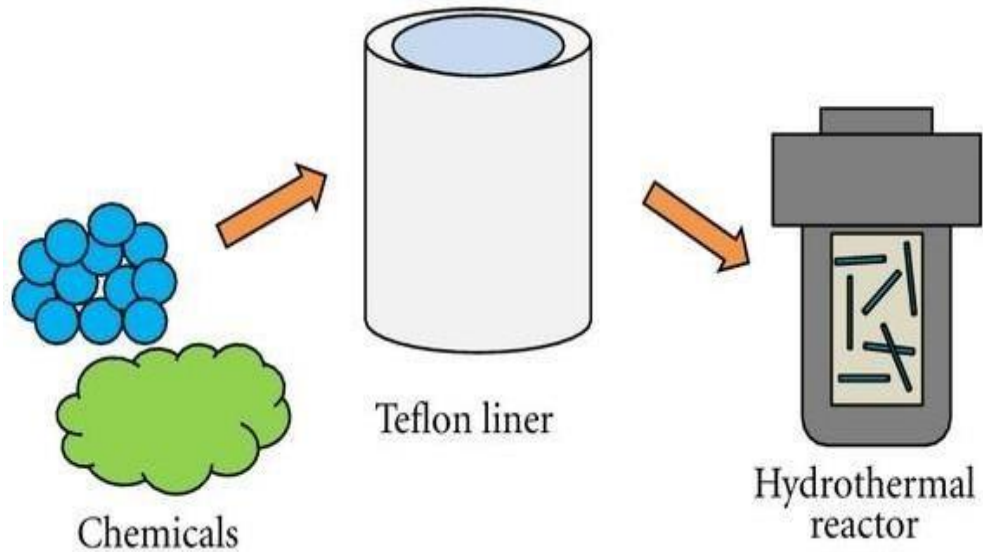
Figure 3.2: Teflon lined autoclave for hydrothermal [151]

3.1.3 Co-precipitation method

Two different reactions requiring different precursors but one reducing agent are put together in a reaction mixture. They precipitate at the same time giving a product with one decorated on another.

We have used co-precipitation method to successfully not only reduce GO to RGO but also synthesize and decorate Co_3O_4 from its salt on RGO. Surfactant and precipitation agents are added to facilitate the growth and size of nanoparticles. Separation of particles from reaction mixture, followed by washing, drying, and calcination is also part of the process.[156]

Advantages

- Cheap

- Eco-friendly

- Synthesis on a large scale

Disadvantages

41

- Size distribution could be a problem

- Careful surfactant selection is required for size control and growth
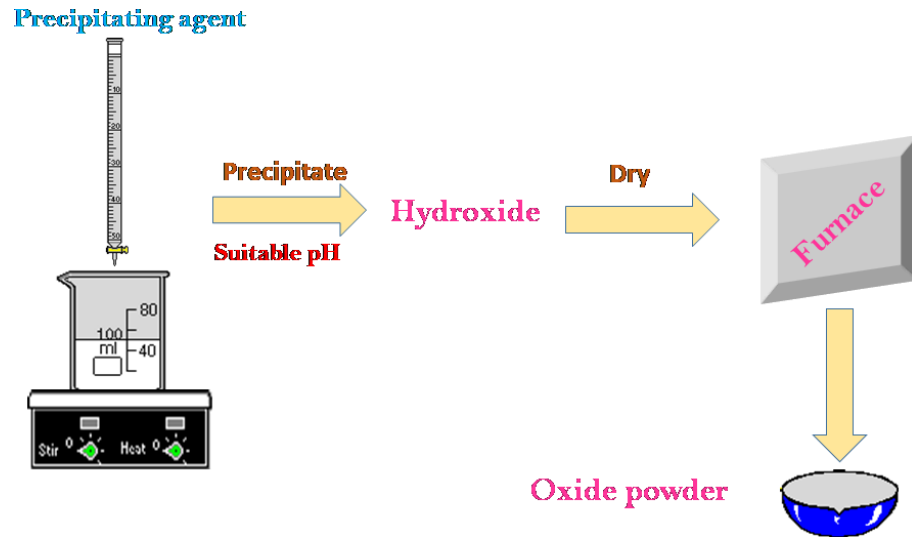
Figure 3.3: Co-precipitation schematics [156]

3.1.4 *Micro-emulsion*

It is another oxide nano particle synthesis technique where two phases are blended, and chemical reaction takes place. Metal salts and surfactants make one phase whereas water and oil make another phase. Direct and reversed micro-emulsions are utilized during which oil is dispersed in water and other water is disseminated in oil.

Advantages

- More uniform characteristics

- Size and pore distribution is good

Disadvantages

- Surfactant removal is a problem

- More precision is required
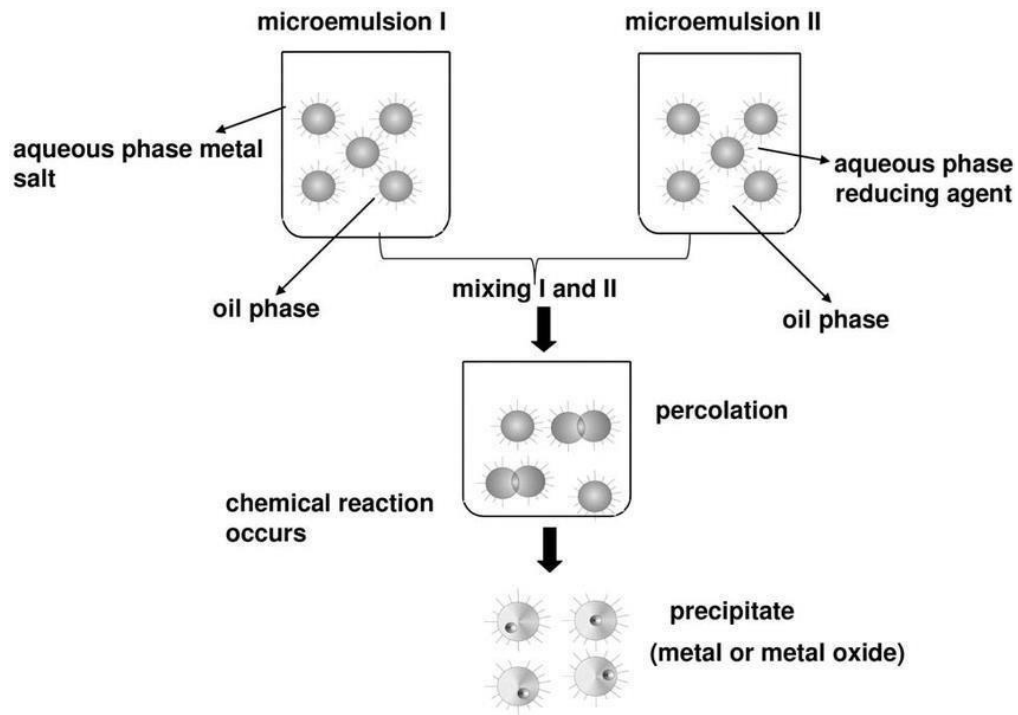
Figure 3.4: Schematics for micro-emulsion method [157]
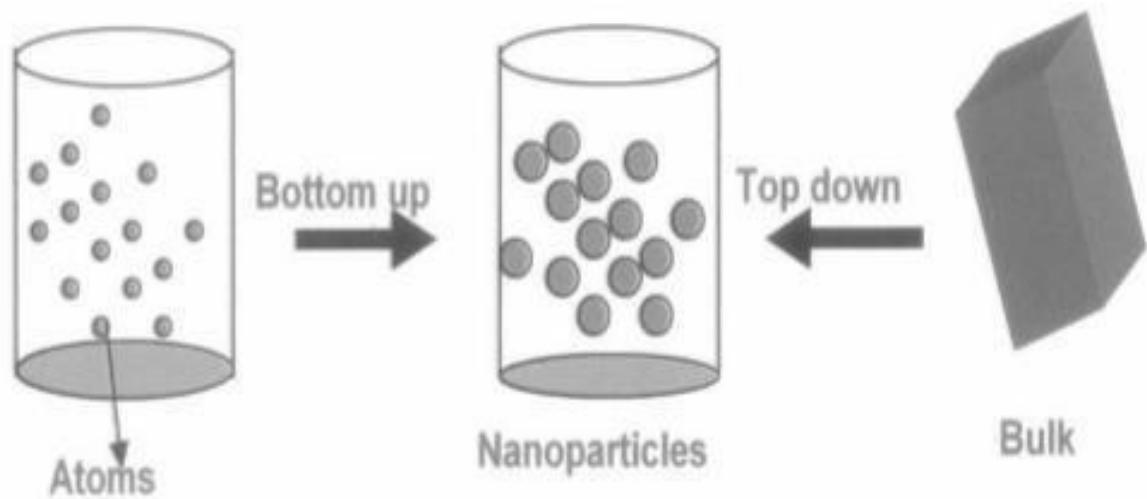
Figure 3.5: Schematics for bottom up and top down approaches for synthesis of nano particles [1]

Recently both top down and bottom-up techniques have been developed to synthesize various metal oxides and grapheme derivatives. However prime focus of top-down approaches still relies on exfoliation.[1]

3.1.5 Wet Chemical Method

Precursors required for desired materials are mixed in solution form either in ethanol or other solvents. Surfactants are used to control the size, form, and morphology of the product. Template synthesis, hydrothermal synthesis, solvothermal synthesis, self-assembly of nanomaterials, and mechanical ball milling are the most extensively utilized wet chemical synthesize types of bottom-up route. We have prepared BNT by using classical ball milling of precursors using the wet chemical synthesis method.[158]

Advantages

- This technology is successful in the synthesis variety of 2D materials including metals

- Cost vs yield is reasonable

- Gives better control over controlling shape of nanomaterials

Disadvantages

- Monolayers of precise size are difficult to achieve

- Difficult to make sophisticated materials with the desired precision

3.1.6 Chemical Vapor Deposition

CVD is an expensive but commercial scale technique where precursors are in the gas phase and reactions take place on a suitable substrate. Thermodynamic parameters are employed to alter reaction kinetics. [159]

Advantages

- Heterogeneous reactions occur when forming high-quality films

- Quick technique for film formation

- Commercial potential for bulk synthesis

Disadvantages

- Energy intensive technique

- Chemicals and particulate contamination might occur

- Cannot be used for 1D materials

- High safety concerns

3.2   Top-Down Approach

Recently top-down and bottom-up methods have been designed to fabricate graphene sheets. Top-down methods mainly focus on exfoliation for the preparation of 2D mono and multilayered sheets. 2D materials hold great importance in view of their tailored properties for desired applications. [160] They have delivered a breakthrough in flexible electronics and optoelectronic devices and revolutionized the overall electronics industry. Their strong in plane bonding and weak out-of-plane bonding offer easy isolation of bulk layers from each other that not only increases surface area but also improve the material's overall optical and electrical properties.[1, 161]

3.2.1   Mechanical Exfoliation

In this technique, material is subjected to mechanical force in the form of vibration or the classic "scotch tape approach" can be used to separate layers by breaking weak out-of-plane bonds in graphene. Temperature assistance can or cannot be used depending on the level of exfoliation required for the desired size and application requirement. [2]

Advantages

- Pristine quality sheets can be produced

Disadvantages

- Generally, yield is low

- Sheet specifications cannot be controlled

- Only be used for lab scale
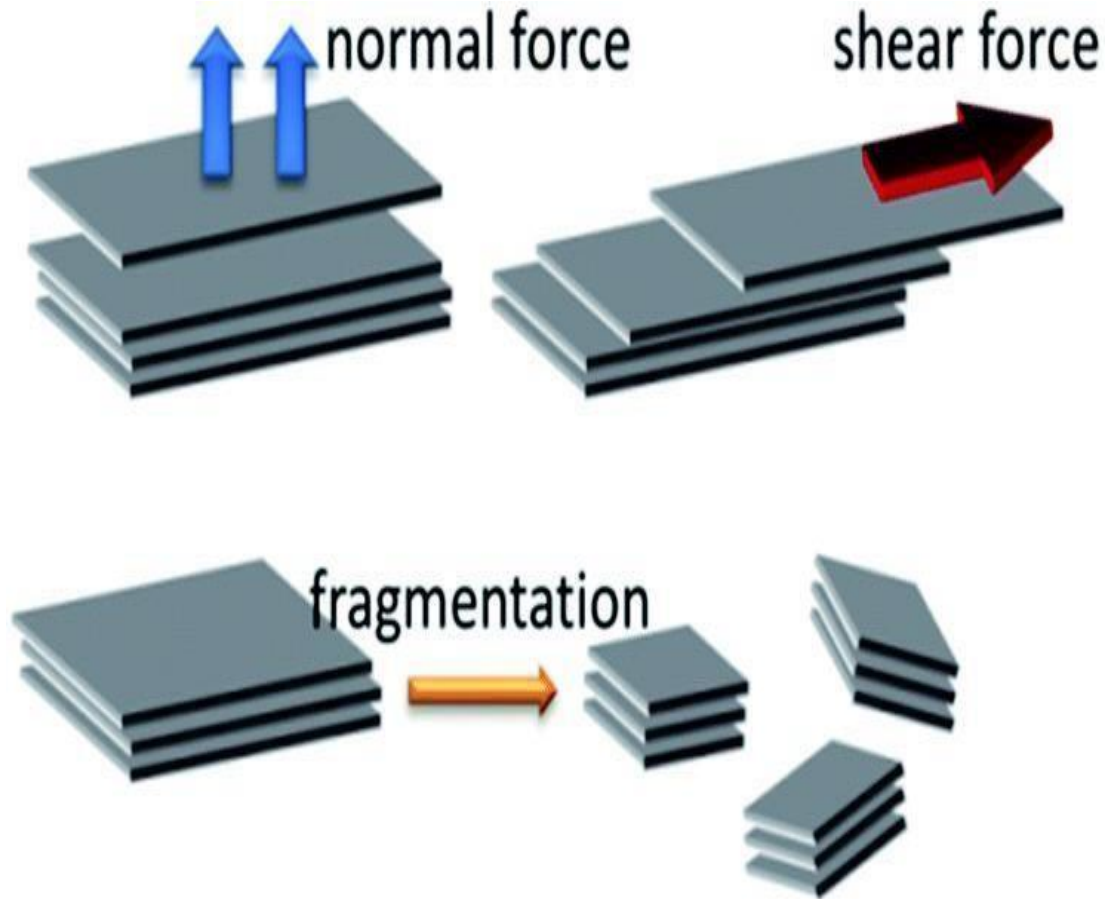
Figure 3.6: Schematics for mechanical exfoliation [2]

3.2.2 Liquid Phase Exfoliation

Solvents and different chemicals with similar surface energy are used to intercalate between layers of graphene. Once the solvent is fully intercalated in crystal lattice then applied sonication resulted into stabilized nanosheets.[160] Sound energy act a shear force to disintegrate out of plane weak bonds linking a layered material. Sonication-assisted exfoliation is widely used these days and we have also used it along with co-precipitation method to decorate our freshly made RGO sheets with Co_3O_4 nanoparticles. For an

effective size distribution and surface properties surfactant and solvent both play a pivotal role. [156]

The solvent is important as it aids in the delimination process. It should be able to maintain highly stabilized dispersion with a high concentration of 2D exfoliated sheets for extended periods. At times mixture of solvents is used n-methyl 2-pyrodine (NMP) is the most common solvent. The surface energy of NMP is 40 mJm^{-2} that is close to the surface energy of a variety of materials. It can be used for stable graphite dispersions with surface energy as high as upto 70 mJm^{-2}[12]
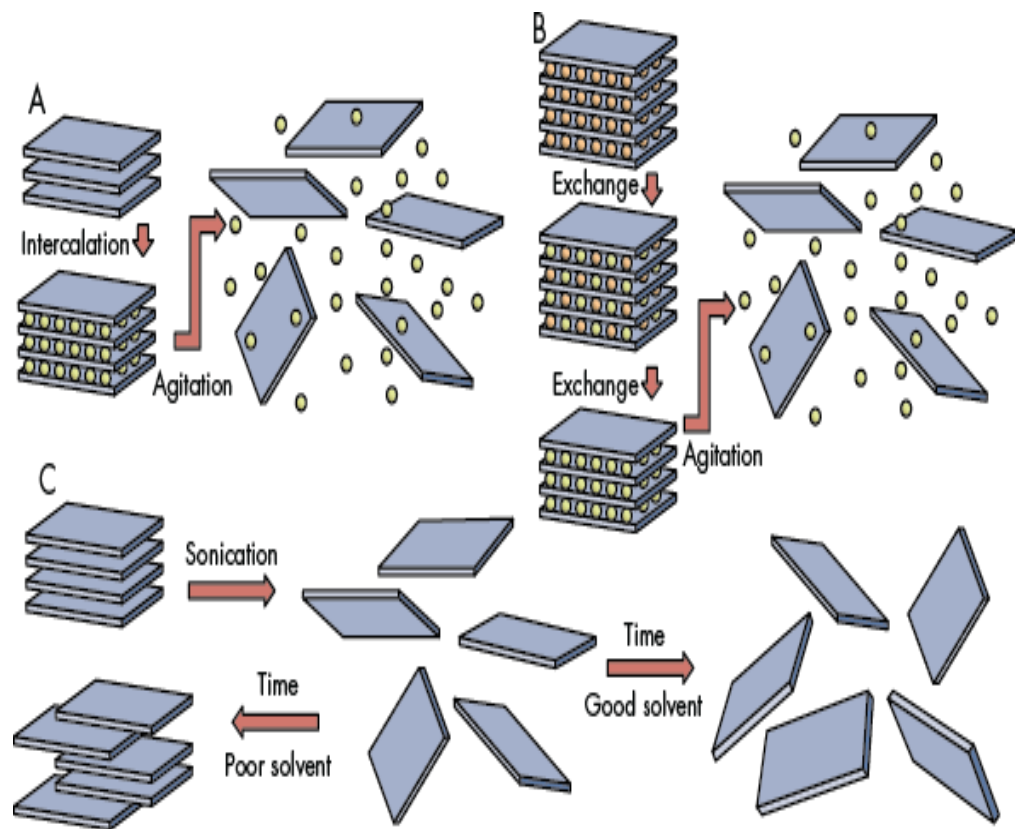
Figure 3.7: Schematics for liquid phase exfoliation [12]

Advantages

- Gives high yield

- Not sensitive to air

- Crystalline product

- Cost-effective method

- Scalability probability

Disadvantages

- Solvents might remain in the end product and affect the properties of the material

- Need rounds of washing at the end

- Faults in sheets are possible

- Range of sheet size from flakes to a few nanometers is possible

3.3   Aim and Objective

This study aims to synthesize Bismuth sodium titanate BNT to be used as a matrix material for making a composite with Reduced Graphene Oxide-cobalt oxide RGO-Co_3O_4 for water splitting through piezo-photo-catalysis. This study includes

- Synthesis of BNT through ball milling method

- Synthesis of RGO-Co_3O_4 through one one-step co-precipitation method with sonication

- Formation of composite catalyst with BNT as matrix and as RGO-Co_3O_4 reinforcement through ball milling method

- Characterization of matrix, reinforcement, and composite materials

- Reaction setup and successful gas collection

- Testing of collected gas using gas chromatography

3.4   Choice of Materials

Piezoelectricity and photoexcitation response of lead-free BNT makes it an excellent candidate for piezo-photo-catalysis. BNT is more balanced in its piezo and photo behaviors as compared to other perovskite oxides that are more piezo-active. [28, 141] Besides perovskite oxides new trends for halides and metal sulfides offer great results but are more toxic and reactive to wet conditions. Furthermore, we were in search of metal-free, non-toxic, environment-friendly, less temperature-intensive method and material for water splitting and BNT fits all criteria with moderate piezo and photo properties[140, 162].

Though its piezoelectric coefficient is poor as compared to other piezo materials however it offers better conductivity than many others and is considered a fundamental element for the performance of certain catalytic reactions. [34]

RGO is a conducting material as well as its optical properties support photo-catalytic processes. Carbon materials such as CNTs, graphene, activated carbon, RGO, and mexenes have been investigated by researchers to improve the photo-catalytic behavior of their catalysts. We have used RGO as a promoter to improve charge mobility inside a material during photon excitations.[8]

Metal oxides have long been tried and tested for catalyzing slow oxygen evolution reaction OER and metals for hydrogen evolution reaction HER.

As we decided not to use metals, we intended to use oxides as co-catalysts to boost OER. Cobalt oxides not only offer a better band gap for photo reaction but also exhibit stable underwater characteristics for prolonged cycles of operation. [163, 164]

3.5   Selected Synthesis Method

For the synthesis of BNT classic ball milling as cost cost-effective and environment-friendly method was used

For reinforcement, we have used single step co-precipitation method to oxidize cobalt chloride and reduce graphene oxide

For composite preparation again ball milling was used to keep the process simple and less temperature-invasive

3.6 Materials Required

- Bismuth oxide Bi_2O_3

- Sodium carbonate Na_2CO_3

- Titanium dioxide TiO_2

- Ethanol

- Distilled water

- Cobalt chloride

- Acetic acid

- Hydrazine anhydrate

- Graphene oxide

- Triethnol amine

- PTFE membrane filter paper 0.45 µm

- Philips bulb (add specs)

- Zirconia balls 12mm

- Apparatus Used

- Media bottles

- Weighing balance

- Ball milling

- Drying oven/vacuum oven/furnace

- Beakers

- Magnetic stirrer

- Hot plate

- Petri dish/ceramic boats/crucibles

- Centrifuge

3.7 Synthesis of Bismuth Sodium Titanate BNT

First 13g of Bi_2O_3, 2.9g of Na_2CO_3, and 8.9g of TiO_2 were weighed and added to a media bottle then filled with 100ml ethanol and 12mm zirconia balls. These raw powders were ball milled for 24hrs followed by 22hrs drying at 70^0C and calcination for 4hrs at 800 ^0C.

The final material obtained was again ball milled with ethanol and BNT followed by drying but this time calcined at much lower temperature and time i.e. 400^0C and 1hrs respectively.
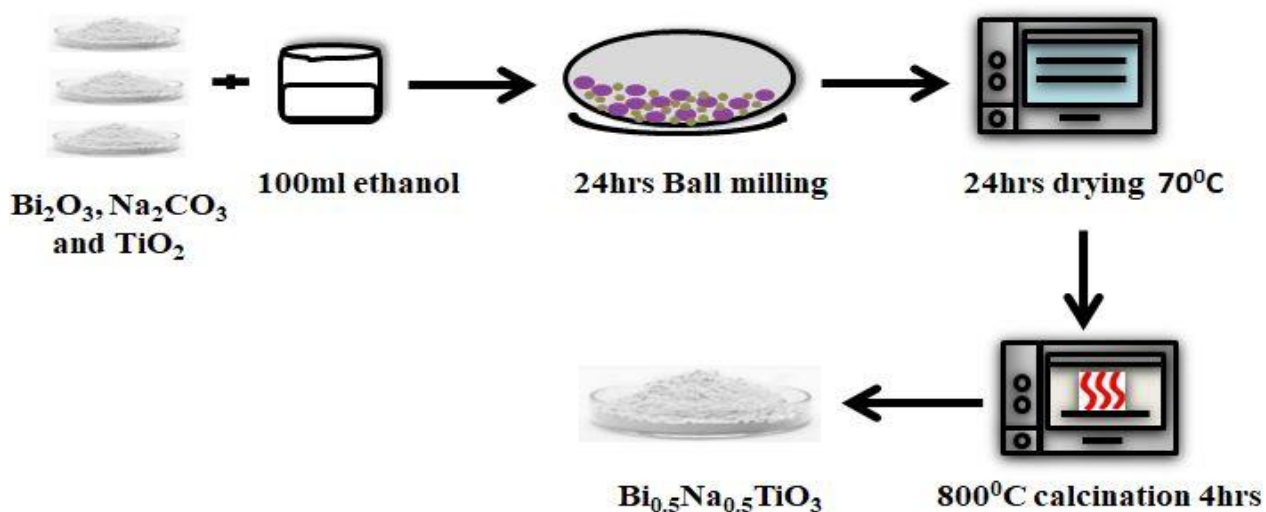
Figure 3.8: Schematics for BNT synthesis

3.8 Synthesis of Reduced Graphene Oxide-cobalt oxide RGO-Co₃O₄

A step process was used to functionalize RGO starting from GO purchased from Sigma Aldrich. 50 of 5mM solution of cobalt chloride and 200mg graphene oxide were prepared and sonicated for 30min. separately 50ml of 4mM solution of citric acid was prepared as capping agent and then added to previous solution.

The mixture was stirred for an hour then drop-wise 1mM hydrazine hydrate was added for simultaneous reduction of Co^{+2} ions and GO. Further one-hour stirring allows better anchoring of cobalt hydroxide on RGO surface $Co(OH)_2$-RGO. The product was filtered using both PTFE membrane and centrifuge at 1200rpms however both gave similar results though filtration was slower due to pore clogging from smaller nano particles.

This process gives a composite material that can be used as is by simply calcining at 400^0C for 1hrs or can be integrated with another process.

The product obtained here is a metal hydroxide gel dispersed on a carbon base where later heat treatment can convert it into respective oxide and metal depending upon the nature of treatment applied and application under consideration.
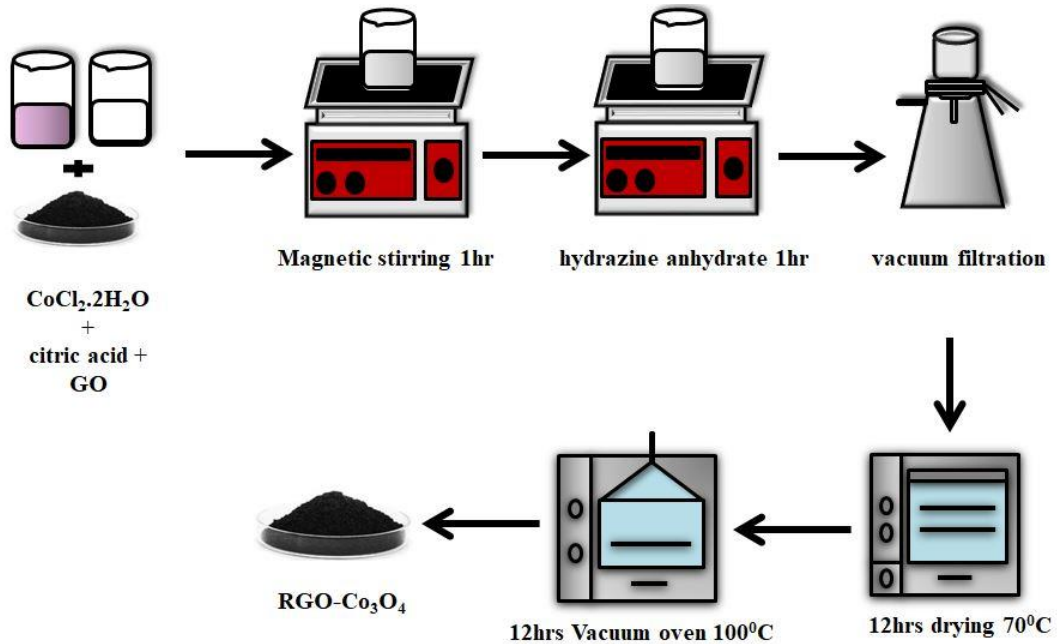
Figure 3.9: Schematics for RGO-Co₃O₄ synthesis

3.9   Synthesis of catalyst

The final materials obtained in the first two processes were ball milled again with ethanol followed by drying. This time it is calcined at a much lower temperature and time i.e. 400 ^{0}C and 1hrs as high temperature may result in loss of RGO active reduced sites.
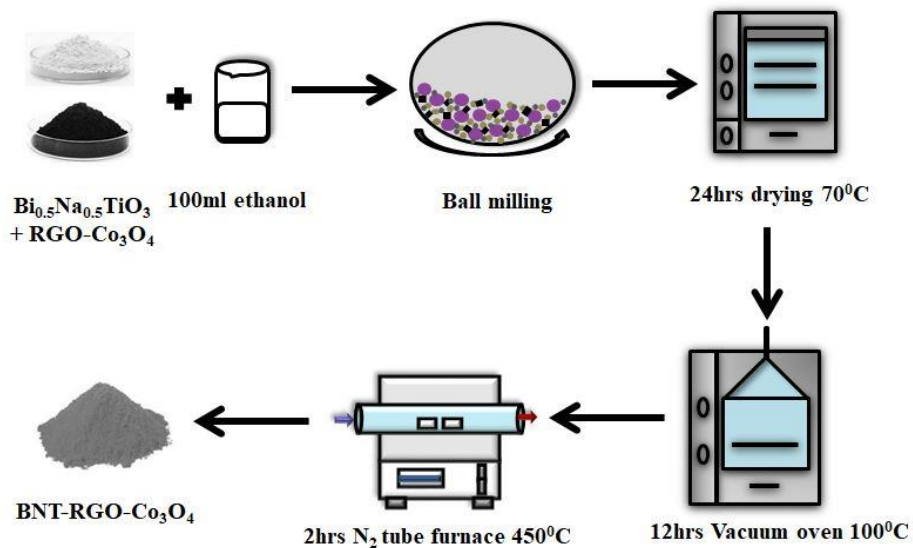
Figure 3.10: Schematics for BNT-RGO-Co$_3$O$_4$ catalyst

CHAPTER 4: CHARACTERIZATION

4.1   Scanning Electron Microscope SEM

This method involves directing a narrow electron beam onto the surface of a specimen. This process causes the ejection of photons or electrons from the material's surface. These emitted electrons are then directed towards a detector. The signal from the detector is used to adjust the brightness of a cathode ray tube CRT. For every location where the beams make contact, a corresponding point is marked on the CRT screen, ultimately creating an image of the material.[165]

The interaction between electrons and the surface of a material leads to the emission of different particles including secondary electrons SE, backscattered electrons BSE and X-rays. In SEM one common mode of detection focuses on secondary electrons which are produced very close to the sample's surface. This approach results in clear and well-defined images of the sample and is capable of revealing minute details even smaller than 1 nanometer in size.

Additionally, incident electrons can undergo elastic scattering and produce backscattering electrons that originate from deeper regions within the sample. However, these electrons have a lower resolution compared to secondary electrons. When an electron from an inner shell is knocked out of its orbit it emits characteristic X-rays.[5]

SEM is a preferred method due to its straightforward sample preparation process allowing us to examine the morphology, chemical composition, crystal structure, and plane orientations of our samples. It offers a wide range of magnification options, spanning from 10 to an impressive 500,000 times.[119]

We studied the materials' physical structure using the JEOL-JSM-6490LA for morphology analysis while we employed the MIRA3 TESCAN for detailed field-emission scanning electron microscopy (FESEM) analysis. Additionally, we determined the elemental composition by utilizing an Energy Dispersive X-ray Spectroscopy (EDS) detector attached to the FESEM.

4.2   X-ray diffraction (XRD)

This method is employed to determine the crystal structure of a material. It's a non-invasive technique that reveals the distinctive patterns of Bragg's reflections in crystalline substances. The setup typically consists of three primary components: a cathode tube, a sample holder, and a detector. X-rays are generated by heating a filament element, which directs electrons toward a target material, resulting in electron collisions. In a crystal, layers and planes are present. When X-rays with wavelengths matching the spacing of these planes strike the crystal at an angle of incidence equal to the angle of reflection, they are reflected. [166, 167] This process enables the identification of a material's crystal structure. "Diffraction" takes place, and it can be described as by Bragg's Law:

$$2d\sin\theta = n\lambda \quad (4)$$
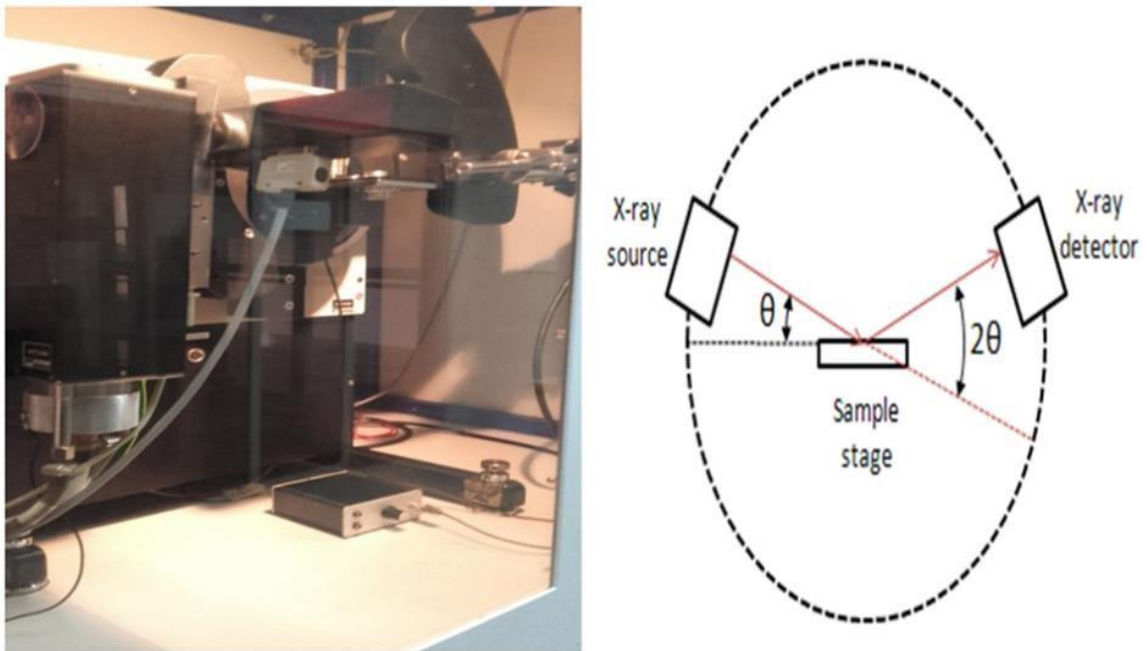
Figure 4.1: X-ray diffractions were performed by STOE diffractometer, showing XRD present at NUST and its schematics

When Bragg's law is met, it indicates that there is constructive interference, and the detector registers what are known as "Bragg's reflections." These reflection positions provide valuable information about the spacing between crystal layers. X-ray diffraction

not only informs us about the arrangement of these layers but also conveys details about the material's phase, crystallinity, and overall purity. This technique is versatile and can even help in identifying lattice mismatches, and dislocations within the crystal structure, and determining the dimensions of the unit cell. [168]

4.3   UV-Vis Spectrophotometer

A typical UV-vis spectrophotometer creates a graph that shows how much a sample absorbs light at different wavelengths. The instrument uses a light source often a tungsten halogen lamp for general visible and UV measurements however deuterium lamp is common for 300 nm and below. This broad spectrum of light is then refined into a single wavelength by a mono-chromatographer before its interaction with the sample.

The sample is usually placed in a 1 cm cuvette. These days chromatographic techniques are being combined with UV spectroscopy for a better understanding of photo reactions where the absorption of light plays an important role. [6]

The photodetector measures the amount of light that passes through the sample (transmitted light intensity). Absorbance is determined by comparing the incoming light (I_{in}) to the outgoing light (I_{out}) using the formula

$$A = \log I_{in}/I_{out}$$

To get accurate results the instrument needs to be calibrated to eliminate any background absorbance caused by factors like the cuvette or buffer. One of the primary uses of this method is to determine the concentration of molecules in a solution as the concentration is directly related to the absorbance.[169]

Bandgap is crucial for opto-electrical properties and can be determined by this technique because it measures materials absorbed light. Bandgaps manifest as light absorption points, so the points from where material transits between transparency to absorption is its band gap. Mathematically we can calculate by formula

$$E_g = 1240/\lambda$$

Where values of λ against absorbance come from UV-Vis spectrophotometer. This technique gives valuable insight into materials' optical and electrical properties along with details about concentration as well.[170]

4.4   Fourier Transform Infrared Spectrophotometer FTIR

FTIR is a powerful analytical tool predominantly used in chemistry and material studies to identify and study chemical compounds through understanding their structure. Its working principle is based on the interaction of molecules with infrared radiation IR. FTIR setup sends an IR beam across the sample and molecules present in the sample absorb light of specific frequencies causing them to vibrate. These resulting vibrations are unique to each compound just like a figure print or a signature.[171]

The transmitted IR beam is detected and processed through the Fourier transform to create an IR spectrum that displays absorbance peaks matching specific functional groups present in the sample. Different functional groups are active in specific FTIR regions for instance OH groups are active in $3000cm^{-1}$ range and 1200cm-1 to 1600cm-1 but the logic is entirely different where one corresponds to hydrogen bonding and other respond to left over OH groups through ethanol processing. Similarly same 3000cm-1 active region also show aromatics active region thus our same and expected materials both confirm the exact type of bond and structure present present in the sample.[156, 172]

It is a nondestructive technique with high precision used for getting valuable insights into molecular structure of materials and can be applicable to variety of fields such as forensics, chemistry, material sciences, pathology, environmental sciences and biological samples. [172]

4.1   Gas Chromatography GC

Gas chromatography was discovered by Russian-Italian botanist, Mikhail Semyonovich Tsvet, in the early 1900s. The separation technique is used to first split the chemical components of a mixture, then determine the presence or absence of each component as well as to measure the level of each detected component. Different types of

GC depending upon the nature of sample and expected gas are available in the form of GC, GC-MS, LC-MS, CE-MSLC-NMR and CE-NMR etc [173]
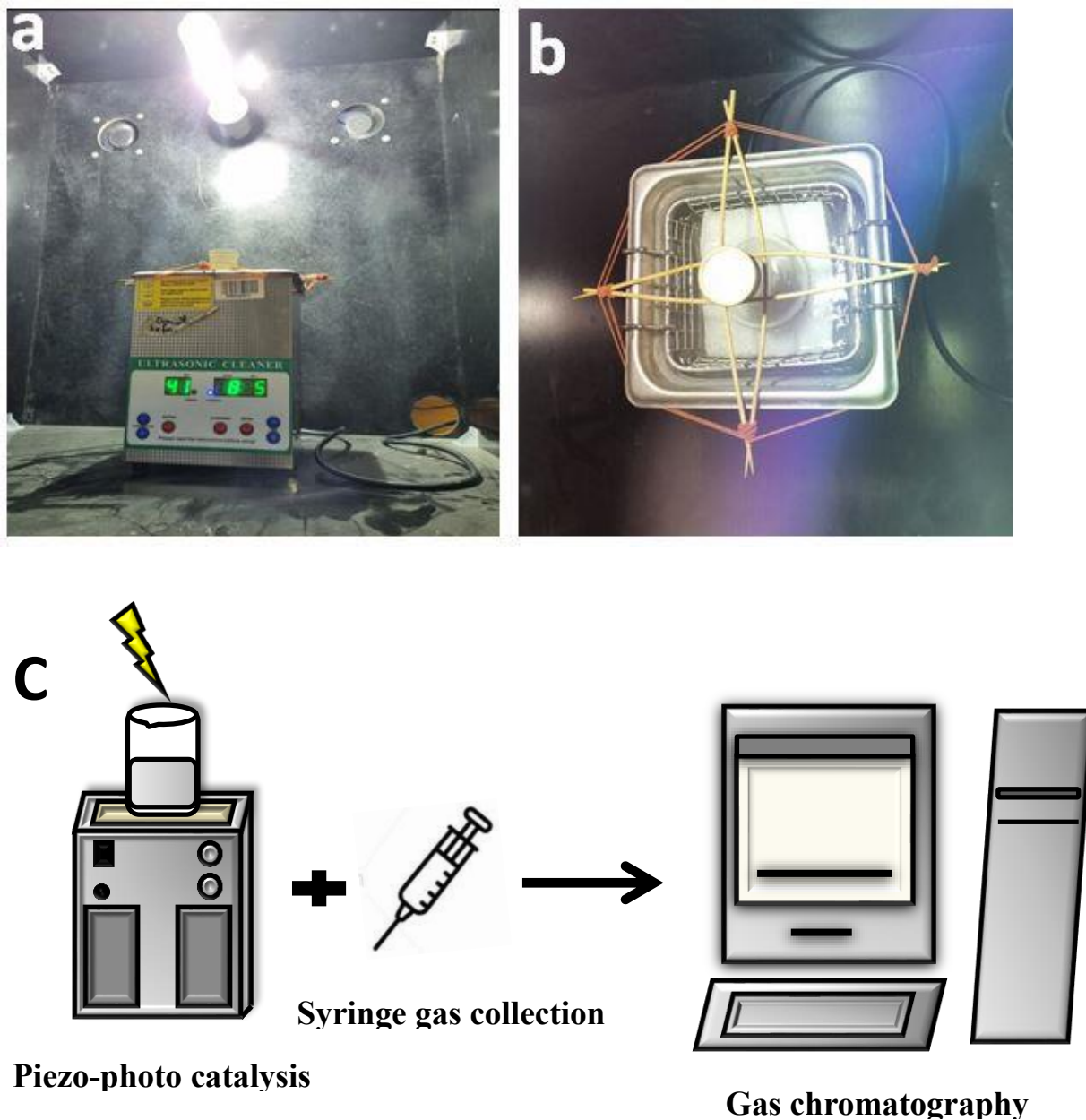
Figure 4.2: a) Experimental setup for reaction and gas collection and b) Skewer arrangement to keep reaction flask upright and c) schematics for gas collection system

Gas chromatography is a common analytical technique used to separate and analyze volatile compounds present in gaseous mixtures. GC works on the principle of differential

partitioning where chromatographic column is filled with stationary gas and sample is injected into the column. As the compound moves through the column they partition between the stationary phase and the carrier gas typically helium. This partition or separation is on the basis of compounds affinity for the stationary phase. The detector records the compound concentrations in terms of percentages forming chromatogram. GC is widely used in chemistry, environmental studies, forensics, qualitative and quantitative analysis of chemical reaction kinetics.[174] we have used gas chromatograph (GC-2010 Pro, Shimadzu. Kyoto, Japan) equipped with a thermal conductivity detector column (30m 0.32mm ID,30 microm; RT-MS5A), and nitrogen as a carrier gas. The extent of hydrogen produced as a consequence of water splitting reaction was investigated.

We have designed our own gas collection system with photo chamber using Philips 635nm bulb and two blowers to remove heat from the system. Sonicator is placed inside chamber and 100ml flask was placed inside with skewers system to keep reaction flask in place. The round bottom reaction flask was covered with rubber septum in order to seal the entire reaction system. 10ml syringe was used to collect gas sample to be injected in GC for chromatography.

We have GC and reading is given in percentage. The sample is extracted in fixed volume and then moles are calculated from standard molar volumes formula

$$n = V/V_m$$

Where V stands for volume of gas collected and V_m for the molar volume i.e. $22.4dm^3$ at STP.

CHAPTER 5:   RESULTS AND DISCUSSION

5.1   XRD

The crystal structure of synthesized bismuth sodium titanate BNT,bismuth sodium titanate with cobalt oxide decorated on reduced graphene oxide BNT-RGO-Co_3O_4, 5%, 10%, and 15% RGO-Co_3O_4 composite catalyst was characterized by an X-ray diffractometer with Cu/Kα radiation. The performed diffractograms spread over the 2θ values from 20^0 to 90^0.
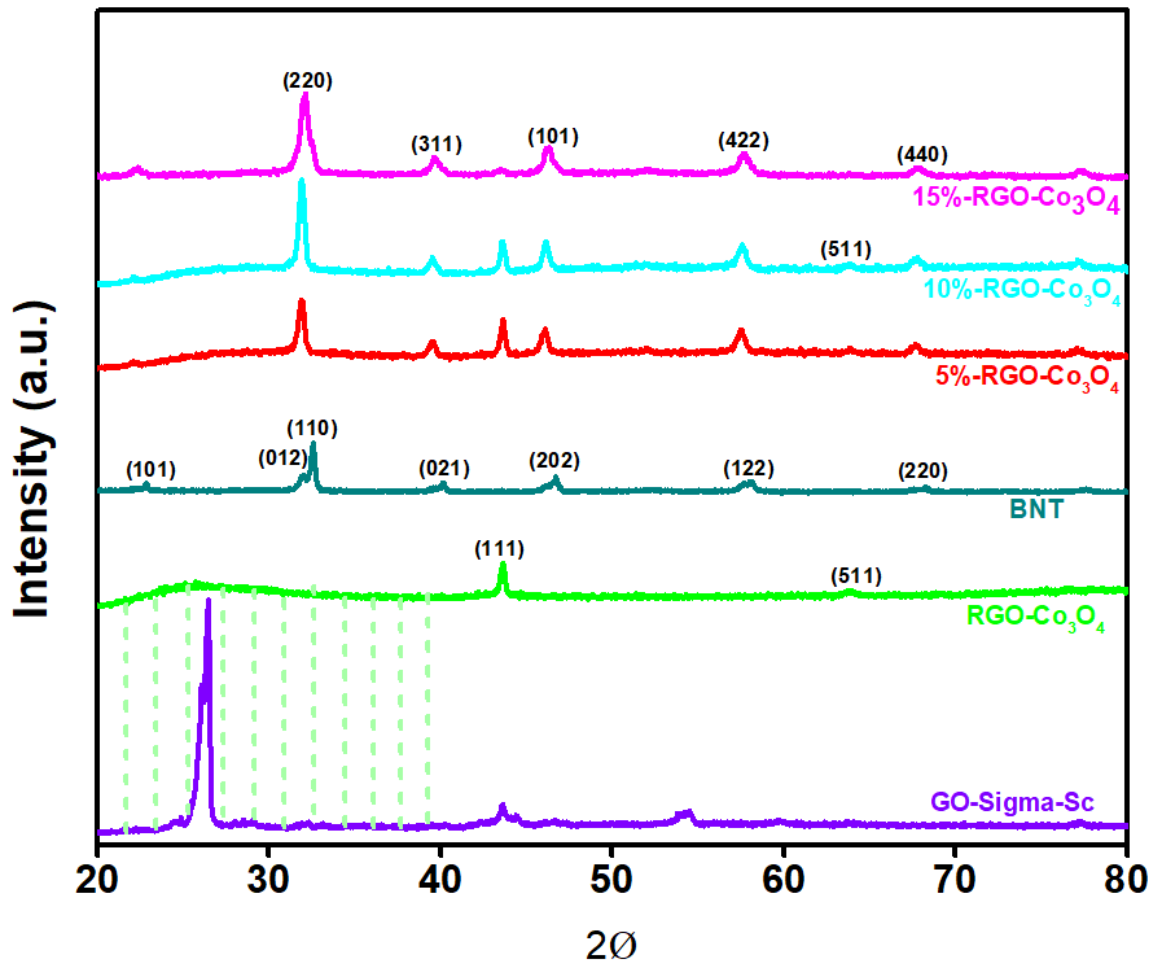
Figure 5.1: Shows XRD pattern for graphene oxide purchased from Sigma Scientific, RGO-Co_3O_4, BNT, 5%, 10% and 15% RGO-Co_3O_4 composite catalyst.

Fig.37 shows the superimposed X-ray diffraction pattern of composite RGO-Co_3O_4, BNT, and its catalysts of varying compositions that were compared with JCPDS cards (Mentioned the number) of their respective materials. Graphene oxide (GO) show a characteristic diffraction signal (002) at 26^0. After reduction is obtained RGO exhibits a hump that covers its two characteristic patterns at 26.8^0 and 42.7^0 with a center around 25^0 due to a change in interplanar spacing of GO sheets.

Besides RGO this hump needs dissection as it underpins diffraction patterns of cobalt oxide that cannot be confirmed otherwise. However, later catalyst patterns confirm Co_3O_4 presence with certainty. The material obtained here is not yet calcined so the presence of moisture along with RGO hump both masks the of cobalt oxide peak. Furthermore at this stage, cobalt is anchored to RGO in the form of hydroxide $Co(OH)_2$-RGO that is later dehydrated to RGO-Co_3O_4 after calcination and is in good agreement with FTIR results shown in fig 42a and b. However a characteristic diffraction peak of RGO (111) at 43.5^o matches with JCPDS no. 15-0806.[156, 175]

All the identical diffraction patterns of the three composites match with the profile of cubic spinel Co_3O_4 JCPDS no. 43-1003. Six remarkable peaks at 31.8^o, 39.48^o, 46°, 57°, 67.8^o, and 62° correspond to (220), (311), (400), (422), (440), and (511) crystal planes. Though the structure remains cubic spinel but a peak appears at 45° corresponding to the hcp (101) crystal lattice that matches JCPDS no. 05-0727.[6]

BNT diffraction pattern confirms rhombohedral crystal structure matching JCPDS no. 36-0340 with significant peaks at 22.8^o, 32°, 32.6^o, 40°, 47°, 57.9^o and 68.2^o corresponding to (101), (012), (110), (021), (202), (122) and (220) respectively.[34]

5.2   SEM

SEM was performed to understand morphology and even dispersion of active sites on best performing catalyst i.e. 5% composition. In figure 38, FE-SEM of 5% BNT-RGO-Co_3O_4 catalyst was performed and the image shows the spherical shape of both BNT and Co_3O_4 nanoparticles.
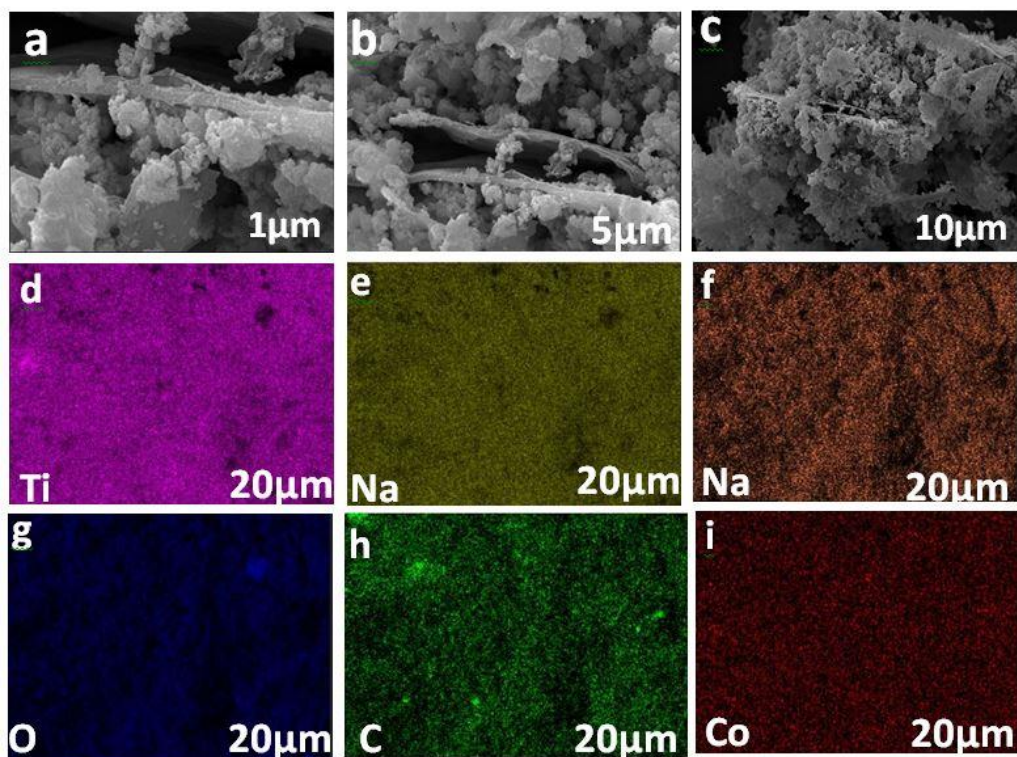
Figure 5.2: a,b, and c show SEM of 5% BNT-RGO-Co₃O₄ catalyst at 1μm, 5μm, and 10μm respectively. Fig. 38 d, e, f, g, h mapping images of 5% BNT-Co₃O₄

Element	Weight %	MDL	Atomic %	Net Int.	Error %	R	A	F
C K	5.3	0.22	14.4	138.2	11.4	0.7803	0.1065	1.0000
O K	28.2	0.09	57.5	1416.7	10.3	0.7952	0.0801	1.0000
Na K	5.7	0.05	8.1	747.3	9.4	0.8139	0.1938	1.0041
Ti K	19.7	0.05	13.4	3680.9	3.4	0.8729	0.8086	1.0345
Co K	0.0	0.10	0.0	2.1	22.3	0.8993	0.9132	1.1044
Sr K	0.6	1.71	0.2	2.4	77.8	0.9813	0.9845	1.2360
Bi M	40.5	0.09	6.3	4016.6	4.1	0.8456	0.7093	1.0199
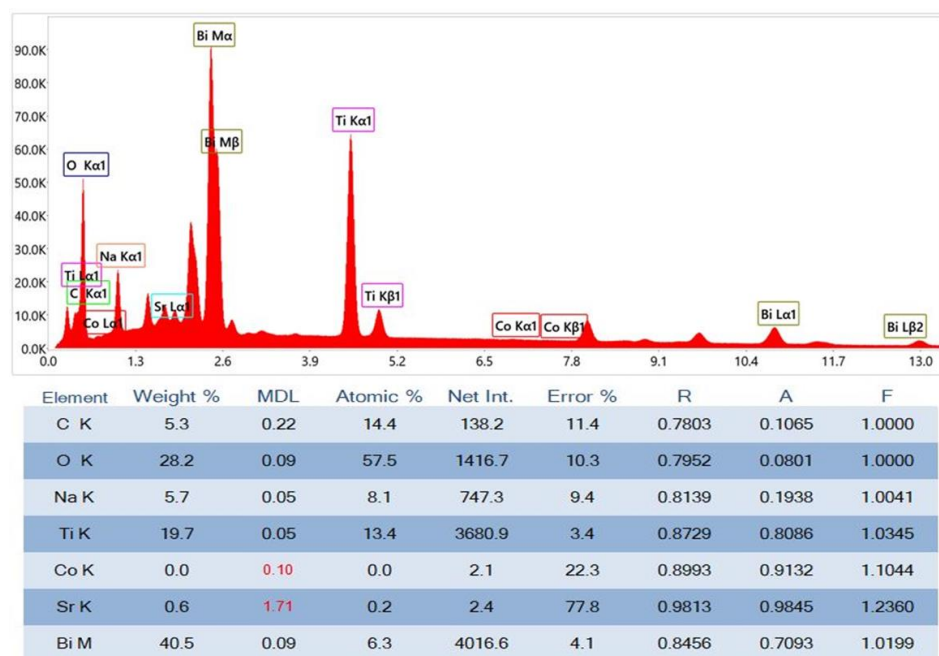
Figure 5.3: EDX image of 5% BNT-RGO-Co₃O₄

62

RGO nanosheets decorated with Co_3O_4 and their uniform dispersion in the BNT matrix can be seen from SEM images. Mapping images show uniform dispersion of active material over the entire surface.

5.3 UV-VIS

UV-Vis was performed to investigate optical properties of pristine BNT, RGO-Co3O4, and their respective varieties of composite catalyst. Through UV-Vis analysis we can propose a reaction mechanism that can be later proved by GC results.

We have performed detailed UV-Vis analysis to investigate maximum absorption by material under specific wavelength. We have found that our matrix and reinforcement material along with their derivative catalysts all are active between 600nm to 800nm. This range not only makes our catalyst ideal for visible light photo reaction but also perfectly befits our light source i.e. designed at 635nm.

In figure 40, UV-vis spectroscopy was done to understand the optical behavior of the catalyst, and maximum absorption was found in the visible region between 600 to 800nm. However, 5% RGO-Co_3O_4 turned out to cover maximum visible light spectra that range from nearly UV to visible range. It shows two distinct peaks corresponding to a clear band gap range offering multiple transitions to facilitate photo catalysis. 1st peak shows maximum absorption around 328nm that is on cusp of UV to visible range of solar spectra i.e. UV and violet region of visible spectrum. 2nd peak shows a flat top of absorption dome with maximum wavelength ranging from 500nm to 600nm covering blue, green and yellow range of visible spectrum. Overall, this specific composition's absorption spectra range from 287nm to 884nm thus making material more suitable to take advantage of full solar spectrum from cusp of UV to cusp of IR region.

However, the remaining materials show one clear absorption peak leading to clear bang gaps instead of range to offer electronic transitions. As the composition of reinforcement increases from 5% to 15% in catalytic matrix it becomes more visible active due to increased amount of RGO as shown by the shift in absorption peak i.e. from 287nm to 600nm.
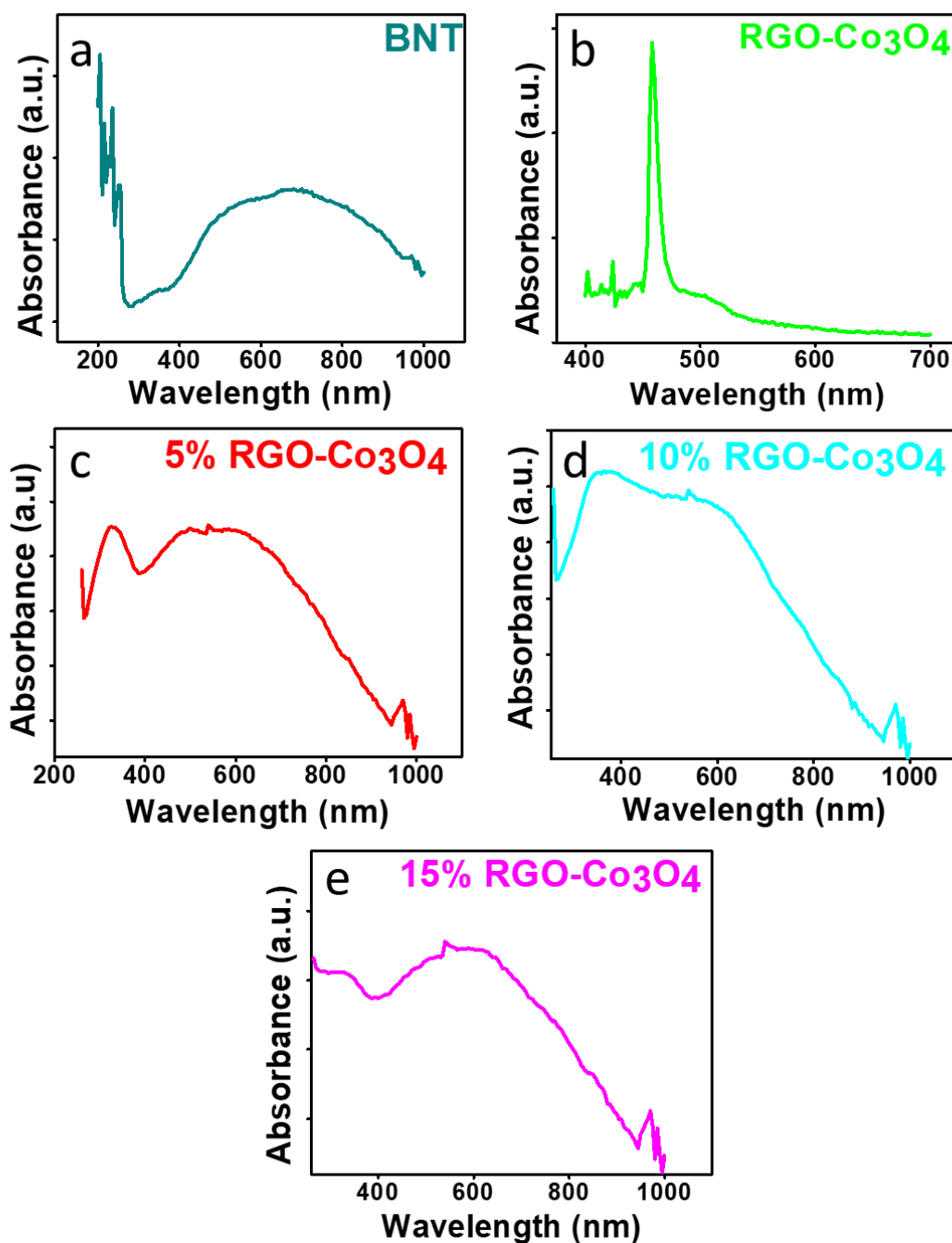
Figure 5.4: a, b, c, d and e UV-Vis adsorption spectra of BNT, RGO-Co_3O_4, 5% RGO-Co_3O_4, 10% RGO-Co_3O_4, 15% RGO-Co_3O_4

Tauc plot was used to determine band gap energies of pristine BNT, RGO-Co_3O_4, and their respective composites by plotting energy versus $(\alpha h v)^2$ and $\alpha h v)^{1/2}$ for both direct

and indirect transitions. Extrapolation of straight lines to the x-axis yields band gaps Eg however, certain materials that do not give crisp straight lines have indirect band gaps rather than direct band gaps.[176]
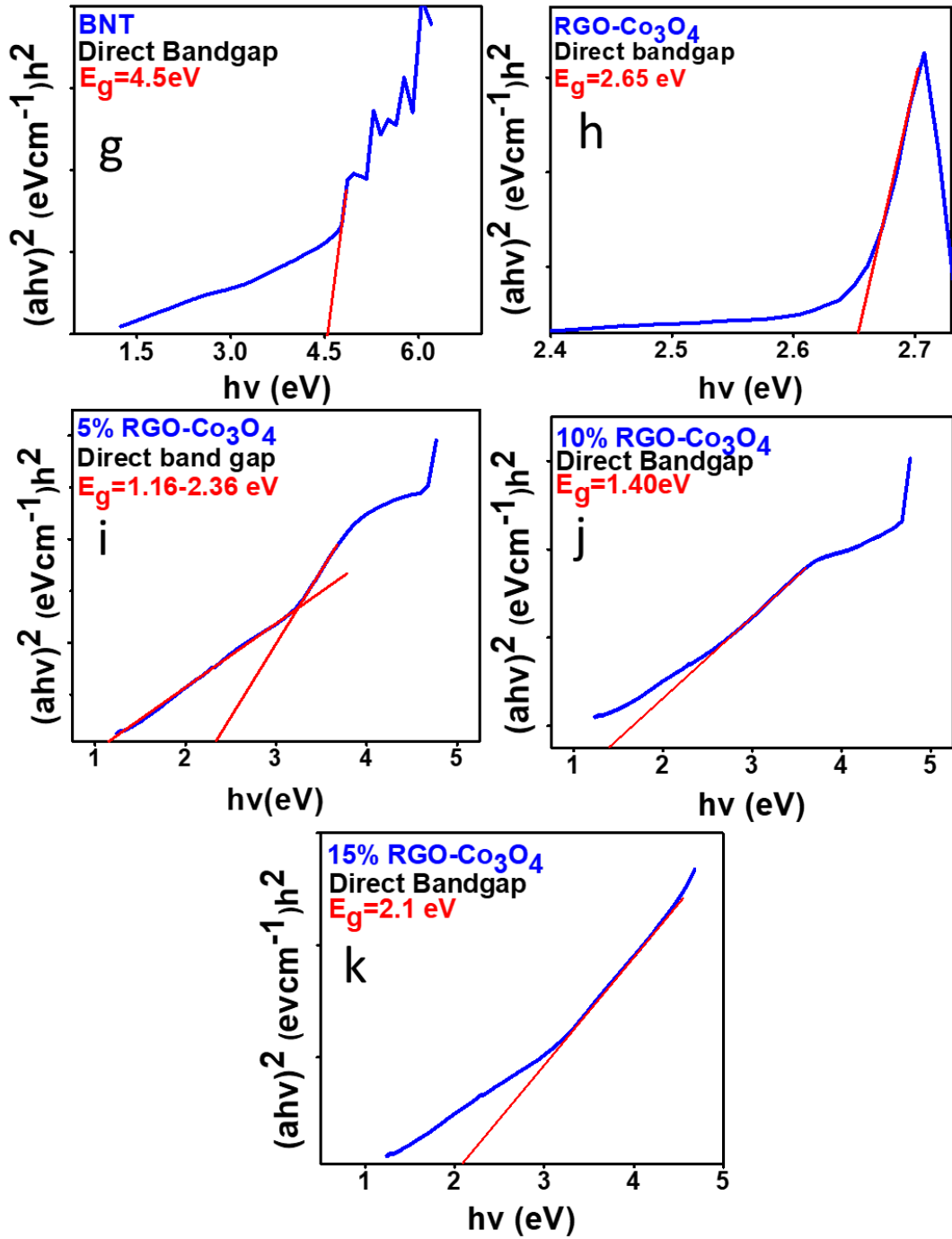
Figure 5.5: g, h, I, j and k direct band gap of BNT, RGO-Co₃O₄, 5% RGO-Co₃O₄, 10% RGO-Co₃O₄, 15% RGO-Co₃O₄
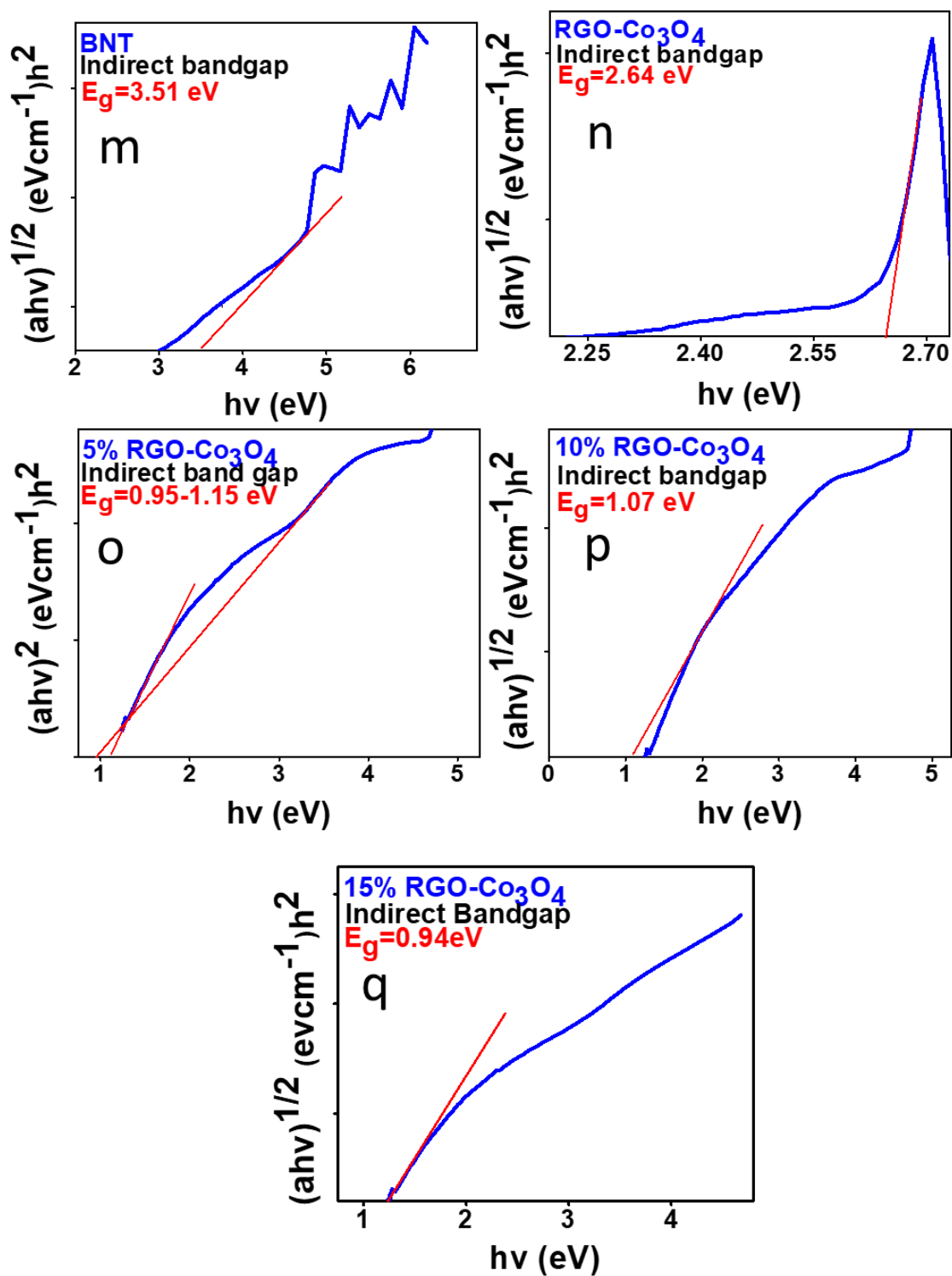
Figure 5.6: m, n, o, p and q indirect band gap of BNT, RGO-Co$_3$O$_4$, 5% RGO-Co$_3$O$_4$, 10% RGO-Co$_3$O$_4$, 15% RGO-Co$_3$O$_4$

RGO-Co$_3$O$_4$ gives a direct band gap where both direct and indirect plots give the same transition energy i.e. 2.64. However, the rest of the materials exhibit both direct and indirect transitions. Though the band gap of reinforcement remains same for both direct and indirect transitions and pristine BNT exhibit both types of bands, hence we can conclude that presence of BNT is responsible for dual bands in all composition catalyst i.e. also our piezo active material.

Optical behavior of BNT as compared to RGO-Co$_3$O$_4$ is comparatively poor but presence of its dual bands along with its piezo sensitivity makes it ideal choice to be used as matrix material. As a result all composites based on BNT exhibit dual bands and further lowering in band edge under piezo strain combined with light irradiation during piezo-photo catalysis.[27]

Furthermore, the role of BNT as water splitting catalyst can be assigned to its inter-band transitions; however, it displays a high direct band gap E$_g$ 4.5eV that limits its straightforward use as a photo-catalyst. The addition of RGO-Co$_3$O$_4$ improves interband transition and lowers the band gap from 4.5eV to 1.4eV depending upon catalytic composition. Catalysts with 5% exhibit a range of band gaps from 1.14eV to 2.36eV that also produce the highest hydrogen yield owing to its lowest band edge. 10% and 15% compositions show 1.02eV and 0.94eV band gaps respectively.

An increase in the concentration of RGO-Co$_3$O$_4$ has a direct impact on materials' optical properties where the band gap declines as concentration increases from 5% to 15% i.e. 1.15eV, 1.02eV and 0.94eV for 5%, 10%, and 15% respectively for indirect band transitions. The lowest band gap range in 5% for direct band gap energy is similar to indirect band energy i.e. 1.15eV. The band gap of BNT for indirect transition is 3.51eV and is lower than the direct band gap value i.e. 4.5eV.

Additions of BNT to RGO-Co$_3$O$_4$ induce strong band tails that were not present previously resulting in the formation of localized sub-energy levels between the valance and conduction band of direct band gap. The striking difference between direct and indirect band gaps is quite noticeable. Direct transitions take place due to photon-electron interaction without being hampered by emitted photons from previous excitations.

However, indirect transitions incorporate combined transitions from both photon-electron and emitted photons.[176]

Furthermore, photon emission from indirect bands is significantly lower than direct bands due to their electron wavenumber being equivalent to direct transitions and the changed wavenumber for indirect transitions. [177] Band tailing and indirect bands with values smaller than direct bands in the same material produce more efficient catalysts due to sufficient availability of photons for indirect transitions. [178]

5.4   Fourier-Transform Infrared Spectroscopy (FTIR)

The functional groups attached to pristine BNT formed in the end catalyst were analyzed using FTIR as shown in figure 43. Both matrix and reinforcement were separately analyzed and then their three compositions such as 5%, 10% and 15% RGO-Co_3O_4 were also analyzed. Consistency has been reported in three compositions and energy points on BNT. However pristine RGO-Co_3O_4 graph needs separate in-depth analysis to clarify the presence of cobalt oxide.

The superimposed FTIR of our composite made from RGO decorated with Co_3O_4 gives a broad band between 3000 to 3400 cm^{-1} that corresponds to symmetric and asymmetric C-OH vibration. A negative shift in O-H stretching is significant due to intermolecular hydrogen bonding present in RGO.

This negative shift in OH could also be possible as Co_3O_4 nanoparticles increase electron density to RGO defective sites that further decrease the band towards lower numbers. This region also exhibits C=C stretching as a result of some unreacted graphitic GO [156]

C-OH stretching present in 1000 to 1187 cm^{-1} range correspond to OH group addition during ethanol processing and it significantly reduces with increasing RGO concentration.[179] The characteristic FTIR absorption peak at 1560 cm^{-1} is allocated to C-O vibration and it not only corresponds to RGO but is also bonded to Co_3O_4 through the C-O bond.
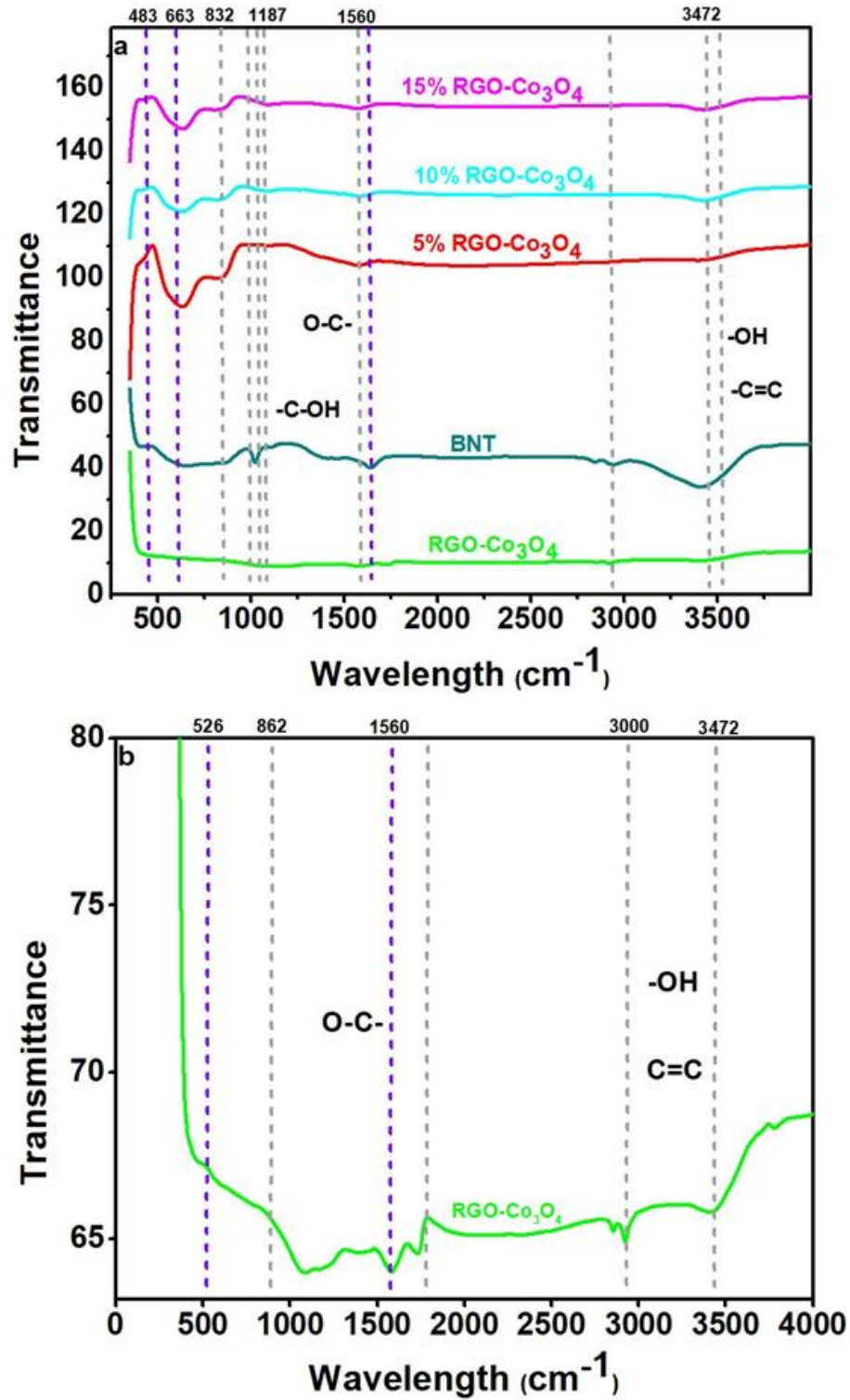
Figure 5.7: a: FTIR plot for pristine BNT, RGO-Co$_3$O$_4$, 5%,10% and 15% RGO-Co$_3$O$_4$ catalyst and fig. 43 b: RGO-Co$_3$O$_4$ extended plot

FTIR analysis of RGO-Co_3O_4 composite catalyst exhibits strong absorption bands around 634 cm^{-1} and 486 cm^{-1} however its pristine version shows 526 cm^{-1} band only. This shift from 526 cm^{-1} to 634 cm^{-1} and 486 cm^{-1} is due to the decomposition of OH functional groups to Co_3O_4 nanoparticles during the calcination step as anchoring hydroxyl links breaks to oxide bonds. [180] Bi-O, Na-O, and Ti-O bands range between 800cm-1 to 1000cm-1 which confirm with literature.[181]

5.5   Gas Chromatography

To demonstrate the effect of piezo-photocatalytic H_2 production performance of prepared samples was first investigated by both light and sonication method. A100ml reaction mixture with 25mg catalyst is constituted with distilled water DI and 15% triethnol amine as a sacrificial agent.Fig. 44 (a) and (b) illustrate the hydrogen production rate of all samples, where BNT and RGO-Co_3O_4 deliver H_2 at the rate of 465 μmol/g-h and 528μmol/g-h respectively. The highest H_2 activity 535 μmol/g-h is observed in composite with 5% RGO-Co_3O_4 loading that is nearest to RGO-Co_3O_4. Excessive co-catalyst loadings beyond 5% reduce H_2 activity but are still above pristine BNT and are 517 μmol/g-h and 515 μmol/g-h for 10% and 15% respectively. A significant increase in activity confirms the role of reinforcement as a co-catalyst in the BNT matrix for H_2 production. [126, 162] We report a 14.79% increase in H_2 activity for BNT from 465 μmol/g-h to 535 μmol/g-h by 5% loading of a metal-free RGO-Co_3O_4 co-catalyst.

Furthermore, H_2 activity is also studied as a function of the trapping agent and is shown in figure 44 (c).15% w/v A_gNO_3 q^- trapper gives 105 μmol/g-h, 15% TEA q+ trapper gives 107 μmol/g-h and DI water produces 103 μmol/g-h. Though the use of a sacrificial agent increases H_2 yield to nearly 3.8% but is not significantly higher thus we conclude that the catalyst produced is effective enough in producing hydrogen without the use of a sacrificial agent.

Furthermore, e^- is critical for HER reaction even the use of q^- trapper yield is slightly increased fundamentally due to the presence of h^+ facilitating catalyst that ensures smooth flow of e^- as a result of OER precedence over HER. An increase in the concentration of q^- trapper is expected to reduce HER yield.[11, 17, 182]
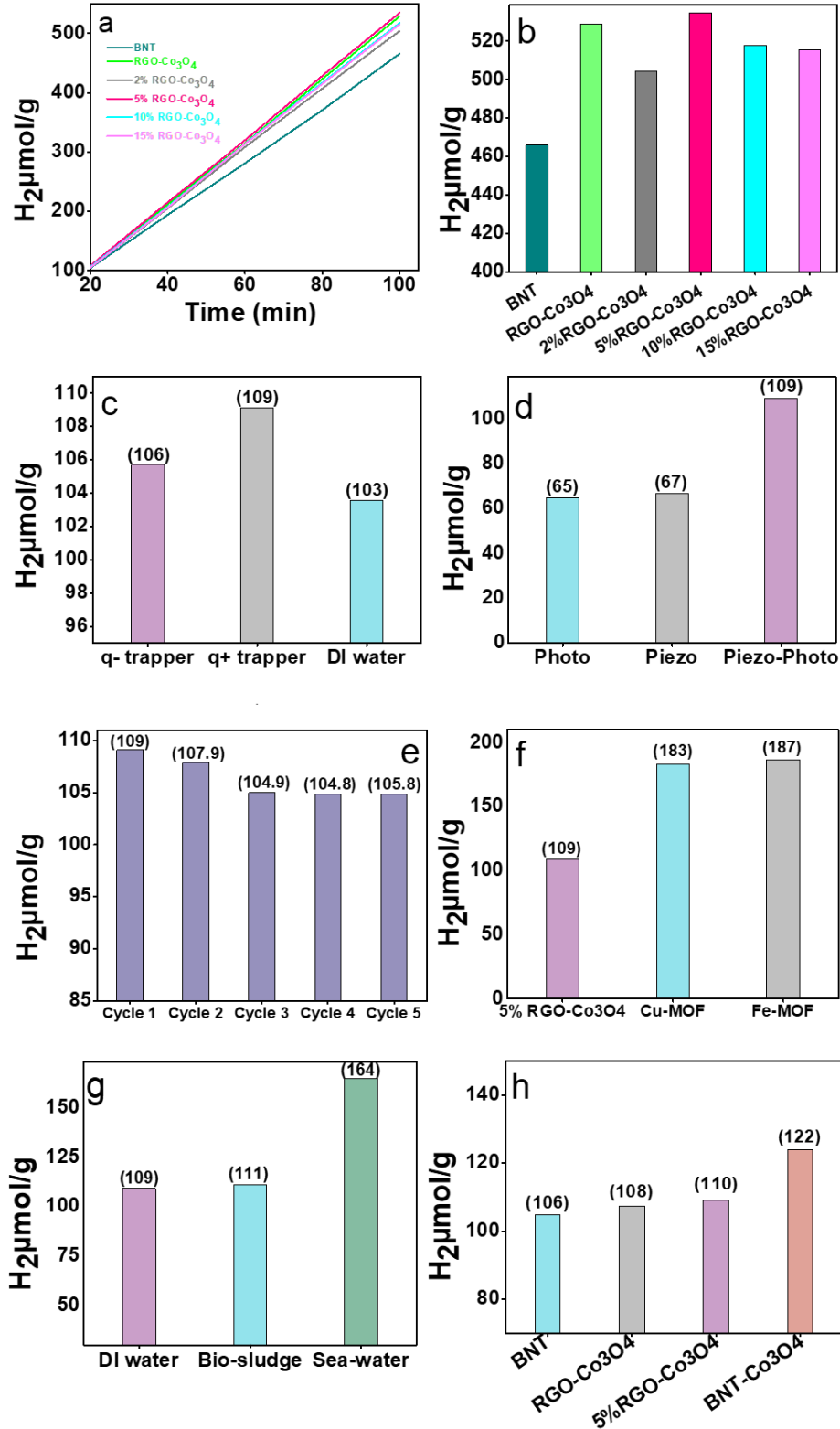
Figure 5.8: (a) shows the compositions for H$_2$ yield, (b) shows the H$_2$ accumulated amount against each composition, (c) shows the charge trappers effect, (d) photo, piezo

and their synergistic effect on H₂ evolution, (d) cyclic stability (e) cyclic strength of catalyst and (f) comparison between metal and non-metal catalyst

To investigate piezo, photo, and its synergistic effects on water splitting reactions three sets of experiments were performed as shown in fig.44 (d). One hour reaction was performed under sonication alone and it nearly produces 67 μmol/g-h hydrogen. Another reaction was performed under light alone and it produces hydrogen around 65 μmol/g-h. In the end, one-hour reaction was carried out under both sonication and light irradiation with a hydrogen yield of around 109 μmol/g-h. Although there isn't a significant difference between piezo and photocatalysis alone however it still confirms materials piezo strain is stronger than photo effect which also confirms well with literature as it happens with few materials.[162] Under application of both piezo and photo effects, a synergistic effect was observed in H₂ production.

The cyclic stability of the pristine catalyst is studied over 5 cycles of 1 hour as shown in figure 44(e) and appears to be stable. A slight decrease is seen in the first cycle that is from 109 μmol/g-h to 107 μmol/g-h and the activity change curve goes flat for the next three cycles i.e. 105 μmol/g-h. On the whole catalyst, it is estimated to be stable under consecutive 5 hours of H₂ activity.

For comparison, Cu-MOF and Fe-MOF were also used to investigate H₂ activity as shown in figure 44 (f) where MOFs were selected due to their prolonged stability under moist conditions. H₂ production rate of Cu-MOF and Fe-MOF are 183 μmol/g-h and 187 μmol/g-h of H₂ respectively. H₂ yield using metals is significantly higher than our catalyst which is nearly 68-70% however we have tried to facilitate HER indirectly by optimizing OER sites primarily due to prolonged stability of oxides underwater as compared to metals.

Moreover, the potential of catalyst for different mediums is also tested for H₂ activity as shown in fig 44 (g). Sea water and manure solutions were used without sacrificial agents and produced nearly 164 μmol/g-h and 111 μmol/g-h H₂ respectively. It nearly produces 50.4% more H₂ for seawater as compared to 1.8% more H₂ in the case of manure. We can conclude sea water has much better potential to be used instead of DI water.

However, the use of RGO as a promotor makes the material more photo-active than usual. Despite its better optical properties when it is combined with BNT it resulted in compromised H_2 activity as a result of poor affinity towards catalyzing HER. However, addition of RGO optimizes optical properties hence slight amounts are recommended.

Furthermore, the use of Co_3O_4 acts as a co-catalyst and it boosts OER that overall speeds up overall water-splitting kinetics. We have confirmed this hypothesis by eliminating RGO and improving Co_3O_4 loading from 1.25% to 9.5% and report similar amounts of H_2 produced i.e. 109 µmol/g-h as shown in fig 44 (h).

We have used both a promoter and a co-catalyst to improve both charge mobility inside the catalyst to speed up negative charge transfer and OER to facilitate water splitting.

Water attack on Co_3O_4 results in oxo coupling and formation of CoOOH. During the oxidation process oxygen vacancies on both Co(III) and Co(IV) provide active oxygen sites for the adsorption of both water and OH- ions that result in surface adsorbed oxygen after proton drifting and release of electrons and forming protons. The surface adsorbed O_2 later converts into O_2 and leaves the catalytic surface.[12] Post O_2 evolution the catalytic surface remains pristine enabling cyclic reactions without compromising catalytic proficiency. Hence Co_3O_4 not only expedites hole migration but also engages in the reaction by providing active oxygen sites. A proposed reaction mechanism is as follows [3, 4, 28, 176, 183]

$$Co_2O_3 + H_2O \leftrightharpoons 2CoOOH + H^+ + e^- \text{ (oxo coupling and proton drifting)}$$

$$Co_2O_3 + OH^- \leftrightharpoons 2CoOOH \qquad \text{(adsorption of OH}^- \text{ ions)}$$

$$2CoOOH \leftrightharpoons O_2(g) + H^+ + e^- + Co_2O_3 \qquad \text{(O}_2 \text{ evolution and catalyst regeneration)}$$

$$2H^+ + 2e^- \leftrightharpoons H_2(g) \qquad \text{(H}_2 \text{ evolution)}$$
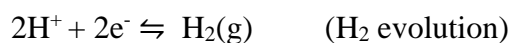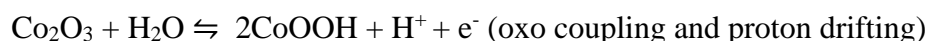
On the other side, RGO aids electron migration from the primary BNT matrix, promoting HER reaction. The experimental result also supports this assumption as we increase Co_3O_4 loading from 2% to 10% by eliminating RGO more H_2 was formed under

similar conditions as shown in fig (f). This suggests that RGO functions as a promoter while Co_3O_4 acts as a co-catalyst within the BNT matrix.

As a piezoelectric material, BNT not only generates but also separates charges under induced polarization. BNT alone without RGO is also fully capable of HER by providing reduction reaction sites.

Yet, trace amounts of RGO enhance the material's overall optical properties making it more visible light active and improving matrix conductivity accelerating charge mobility within the matrix.

BNT directly catalysis HER by following a series of reactions

$$BNT \leftrightharpoons BNT + h^+ + e^-$$

$$H2O + 2h^+ \leftrightharpoons 2H^+ + 1/2O_2$$

$$2H^+ + 2e^- \leftrightharpoons H_2$$
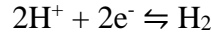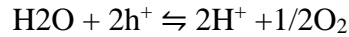
Electrons generated in a material with higher reduction potential are combined with holes generated in a material with lower oxidation potential. This results in e^- h^+ isolation in direct z-scheme. Thus, reduction reactions take place in a material with the lowest reduction potential while oxidation reactions take place in a material with the highest oxidation potential.

As a result, it optimizes redox reactions.[183, 184] Traditional z-schemes typically require a mediator i.e. a conductive material to act as a buffer zone to allow maximum flow of e^- h^+ between two semiconductor materials. Direct z-schemes are more efficient than z-schemes requiring a mediator for redox reaction catalysis.[134, 185] We have found that the mediator requirement is directly dependent on the concentration of the co-catalyst not the promoter.

Our GC results show similar H_2 yield for both 5%RGO-Co_3O_4 and without RGO. The presence of nearly 10% Co_3O_4 eliminates the need for a mediator and shows a direct z-scheme for HER and OER to take place at their respective redox sites. However, for low

concentrations around 1.25% for Co_3O_4 roughly 3.75% for RGO as in 5%RGO-Co_3O_4 is required as a mediator to promote e^- h^+ flow to optimize reaction to the same level.
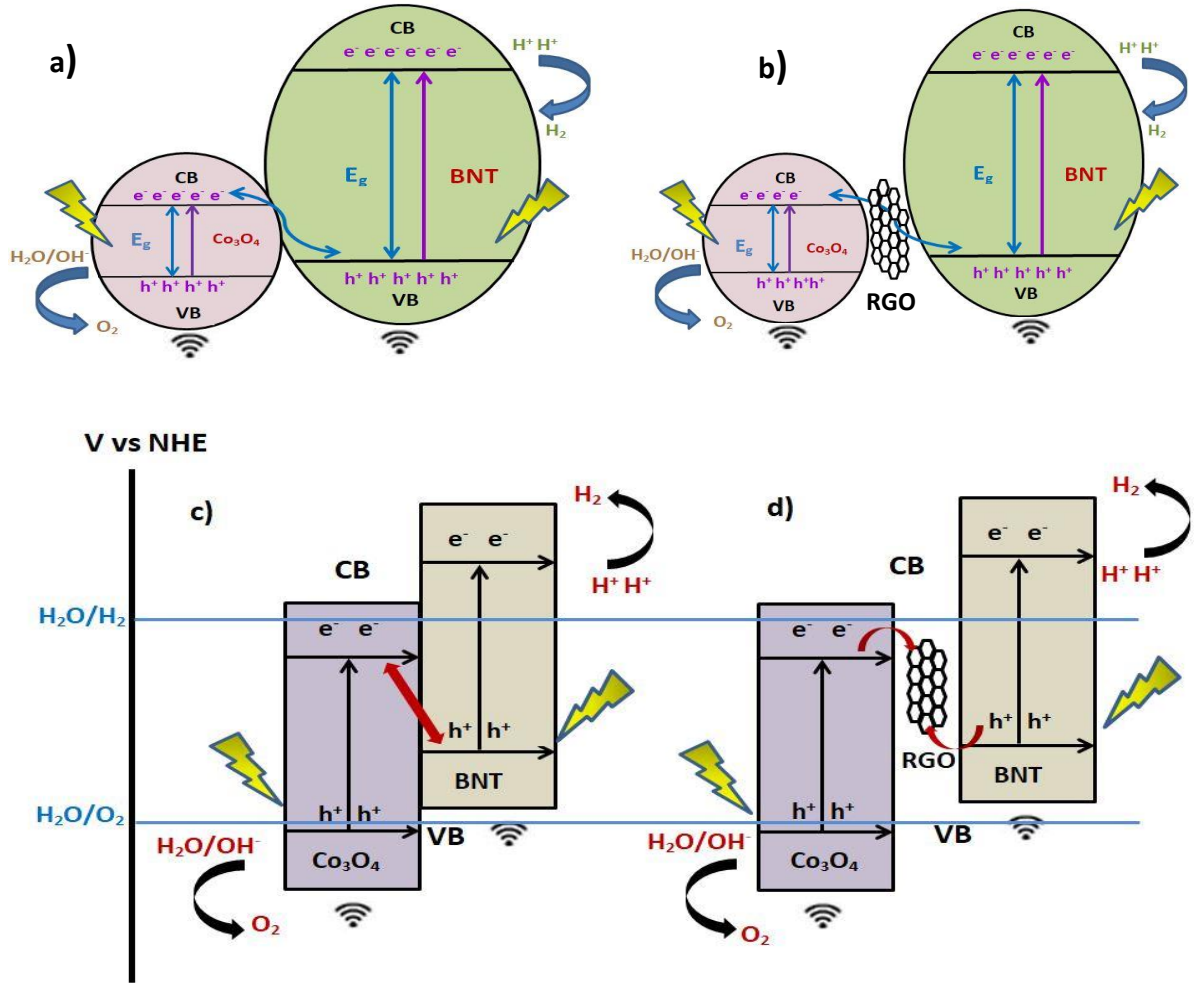
Figure 5.9: (a) and (c) direct z-schemes without mediator for BNT-Co_3O_4. Figure 45 (b) and (d) z-schemes with mediator for BNT-RGO-Co_3O_4

CHAPTER 6: CONCLUSIONS AND FUTURE RECOMMENDATION

6.1   Conclusion

We have achieved success in creating an OER catalyst that enhances water splitting through low-temperature synthesis techniques, such as traditional ball milling. Additionally, we have made significant strides by employing metal-free, stable underwater suspensions of metal oxides. This ingenious approach minimizes the use of metals in unstable reduced form while efficiently generating hydrogen at a reasonable rate.

A comprehensive analysis of our superimposed RGO-Co_3O_4 as a reinforcement has been conducted. It has been observed that RGO serves as a promoter, while Co_3O_4 acts as the main primary co-catalyst in water splitting system. We conclude from this investigation that minute traces of RGO only enhance the optical properties of our catalyst. Moreover, an increase in the quantity of Co_3O_4 has direct correlation with the hydrogen yield. Notable, by increasing Co_3O_4 concentrations from 1.25% to 10% demonstrated a consistent hydrogen yield this eliminating the necessity for separate promoter. However, for more efficient water splitting system, a detailed examination is recommended to determine the optimized percentages of both the promoter and the co-catalyst. This study is aimed at investigating the role of promoter and co-catalyst in overall catalytic matrix.

An in-depth investigation of piezo-catalysis, photo-catalysis and their combined effects has revealed a synergistic interplay between these catalytic processes within single reaction system. The piezo nature of BNT fundamentally governs piezo catalysis. Conversely, the RGO-Co3O4 composite reinforcement not only enhances optical properties of material but also serves as an OER site, initiating water-splitting reaction. Our findings indicate similar hydrogen yields from both piezo-catalysis and photo-catalysis due to optimized characteristics of our material that leverage both piezoelectric and photonic properties. Moreover, the synergy arising from simultaneous piezo-photo catalysis is primarily attributed from reduced charge recombination induced by piezo-induced strain.

Our findings additionally reveal a decrease in charge recombination facilitating better catalytic performance due to the formation of z-scheme heterojunction between BNT

76

and Co3O4. In traditional z-scheme, a low concentration of co-catalyst typically necessitates the use of mediator i.e. promoter to facilitate the smooth flow of electrons across heterojunction. We also report our material to exhibit both direct and indirect bands with band tails that improves efficiency of photo-initiated reactions.

We have also investigated various solvent systems and report seawater as a superior alternative to DI water, attributing its high hydrogen yield. We report 12.8% more hydrogen produced as compared to 1.8% for manure as compared to DI water

6.2   Future Recommendations

Yet, potential formation of chlorine over oxygen necessitates ingenuous optimization of oxygen sites that remains out of scope of this study. Furthermore, MOF's have also been studied and we report Fe MOF's outsmart Cu MOF's in-view of their water splitting capability.

REFERENCES

[1]   N. Abid *et al.*, "Synthesis of nanomaterials using various top-down and bottom-up approaches, influencing factors, advantages, and disadvantages: A review," *Adv Colloid Interface Sci,* vol. 300, p. 102597, Feb 2022.

[2]   M. Yi and Z. Shen, "A review on mechanical exfoliation for the scalable production of graphene," *Journal of Materials Chemistry A,* vol. 3, no. 22, pp. 11700-11715, 2015.

[3]   S. K. Dash, S. Chakraborty, and D. Elangovan, "A Brief Review of Hydrogen Production Methods and Their Challenges," *Energies,* vol. 16, no. 3, 2023.

[4]   J. L. Holechek, H. M. E. Geli, M. N. Sawalhah, and R. Valdez, "A Global Assessment: Can Renewable Energy Replace Fossil Fuels by 2050?," *Sustainability,* vol. 14, no. 8, 2022.

[5]   M. Cheng *et al.*, "Hydroxyl radicals based advanced oxidation processes (AOPs) for remediation of soils contaminated with organic compounds: A review," *Chemical Engineering Journal,* vol. 284, pp. 582-598, 2016.

[6]   M. Rivarolo, E. Porcheddu, and L. Magistri, "DISTRIBUTED HYDRO-METHANE GENERATION FROM RENEWABLE SOURCES: INFLUENCE OF ECONOMIC SCENARIO," presented at the International Conference on Applied Energy Pretoria, South Africa, July, 1-4, 2013, 2013.

[7]   Z. Zhou *et al.*, "Persulfate-based advanced oxidation processes (AOPs) for organic-contaminated soil remediation: A review," *Chemical Engineering Journal,* vol. 372, pp. 836-851, 2019.

[8]   Z. Liang, C.-F. Yan, S. Rtimi, and J. Bandara, "Piezoelectric materials for catalytic/photocatalytic removal of pollutants: Recent advances and outlook," *Applied Catalysis B: Environmental,* vol. 241, pp. 256-269, 2019.

[9]   S. Tasleem and M. Tahir, "Recent progress in structural development and band engineering of perovskites materials for photocatalytic solar hydrogen production: A review," *International Journal of Hydrogen Energy,* vol. 45, no. 38, pp. 19078-19111, 2020.

[10]   T. Puangpetch, T. Sreethawong, S. Yoshikawa, and S. Chavadej, "Hydrogen production from photocatalytic water splitting over mesoporous-assembled SrTiO3 nanocrystal-based photocatalysts," *Journal of Molecular Catalysis A: Chemical,* vol. 312, no. 1-2, pp. 97-106, 2009.

[11]   N. Denisov, J. Yoo, and P. Schmuki, "Effect of different hole scavengers on the photoelectrochemical properties and photocatalytic hydrogen evolution performance of pristine and Pt-decorated TiO2 nanotubes," *Electrochimica Acta,* vol. 319, pp. 61-71, 2019.

[12]   F. E. Osterloh and B. A. Parkinson, "Recent developments in solar water-splitting photocatalysis," *MRS Bulletin,* vol. 36, no. 1, pp. 17-22, 2011.

[13]   L. Pan *et al.*, "Advances in Piezo-Phototronic Effect Enhanced Photocatalysis and Photoelectrocatalysis," *Advanced Energy Materials,* vol. 10, no. 15, 2020.

[14]   J. Tang, T. Liu, S. Miao, and Y. Cho, "Emerging Energy Harvesting Technology for Electro/Photo-Catalytic Water Splitting Application," *Catalysts,* vol. 11, no. 1, 2021.

[15]   X. Li *et al.*, "Water Splitting: From Electrode to Green Energy System," *Nanomicro Lett,* vol. 12, no. 1, p. 131, Jun 17 2020.

[16]   S. Y. Tee *et al.*, "Recent Progress in Energy-Driven Water Splitting," *Adv Sci (Weinh),* vol. 4, no. 5, p. 1600337, May 2017.

[17]   Y. Zhang *et al.*, "High Efficiency Water Splitting using Ultrasound Coupled to a BaTiO(3) Nanofluid," *Adv Sci (Weinh),* vol. 9, no. 9, p. e2105248, Mar 2022.

[18]   R. Su *et al.*, "Strain-Engineered Nano-Ferroelectrics for High-Efficiency Piezocatalytic Overall Water Splitting," *Angew Chem Int Ed Engl,* vol. 60, no. 29, pp. 16019-16026, Jul 12 2021.

[19]   P. Wu *et al.*, "Electronic, Optical, piezoelectric properties and photocatalytic water splitting performance of Two-dimensional group IV-V compounds," *Applied Surface Science,* vol. 627, 2023.

[20]   Y. Feng *et al.*, "Engineering spherical lead zirconate titanate to explore the essence of piezo-catalysis," *Nano Energy,* vol. 40, pp. 481-486, 2017.

[21]   L. Song, S. Sun, S. Zhang, and J. Wei, "Hydrogen production and mechanism from water splitting by metal-free organic polymers PVDF/PVDF-HFP under drive by vibrational energy," *Fuel,* vol. 324, 2022.

[22]   S. Tu *et al.*, "Piezocatalysis and Piezo-Photocatalysis: Catalysts Classification and Modification Strategy, Reaction Mechanism, and Practical Application," *Advanced Functional Materials,* vol. 30, no. 48, 2020.

[23]   X. Zhou, F. Yan, S. Wu, B. Shen, H. Zeng, and J. Zhai, "Remarkable Piezophoto Coupling Catalysis Behavior of BiOX/BaTiO(3) (X = Cl, Br, Cl(0.166) Br(0.834)) Piezoelectric Composites," *Small,* vol. 16, no. 26, p. e2001573, Jul 2020.

[24] S. A. Ali and T. Ahmad, "Treasure trove for efficient hydrogen evolution through water splitting using diverse perovskite photocatalysts," *Materials Today Chemistry,* vol. 29, 2023.

[25] M. L. Xu *et al.*, "Piezo-Photocatalytic Synergy in BiFeO(3) @COF Z-Scheme Heterostructures for High-Efficiency Overall Water Splitting," *Angew Chem Int Ed Engl,* vol. 61, no. 44, p. e202210700, Nov 2 2022.

[26] M. Irshad *et al.*, "Photocatalysis and perovskite oxide-based materials: a remedy for a clean and sustainable future," *RSC Adv,* vol. 12, no. 12, pp. 7009-7039, Mar 1 2022.

[27] L. Chen *et al.*, "Facile preparation of Ag2S/KTa0.5Nb0.5O3 heterojunction for enhanced performance in catalytic nitrogen fixation via photocatalysis and piezo-photocatalysis," *Green Energy & Environment,* vol. 8, no. 6, pp. 1630-1643, 2023.

[28] X. Zhou, Q. Sun, D. Zhai, G. Xue, H. Luo, and D. Zhang, "Excellent catalytic performance of molten-salt-synthesized Bi0.5Na0.5TiO3 nanorods by the piezo-phototronic coupling effect," *Nano Energy,* vol. 84, 2021.

[29] Y. H. Chen, B. K. Wang, and W. C. Hou, "Graphitic carbon nitride embedded with graphene materials towards photocatalysis of bisphenol A: The role of graphene and mediation of superoxide and singlet oxygen," *Chemosphere,* vol. 278, p. 130334, Sep 2021.

[30] S. Singh and N. Khare, "Coupling of piezoelectric, semiconducting and photoexcitation properties in NaNbO 3 nanostructures for controlling electrical transport: Realizing an efficient piezo-photoanode and piezo-photocatalyst," *Nano Energy,* vol. 38, pp. 335-341, 2017.

[31] Y. Jiang *et al.*, "Efficient Cocatalyst-Free Piezo-Photocatalytic Hydrogen Evolution of Defective BaTiO3–x Nanoparticles from Seawater," *ACS Sustainable Chemistry & Engineering,* vol. 11, no. 8, pp. 3370-3389, 2023.

[32] M. Zelisko *et al.*, "Anomalous piezoelectricity in two-dimensional graphene nitride nanosheets," *Nat Commun,* vol. 5, p. 4284, Jun 27 2014.

[33] J. Wang *et al.*, "Energy and environmental catalysis driven by stress and temperature-variation," *Journal of Materials Chemistry A,* vol. 9, no. 21, pp. 12400-12432, 2021.

[34] Z. Zhao *et al.*, "Exclusive enhancement of catalytic activity in Bi0.5Na0.5TiO3nanostructures: new insights into the design of efficient piezocatalysts and piezo-photocatalysts," *Journal of Materials Chemistry A,* vol. 8, no. 32, pp. 16238-16245, 2020.

[35] J. Zhang *et al.*, "Metal-Organic-Framework-Based Photocatalysts Optimized by Spatially Separated Cocatalysts for Overall Water Splitting," *Adv Mater,* vol. 32, no. 49, p. e2004747, Dec 2020.

[36] A. M. K. Fehr *et al.*, "Integrated halide perovskite photoelectrochemical cells with solar-driven water-splitting efficiency of 20.8," *Nat Commun,* vol. 14, no. 1, p. 3797, Jun 26 2023.

[37] R. Li, "Latest progress in hydrogen production from solar water splitting via photocatalysis, photoelectrochemical, and photovoltaic-photoelectrochemical solutions," *Chinese Journal of Catalysis,* vol. 38, no. 1, pp. 5-12, 2017.

[38] A. Wei *et al.*, "Triboelectric Nanogenerator Driven Self-Powered Photoelectrochemical Water Splitting Based on Hematite Photoanodes," *ACS Nano,* vol. 12, no. 8, pp. 8625-8632, Aug 28 2018.

[39] Q. Fu *et al.*, "Improved Capture and Removal Efficiency of Gaseous Acetaldehyde by a Self-Powered Photocatalytic System with an External Electric Field," *ACS Nano,* vol. 15, no. 6, pp. 10577-10586, Jun 22 2021.

[40] N. A. Owen, O. R. Inderwildi, and D. A. King, "The status of conventional world oil reserves—Hype or cause for concern?," *Energy Policy,* vol. 38, no. 8, pp. 4743-4749, 2010.

[41] M. Guo, W. Song, and J. Buhain, "Bioenergy and biofuels: History, status, and perspective," *Renewable and Sustainable Energy Reviews,* vol. 42, pp. 712-725, 2015.

[42] F. Liu *et al.*, "Prehistoric firewood gathering on the northeast Tibetan plateau: environmental and cultural determinism," *Vegetation History and Archaeobotany,* vol. 31, no. 4, pp. 431-441, 2021.

[43] J. Gasparotto and K. Da Boit Martinello, "Coal as an energy source and its impacts on human health," *Energy Geoscience,* vol. 2, no. 2, pp. 113-120, 2021.

[44] L. J. R. Nunes, M. Casau, J. C. O. Matias, and M. F. Dias, "Coal to Biomass Transition as the Path to Sustainable Energy Production: A Hypothetical Case Scenario with the Conversion of Pego Power Plant (Portugal)," *Applied Sciences,* vol. 13, no. 7, 2023.

[45] M. Qiu1 *et al.*, "Earliest systematic coal exploitation for fuel extended to

~3600 B.P.," *SCIENCE ADVANCES,* vol. 9, no. 30, 2023.

[46] R. Fouquet, "The slow search for solutions: Lessons from historical energy transitions by sector and service," *Energy Policy,* vol. 38, no. 11, pp. 6586-6596, 2010.

[47] P. A. O'Connor, "Energy Transitions," The Frederick S; Pardee Centre for the study of the Longer-Range Future, Boston UniversityISBN 978-0-9825683-7-8, 2010.

[48] E. Ostadzadeh, A. Elshorbagy, M. Tuninetti, F. Laio, and A. Abdelkader, "Who will dominate the global fossil fuel trade?," *Economic Systems Research,* vol. 35, no. 3, pp. 354-375, 2023.

[49] T. Haas, "Comparing energy transitions in Germany and Spain using a political economy perspective," *Environmental Innovation and Societal Transitions,* vol. 31, pp. 200-210, 2019.

[50] R. Vakulchuk, I. Overland, and D. Scholten, "Renewable energy and geopolitics: A review," *Renewable and Sustainable Energy Reviews,* vol. 122, 2020.

[51] L. C. Stokes and H. L. Breetz, "Politics in the U.S. energy transition: Case studies of solar, wind, biofuels and electric vehicles policy," *Energy Policy,* vol. 113, pp. 76-86, 2018.

[52] C. J. Cleveland, "The direct and indirect use of fossil fuels and electricity in USA agriculture, 1910-1990," *Agriculture*

Ecosystems &

Environment vol. 55, pp. 111-121, 1995.

[53] M. L. Perry and T. F. Fuller, "A Historical Perspective of Fuel Cell Technology

in the 20th Century," *Journal of The Electrochemical Society,* vol. 149, no. 7, pp. 59-67, 2002.

[54] Z.-b. Cai, Z.-y. Li, M.-g. Yin, M.-h. Zhu, and Z.-r. Zhou, "A review of fretting study on nuclear power equipment," *Tribology International,* vol. 144, 2020.

[55] M. Zeng, S. Wang, J. Duan, J. Sun, P. Zhong, and Y. Zhang, "Review of nuclear power development in China: Environment analysis, historical stages, development status, problems and countermeasures," *Renewable and Sustainable Energy Reviews,* vol. 59, pp. 1369-1383, 2016.

[56] J. M. Pearce, "Limitations of Nuclear Power as a Sustainable Energy Source," *Sustainability,* vol. 4, no. 6, pp. 1173-1187, 2012.

[57] J. Skovgaard and H. van Asselt, "The politics of fossil fuel subsidies and their reform: Implications for climate change mitigation," *WIREs Climate Change,* vol. 10, no. 4, 2019.

[58] J. Syvitski *et al.*, "Extraordinary human energy consumption and resultant geological impacts beginning around 1950 CE initiated the proposed Anthropocene Epoch," *Communications Earth & Environment,* vol. 1, no. 1, 2020.

[59]   Y. F. Makogon, "Natural gas hydrates – A promising source of energy," *Journal of Natural Gas Science and Engineering,* vol. 2, no. 1, pp. 49-59, 2010.

[60]   J. Curtin, C. McInerney, B. Ó Gallachóir, C. Hickey, P. Deane, and P. Deeney, "Quantifying stranding risk for fossil fuel assets and implications for renewable energy investment: A review of the literature," *Renewable and Sustainable Energy Reviews,* vol. 116, 2019.

[61]   M. Lockwood, C. Kuzemko, C. Mitchell, and R. Hoggett, "Historical institutionalism and the politics of sustainable energy transitions: A research agenda," *Environment and Planning C: Politics and Space,* vol. 35, no. 2, pp. 312-333, 2016.

[62]   D. Shindell and C. J. Smith, "Climate and air-quality benefits of a realistic phase-out of fossil fuels," *Nature,* vol. 573, no. 7774, pp. 408-411, Sep 2019.

[63]   K. Bhattarai, W. M. Stalick, S. McKay, G. Geme, and N. Bhattarai, "Biofuel: an alternative to fossil fuel for alleviating world energy and economic crises," *J Environ Sci Health A Tox Hazard Subst Environ Eng,* vol. 46, no. 12, pp. 1424-42, 2011.

[64]   K. Bos and J. Gupta, "Climate change: the risks of stranded fossil fuel assets and resources to the developing world," *Third World Quarterly,* vol. 39, no. 3, pp. 436-453, 2017.

[65]   N. Scovronick *et al.*, "Air Quality and Health Impacts of Future Ethanol Production and Use in Sao Paulo State, Brazil," *Int J Environ Res Public Health,* vol. 13, no. 7, Jul 11 2016.

[66]   G. Nicoletti, N. Arcuri, G. Nicoletti, and R. Bruno, "A technical and environmental comparison between hydrogen and some fossil fuels," *Energy Conversion and Management,* vol. 89, pp. 205-213, 2015.

[67]   K. Moustakas, M. Loizidou, M. Rehan, and A. S. Nizami, "A review of recent developments in renewable and sustainable energy systems: Key challenges and future perspective," *Renewable and Sustainable Energy Reviews,* vol. 119, 2020.

[68]   A. K. Azad, M. G. Rasul, M. M. K. Khan, S. C. Sharma, and M. A. Hazrat, "Prospect of biofuels as an alternative transport fuel in Australia," *Renewable and Sustainable Energy Reviews,* vol. 43, pp. 331-351, 2015.

[69]   Suyarov A.O., Sorimsokov U.S., and B. A.M, "RENEWABLE ENERGY RESEARCH IN UZBEKISTAN: PROSPECTS

AND CHALLENGES," *Web of Scientist: International Scientific Research Journal,* vol. 4, no. 4, 2023.

[70] H. A. Kazem and M. T. Chaichan, "Status and future prospects of renewable energy in Iraq," *Renewable and Sustainable Energy Reviews,* vol. 16, no. 8, pp. 6007-6012, 2012.

[71] P. A. Østergaard, N. Duic, Y. Noorollahi, and S. Kalogirou, "Renewable energy for sustainable development," *Renewable Energy,* vol. 199, pp. 1145-1152, 2022.

[72] N. Kannan and D. Vakeesan, "Solar energy for future world: - A review," *Renewable and Sustainable Energy Reviews,* vol. 62, pp. 1092-1105, 2016.

[73] Z. Zakaria, S. K. Kamarudin, K. A. Abd Wahid, and S. H. Abu Hassan, "The progress of fuel cell for malaysian residential consumption: Energy status and prospects to introduction as a renewable power generation system," *Renewable and Sustainable Energy Reviews,* vol. 144, 2021.

[74] M. Ji and J. Wang, "Review and comparison of various hydrogen production methods based on costs and life cycle impact assessment indicators," *International Journal of Hydrogen Energy,* vol. 46, no. 78, pp. 38612-38635, 2021.

[75] M. T. Ross and B. C. Murray, "What is the fuel of the future? Prospects under the Clean Power Plan," *Energy Economics,* vol. 60, pp. 451-459, 2016.

[76] H. T. Arat and M. G. SÜRer, "State of art of hydrogen usage as a fuel on aviation," *European Mechanical Science,* vol. 2, no. 1, pp. 20-30, 2017.

[77] S. Masoudi Soltani, A. Lahiri, H. Bahzad, P. Clough, M. Gorbounov, and Y. Yan, "Sorption-enhanced Steam Methane Reforming for Combined CO_2 Capture and Hydrogen Production: A State-of-the-Art Review," *Carbon Capture Science & Technology,* vol. 1, 2021.

[78] S. Wang, S. A. Nabavi, and P. T. Clough, "A review on bi/polymetallic catalysts for steam methane reforming," *International Journal of Hydrogen Energy,* vol. 48, no. 42, pp. 15879-15893, 2023.

[79] S. A. Bhat and J. Sadhukhan, "Process intensification aspects for steam methane reforming: An overview," *AIChE Journal,* vol. 55, no. 2, pp. 408-422, 2009.

[80] F. Safari and I. Dincer, "A review and comparative evaluation of thermochemical water splitting cycles for hydrogen production," *Energy Conversion and Management,* vol. 205, 2020.

[81] M. Mehrpooya and R. Habibi, "A review on hydrogen production thermochemical water-splitting cycles," *Journal of Cleaner Production,* vol. 275, 2020.

[82] C. L. Muhich, B. D. Ehrhart, I. Al-Shankiti, B. J. Ward, C. B. Musgrave, and A. W. Weimer, "A review and perspective of efficient hydrogen generation via solar thermal water splitting," *WIREs Energy and Environment,* vol. 5, no. 3, pp. 261-287, 2015.

[83]   A. A. Ahmad, N. A. Zawawi, F. H. Kasim, A. Inayat, and A. Khasri, "Assessing the gasification performance of biomass: A review on biomass gasification process conditions, optimization and economic evaluation," *Renewable and Sustainable Energy Reviews,* vol. 53, pp. 1333-1347, 2016.

[84]   S. Singh Siwal, Q. Zhang, C. Sun, S. Thakur, V. Kumar Gupta, and V. Kumar Thakur, "Energy production from steam gasification processes and parameters that contemplate in biomass gasifier - A review," *Bioresour Technol,* vol. 297, p. 122481, Feb 2020.

[85]   T. K. Patra and P. N. Sheth, "Biomass gasification models for downdraft gasifier: A state-of-the-art review," *Renewable and Sustainable Energy Reviews,* vol. 50, pp. 583-593, 2015.

[86]   S. K. Sansaniwal, K. Pal, M. A. Rosen, and S. K. Tyagi, "Recent advances in the development of biomass gasification technology: A comprehensive review," *Renewable and Sustainable Energy Reviews,* vol. 72, pp. 363-384, 2017.

[87]   S. Safarian, R. Unnþórsson, and C. Richter, "A review of biomass gasification modelling," *Renewable and Sustainable Energy Reviews,* vol. 110, pp. 378-391, 2019.

[88]   L. Singh and Z. A. Wahid, "Methods for enhancing bio-hydrogen production from biological process: A review," *Journal of Industrial and Engineering Chemistry,* vol. 21, pp. 70-80, 2015.

[89]   I. K. Kapdan and F. Kargi, "Bio-hydrogen production from waste materials," *Enzyme and Microbial Technology,* vol. 38, no. 5, pp. 569-582, 2006.

[90]   D. D. T. Ferraren-De Cagalitan and M. L. S. Abundo, "A review of biohydrogen production technology for application towards hydrogen fuel cells," *Renewable and Sustainable Energy Reviews,* vol. 151, 2021.

[91]   M. Wang, Z. Wang, X. Gong, and Z. Guo, "The intensification technologies to water electrolysis for hydrogen production – A review," *Renewable and Sustainable Energy Reviews,* vol. 29, pp. 573-588, 2014.

[92]   J. Chi and H. Yu, "Water electrolysis based on renewable energy for hydrogen production," *Chinese Journal of Catalysis,* vol. 39, no. 3, pp. 390-394, 2018.

[93]   W. Han, M. Li, Y. Ma, and J. Yang, "Cobalt-Based Metal-Organic Frameworks and Their Derivatives for Hydrogen Evolution Reaction," *Front Chem,* vol. 8, p. 592915, 2020.

[94]   A. Ursua, L. M. Gandia, and P. Sanchis, "Hydrogen Production From Water Electrolysis: Current Status and Future Trends," *Proceedings of the IEEE,* vol. 100, no. 2, pp. 410-426, 2012.

[95]   S. Shiva Kumar and V. Himabindu, "Hydrogen production by PEM water electrolysis – A review," *Materials Science for Energy Technologies,* vol. 2, no. 3, pp. 442-454, 2019.

[96]   S. Shiva Kumar and H. Lim, "An overview of water electrolysis technologies for green hydrogen production," *Energy Reports,* vol. 8, pp. 13793-13813, 2022.

[97]   S. Wang, A. Lu, and C. J. Zhong, "Hydrogen production from water electrolysis: role of catalysts," *Nano Converg,* vol. 8, no. 1, p. 4, Feb 11 2021.

[98]   M. Ahmed and I. Dincer, "A review on photoelectrochemical hydrogen production systems: Challenges and future directions," *International Journal of Hydrogen Energy,* vol. 44, no. 5, pp. 2474-2507, 2019.

[99]   L. Clarizia, M. N. Nadagouda, and D. D. Dionysiou, "Recent advances and challenges of photoelectrochemical cells for hydrogen production," *Current Opinion in Green and Sustainable Chemistry,* vol. 41, 2023.

[100]   M. D. Bhatt and J. S. Lee, "Recent theoretical progress in the development of photoanode materials for solar water splitting photoelectrochemical cells," *Journal of Materials Chemistry A,* vol. 3, no. 20, pp. 10632-10659, 2015.

[101]   N. S. Hassan *et al.*, "Recent review and evaluation of green hydrogen production via water electrolysis for a sustainable and clean energy society," *International Journal of Hydrogen Energy,* 2023.

[102]   B. Y. Alfaifi, H. Ullah, S. Alfaifi, A. A. Tahir, and T. K. Mallick, "Photoelectrochemical solar water splitting: From basic principles to advanced devices," *Veruscript Functional Nanomaterials,* vol. 2, 2018.

[103]   C. Acar and I. Dincer, "A review and evaluation of photoelectrode coating materials and methods for photoelectrochemical hydrogen production," *International Journal of Hydrogen Energy,* vol. 41, no. 19, pp. 7950-7959, 2016.

[104]   J. Ekspong *et al.*, "Solar-Driven Water Splitting at 13.8% Solar-to-Hydrogen Efficiency by an Earth-Abundant Electrolyzer," *ACS Sustainable Chemistry & Engineering,* vol. 9, no. 42, pp. 14070-14078, 2021.

[105]   J. M. Yu *et al.*, "High-performance and stable photoelectrochemical water splitting cell with organic-photoactive-layer-based photoanode," *Nat Commun,* vol. 11, no. 1, p. 5509, Nov 2 2020.

[106]   M. F. R. Samsudin, "Photovoltaic-Assisted Photo(electro)catalytic Hydrogen Production: A Review," *Energies,* vol. 16, no. 15, 2023.

[107]   M. Tayebi and B.-K. Lee, "Recent advances in BiVO4 semiconductor materials for hydrogen production using photoelectrochemical water splitting," *Renewable and Sustainable Energy Reviews,* vol. 111, pp. 332-343, 2019.

[108] P. Varadhan, H. C. Fu, Y. C. Kao, R. H. Horng, and J. H. He, "An efficient and stable photoelectrochemical system with 9% solar-to-hydrogen conversion efficiency via InGaP/GaAs double junction," *Nat Commun,* vol. 10, no. 1, p. 5282, Nov 21 2019.

[109] M. P. Browne, Z. Sofer, and M. Pumera, "Layered and two dimensional metal oxides for electrochemical energy conversion," *Energy & Environmental Science,* vol. 12, no. 1, pp. 41-58, 2019.

[110] J. H. Kim, D. Hansora, P. Sharma, J. W. Jang, and J. S. Lee, "Toward practical solar hydrogen production - an artificial photosynthetic leaf-to-farm challenge," *Chem Soc Rev,* vol. 48, no. 7, pp. 1908-1971, Apr 1 2019.

[111] V. Preethi and S. Kanmani, "Photocatalytic hydrogen production," *Materials Science in Semiconductor Processing,* vol. 16, no. 3, pp. 561-575, 2013.

[112] A. R. Araujo Scharnberg, A. Carvalho de Loreto, and A. Kopp Alves, "Optical and Structural Characterization of Bi2FexNbO7 Nanoparticles for Environmental Applications," *Emerging Science Journal,* vol. 4, no. 1, pp. 11-17, 2020.

[113] H. Idriss, "Hydrogen production from water: past and present," *Current Opinion in Chemical Engineering,* vol. 29, pp. 74-82, 2020.

[114] Y. Lim, D. K. Lee, S. M. Kim, W. Park, S. Y. Cho, and U. Sim, "Low Dimensional Carbon-Based Catalysts for Efficient Photocatalytic and Photo/Electrochemical Water Splitting Reactions," *Materials (Basel),* vol. 13, no. 1, Dec 25 2019.

[115] C. Acar, I. Dincer, and C. Zamfirescu, "A review on selected heterogeneous photocatalysts for hydrogen production," *International Journal of Energy Research,* vol. 38, no. 15, pp. 1903-1920, 2014.

[116] M. Xiao *et al.*, "Addressing the stability challenge of metal halide perovskite based photocatalysts for solar fuel production," *Journal of Physics: Energy,* vol. 4, no. 4, 2022.

[117] S. Cao, J. Low, J. Yu, and M. Jaroniec, "Polymeric photocatalysts based on graphitic carbon nitride," *Adv Mater,* vol. 27, no. 13, pp. 2150-76, Apr 1 2015.

[118] L. Jiang *et al.*, "Doping of graphitic carbon nitride for photocatalysis: A review," *Applied Catalysis B: Environmental,* vol. 217, pp. 388-406, 2017.

[119] G. Liu *et al.*, "Enhancement of the photoelectrochemical water splitting by perovskite BiFeO3 via interfacial engineering," *Solar Energy,* vol. 202, pp. 198-203, 2020.

[120] S. Das *et al.*, "High performance BiFeO(3) ferroelectric nanostructured photocathodes," *J Chem Phys,* vol. 153, no. 8, p. 084705, Aug 28 2020.

[121] T. Hisatomi, K. Takanabe, and K. Domen, "Photocatalytic Water-Splitting Reaction from Catalytic and Kinetic Perspectives," *Catalysis Letters,* vol. 145, no. 1, pp. 95-108, 2014.

[122] Y. Yan, Z. Chen, X. Cheng, and W. Shi, "Research Progress of ZnIn2S4-Based Catalysts for Photocatalytic Overall Water Splitting," *Catalysts,* vol. 13, no. 6, 2023.

[123] A. V. Zhurenok, D. B. Vasilchenko, and E. A. Kozlova, "Comprehensive Review on g-C(3)N(4)-Based Photocatalysts for the Photocatalytic Hydrogen Production under Visible Light," *Int J Mol Sci,* vol. 24, no. 1, Dec 25 2022.

[124] J. Y. Kim and D. H. Youn, "Nanomaterials for Advanced Photocatalytic Plastic Conversion," *Molecules,* vol. 28, no. 18, Sep 7 2023.

[125] K. H. Ng, S. Y. Lai, C. K. Cheng, Y. W. Cheng, and C. C. Chong, "Photocatalytic water splitting for solving energy crisis: Myth, Fact or Busted?," *Chemical Engineering Journal,* vol. 417, 2021.

[126] Z. Yan, H. Wu, A. Han, X. Yu, and P. Du, "Noble metal-free cobalt oxide (CoO) nanoparticles loaded on titanium dioxide/cadmium sulfide composite for enhanced photocatalytic hydrogen production from water," *International Journal of Hydrogen Energy,* vol. 39, no. 25, pp. 13353-13360, 2014.

[127] C. Acar, I. Dincer, and G. F. Naterer, "Review of photocatalytic water-splitting methods for sustainable hydrogen production," *International Journal of Energy Research,* vol. 40, no. 11, pp. 1449-1473, 2016.

[128] V. Dal Santo and A. Naldoni, "Titanium Dioxide Photocatalysis," *Catalysts,* vol. 8, no. 12, 2018.

[129] S. Horikoshi and N. Serpone, "Can the photocatalyst TiO2 be incorporated into a wastewater treatment method? Background and prospects," *Catalysis Today,* vol. 340, pp. 334-346, 2020.

[130] B. A. Bhanvase, T. P. Shende, and S. H. Sonawane, "A review on graphene–TiO2 and doped graphene–TiO2 nanocomposite photocatalyst for water and wastewater treatment," *Environmental Technology Reviews,* vol. 6, no. 1, pp. 1-14, 2016.

[131] Z. Mamiyev and N. O. Balayeva, "Metal Sulfide Photocatalysts for Hydrogen Generation: A Review of Recent Advances," *Catalysts,* vol. 12, no. 11, 2022.

[132] D. J. Martin, P. J. Reardon, S. J. Moniz, and J. Tang, "Visible light-driven pure water splitting by a nature-inspired organic semiconductor-based system," *J Am Chem Soc,* vol. 136, no. 36, pp. 12568-71, Sep 10 2014.

[133] T. F. Qahtan, T. O. Owolabi, O. E. Olubi, and A. Hezam, "State-of-the-art, challenges and prospects of heterogeneous tandem photocatalysis," *Coordination Chemistry Reviews,* vol. 492, 2023.

[134] T. Li, N. Tsubaki, and Z. Jin, "S-scheme heterojunction in photocatalytic hydrogen production," *Journal of Materials Science & Technology,* vol. 169, pp. 82-104, 2024.

[135] S. Liu, K. Yin, W. Ren, B. Cheng, and J. Yu, "Tandem photocatalytic oxidation of Rhodamine B over surface fluorinated bismuth vanadate crystals," *Journal of Materials Chemistry,* vol. 22, no. 34, 2012.

[136] Y. Jing, Z. Zhou, W. Geng, X. Zhu, and T. Heine, "2D Honeycomb-Kagome Polymer Tandem as Effective Metal-Free Photocatalysts for Water Splitting," *Adv Mater,* vol. 33, no. 21, p. e2008645, May 2021.

[137] S. Navalon, A. Dhakshinamoorthy, M. Alvaro, B. Ferrer, and H. Garcia, "Metal-Organic Frameworks as Photocatalysts for Solar-Driven Overall Water Splitting," *Chem Rev,* vol. 123, no. 1, pp. 445-490, Jan 11 2023.

[138] Y. Bai *et al.*, "Photocatalytic Overall Water Splitting Under Visible Light Enabled by a Particulate Conjugated Polymer Loaded with Palladium and Iridium," *Angew Chem Int Ed Engl,* vol. 61, no. 26, p. e202201299, Jun 27 2022.

[139] J. Liu *et al.*, "Enhanced visible-light photocatalytic performances of ZnO through loading AgI and coupling piezo-photocatalysis," *Journal of Alloys and Compounds,* vol. 852, 2021.

[140] G. Cilaveni, K. V. Ashok Kumar, S. S. K. Raavi, C. Subrahmanyam, and S. Asthana, "Control over relaxor, piezo-photocatalytic and energy storage properties in Na0.5Bi0.5TiO3 via processing methodologies," *Journal of Alloys and Compounds,* vol. 798, pp. 540-552, 2019.

[141] X. Xu, X. Lin, F. Yang, S. Huang, and X. Cheng, "Piezo-photocatalytic Activity of Bi0.5Na0.5TiO3@TiO2 Composite Catalyst with Heterojunction for Degradation of Organic Dye Molecule," *The Journal of Physical Chemistry C,* vol. 124, no. 44, pp. 24126-24134, 2020.

[142] W. Qian, K. Zhao, D. Zhang, C. R. Bowen, Y. Wang, and Y. Yang, "Piezoelectric Material-Polymer Composite Porous Foam for Efficient Dye Degradation via the Piezo-Catalytic Effect," *ACS Appl Mater Interfaces,* vol. 11, no. 31, pp. 27862-27869, Aug 7 2019.

[143] S. Li, Z. Zhao, J. Zhao, Z. Zhang, X. Li, and J. Zhang, "Recent Advances of Ferro-, Piezo-, and Pyroelectric Nanomaterials for Catalytic Applications," *ACS Applied Nano Materials,* vol. 3, no. 2, pp. 1063-1079, 2020.

[144] Y. Xia *et al.*, "Pyroelectrically Induced Pyro-Electro-Chemical Catalytic Activity of BaTiO3 Nanofibers under Room-Temperature Cold–Hot Cycle Excitations," *Metals,* vol. 7, no. 4, 2017.

[145] X. Xu *et al.*, "Strong piezo-electro-chemical effect of piezoelectric BaTiO3 nanofibers for vibration-catalysis," *Journal of Alloys and Compounds,* vol. 762, pp. 915-921, 2018.

[146] A. Al Nafiey *et al.*, "Reduced graphene oxide decorated with Co3O4 nanoparticles (rGO-Co3O4) nanocomposite: A reusable catalyst for highly efficient reduction of 4-nitrophenol, and Cr(VI) and dye removal from aqueous solutions," *Chemical Engineering Journal,* vol. 322, pp. 375-384, 2017.

[147] Y. Wang *et al.*, "Piezo-catalysis for nondestructive tooth whitening," *Nat Commun,* vol. 11, no. 1, p. 1328, Mar 12 2020.

[148] R. Su *et al.*, "Nano-Ferroelectric for High Efficiency Overall Water Splitting under Ultrasonic Vibration," *Angew Chem Int Ed Engl,* vol. 58, no. 42, pp. 15076-15081, Oct 14 2019.

[149] D. Masekela, N. C. Hintsho-Mbita, B. Ntsendwana, and N. Mabuba, "Thin Films (FTO/BaTiO(3)/AgNPs) for Enhanced Piezo-Photocatalytic Degradation of Methylene Blue and Ciprofloxacin in Wastewater," *ACS Omega,* vol. 7, no. 28, pp. 24329-24343, Jul 19 2022.

[150] F. Bößl and I. Tudela, "Piezocatalysis: Can catalysts really dance?," *Current Opinion in Green and Sustainable Chemistry,* vol. 32, 2021.

[151] L. Chen *et al.*, "Strong piezocatalysis in barium titanate/carbon hybrid nanocomposites for dye wastewater decomposition," *J Colloid Interface Sci,* vol. 586, pp. 758-765, Mar 15 2021.

[152] S. Tu *et al.*, "Band shifting triggered ·OH evolution and charge separation enhanced H2O2 generation in piezo-photocatalysis of Silleń-Aurivillius-structured Bi4W0.5Ti0.5O8Cl," *Chemical Engineering Journal,* vol. 465, 2023.

[153] P. Wang, Y. Zong, H. Liu, H. Wen, H.-B. Wu, and J.-B. Xia, "Highly efficient photocatalytic water splitting and enhanced piezoelectric properties of 2D Janus group-III chalcogenides," *Journal of Materials Chemistry C,* vol. 9, no. 14, pp. 4989-4999, 2021.

[154] M. K. Mohanta, A. Rawat, Dimple, N. Jena, R. Ahammed, and A. De Sarkar, "Superhigh out-of-plane piezoelectricity, low thermal conductivity and photocatalytic abilities in ultrathin 2D van der Waals heterostructures of boron monophosphide and gallium nitride," *Nanoscale,* vol. 11, no. 45, pp. 21880-21890, Nov 21 2019.

[155] Q. Zhang, S. Zuo, P. Chen, and C. Pan, "Piezotronics in two-dimensional materials," *InfoMat,* vol. 3, no. 9, pp. 987-1007, 2021.

[156] A. V. Munde, B. B. Mulik, R. P. Dighole, and B. R. Sathe, "Cobalt oxide nanoparticle-decorated reduced graphene oxide (Co3O4–rGO): active and sustainable nanoelectrodes for water oxidation reaction," *New Journal of Chemistry,* vol. 44, no. 36, pp. 15776-15784, 2020.

[157] M. R. Kaiser *et al.*, "Reverse Microemulsion Synthesis of Sulfur/Graphene Composite for Lithium/Sulfur Batteries," *ACS Nano,* vol. 11, no. 9, pp. 9048-9056, Sep 26 2017.

[158] M. Saleem, M.-S. Kim, I.-S. Kim, and S.-J. Jeong, "Polarization and strain behaviors of 0.74BiNaTiO3–0.26SrTiO3/Bi0.5(Na0.8K0.2)0.5TiO3 ceramic composite," *Ceramics International,* vol. 42, no. 12, pp. 13960-13968, 2016.

[159] L. Cai and G. Yu, "Recent Advances in Growth and Modification of Graphene-Based Energy Materials: From Chemical Vapor Deposition to Reduction of Graphene Oxide," *Small Methods,* vol. 3, no. 7, 2019.

[160] M. A. Aldosari, A. A. Othman, and E. H. Alsharaeh, "Synthesis and characterization of the in situ bulk polymerization of PMMA containing graphene sheets using microwave irradiation," *Molecules,* vol. 18, no. 3, pp. 3152-67, Mar 11 2013.

[161] X.-Y. Wang, A. Narita, and K. Müllen, "Precision synthesis versus bulk-scale fabrication of graphenes," *Nature Reviews Chemistry,* vol. 2, no. 1, 2017.

[162] X. Huang *et al.*, "Insight into the piezo-photo coupling effect of PbTiO3/CdS composites for piezo-photocatalytic hydrogen production," *Applied Catalysis B: Environmental,* vol. 282, 2021.

[163] A. Numan, M. M. Shahid, F. S. Omar, K. Ramesh, and S. Ramesh, "Facile fabrication of cobalt oxide nanograin-decorated reduced graphene oxide composite as ultrasensitive platform for dopamine detection," *Sensors and Actuators B: Chemical,* vol. 238, pp. 1043-1051, 2017.

[164] J. E. Ellis *et al.*, "Modification of Carbon Nitride/Reduced Graphene Oxide van der Waals Heterostructure with Copper Nanoparticles To Improve CO(2) Sensitivity," *ACS Appl Mater Interfaces,* vol. 11, no. 44, pp. 41588-41594, Nov 6 2019.

[165] M. Suga *et al.*, "Recent progress in scanning electron microscopy for the characterization of fine structural details of nano materials," *Progress in Solid State Chemistry,* vol. 42, no. 1-2, pp. 1-21, 2014.

[166] J. Epp, "X-ray diffraction (XRD) techniques for materials characterization," in *Materials Characterization Using Nondestructive Evaluation (NDE) Methods*, 2016, pp. 81-124.

[167] V. Gonzalez, M. Cotte, F. Vanmeert, W. de Nolf, and K. Janssens, "X-ray Diffraction Mapping for Cultural Heritage Science: a Review of Experimental Configurations and Applications," *Chemistry,* vol. 26, no. 8, pp. 1703-1719, Feb 6 2020.

[168] N. Widjonarko, "Introduction to Advanced X-ray Diffraction Techniques for Polymeric Thin Films," *Coatings,* vol. 6, no. 4, 2016.

[169] Z. Xue, Z. Lv, and L. Li, "Combination of chromatographic and spectroscopic characterization based on primitive ultraviolet absorbance detection to fulfill advanced monitoring of dissolved organic matter in municipal wastewater treatment plant," *Journal of Environmental Chemical Engineering,* vol. 10, no. 3, 2022.

[170] N. Tsolekile, S. Parani, M. C. Matoetoe, S. P. Songca, and O. S. Oluwafemi, "Evolution of ternary I–III–VI QDs: Synthesis, characterization and application," *Nano-Structures & Nano-Objects,* vol. 12, pp. 46-56, 2017.

[171] S. Lefrant, M. Baibarac, and I. Baltog, "Raman and FTIR spectroscopy as valuable tools for the characterization of polymer and carbon nanotube based composites," *Journal of Materials Chemistry,* vol. 19, no. 32, 2009.

[172] A. Ricci, K. J. Olejar, G. P. Parpinello, P. A. Kilmartin, and A. Versari, "Application of Fourier Transform Infrared (FTIR) Spectroscopy in the Characterization of Tannins," *Applied Spectroscopy Reviews,* vol. 50, no. 5, pp. 407-442, 2015.

[173] S. Singh, T. Handa, M. Narayanam, A. Sahu, M. Junwal, and R. P. Shah, "A critical review on the use of modern sophisticated hyphenated tools in the characterization of impurities and degradation products," *J Pharm Biomed Anal,* vol. 69, pp. 148-73, Oct 2012.

[174] A. F. Al-Rubaye, I. H. Hameed, and M. J. Kadhim, "A Review: Uses of Gas Chromatography-Mass Spectrometry (GC-MS) Technique for Analysis of Bioactive Natural Compounds of Some Plants," *International Journal of Toxicological and Pharmacological Research,* vol. 9, no. 01, 2017.

[175] L. Cheng, Q. Wang, and J. Ding, "Synthesis of Co/CoO@RGO composite for enhanced electromagnetic microwave absorption performance," *Applied Physics A,* vol. 127, no. 1, 2021.

[176] L. L. G. Al-Mahamad, "Analytical study to determine the optical properties of gold nanoparticles in the visible solar spectrum," *Heliyon,* vol. 8, no. 7, p. e09966, Jul 2022.

[177] N. Serpone, "Is the Band Gap of Pristine TiO2 Narrowed by Anion- and Cation-Doping of Titanium Dioxide in Second-Generation Photocatalysts?," *J. Phys. Chem. B,* vol. 110, no. 48, pp. 24287-24293, 2006.

[178] N. Saha *et al.*, "Highly active spherical amorphous MoS2: facile synthesis and application in photocatalytic degradation of rose bengal dye and hydrogenation of nitroarenes," *RSC Advances,* vol. 5, no. 108, pp. 88848-88856, 2015.

[179] T. F. Emiru and D. W. Ayele, "Controlled synthesis, characterization and reduction of graphene oxide: A convenient method for large scale production," *Egyptian Journal of Basic and Applied Sciences,* vol. 4, no. 1, pp. 74-79, 2019.

[180] S. H. Alwan, H. A. H. Alshamsi, and L. S. Jasim, "Rhodamine B removal on A-rGO/cobalt oxide nanoparticles composite by adsorption from contaminated water," *Journal of Molecular Structure,* vol. 1161, pp. 356-365, 2018.

[181] T. Salehi, M. Shirvani, M. Dinari, and E. Gavili, "Adsorptive Removal of Lead from Water Using a Novel Cysteine-Bentonite/Poly(vinyl alcohol)/Alginate Nanocomposite," *Journal of Polymers and the Environment,* vol. 30, no. 10, pp. 4463-4478, 2022.

[182] N. Denisov, S.-J. Jeong, and P. Schmuki, "Effect of different hole scavengers on the photoelectrochemical properties and photocatalytic hydrogen evolution performance of pristine and Pt-decorated TiO2 nanotubes," *Electrochimica Acta,* vol. 319, 2019.

[183] J. Wang, L. Yu, Z. Wang, W. Wei, K. Wang, and X. Wei, "Constructing 0D/2D Z-Scheme Heterojunction of CdS/g-C3N4 with Enhanced Photocatalytic Activity for H2 Evolution," *Catalysis Letters,* vol. 151, no. 12, pp. 3550-3561, 2021.

[184] J. Fernández-Catalá, R. Greco, M. Navlani-García, W. Cao, Á. Berenguer-Murcia, and D. Cazorla-Amorós, "g-C3N4-Based Direct Z-Scheme Photocatalysts for Environmental Applications," *Catalysts,* vol. 12, no. 10, 2022.

[185] Q. Xu, L. Zhang, B. Cheng, J. Fan, and J. Yu, "S-Scheme Heterojunction Photocatalyst," *Chem,* vol. 6, no. 7, pp. 1543-1559, 2020.